

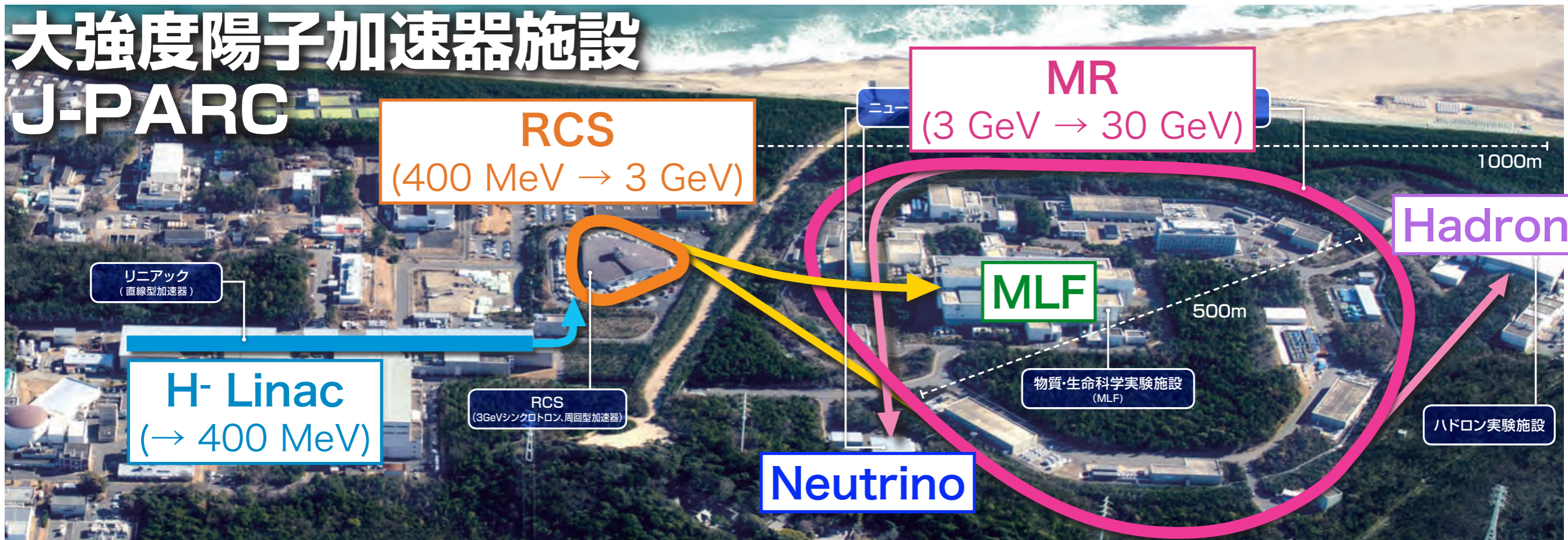


Space charge domain beam dynamics in J-PARC MR

Takaaki Yasui (KEK/J-PARC)

Space Charge Workshop 2024,
Dongguan, China, September 12, 2024

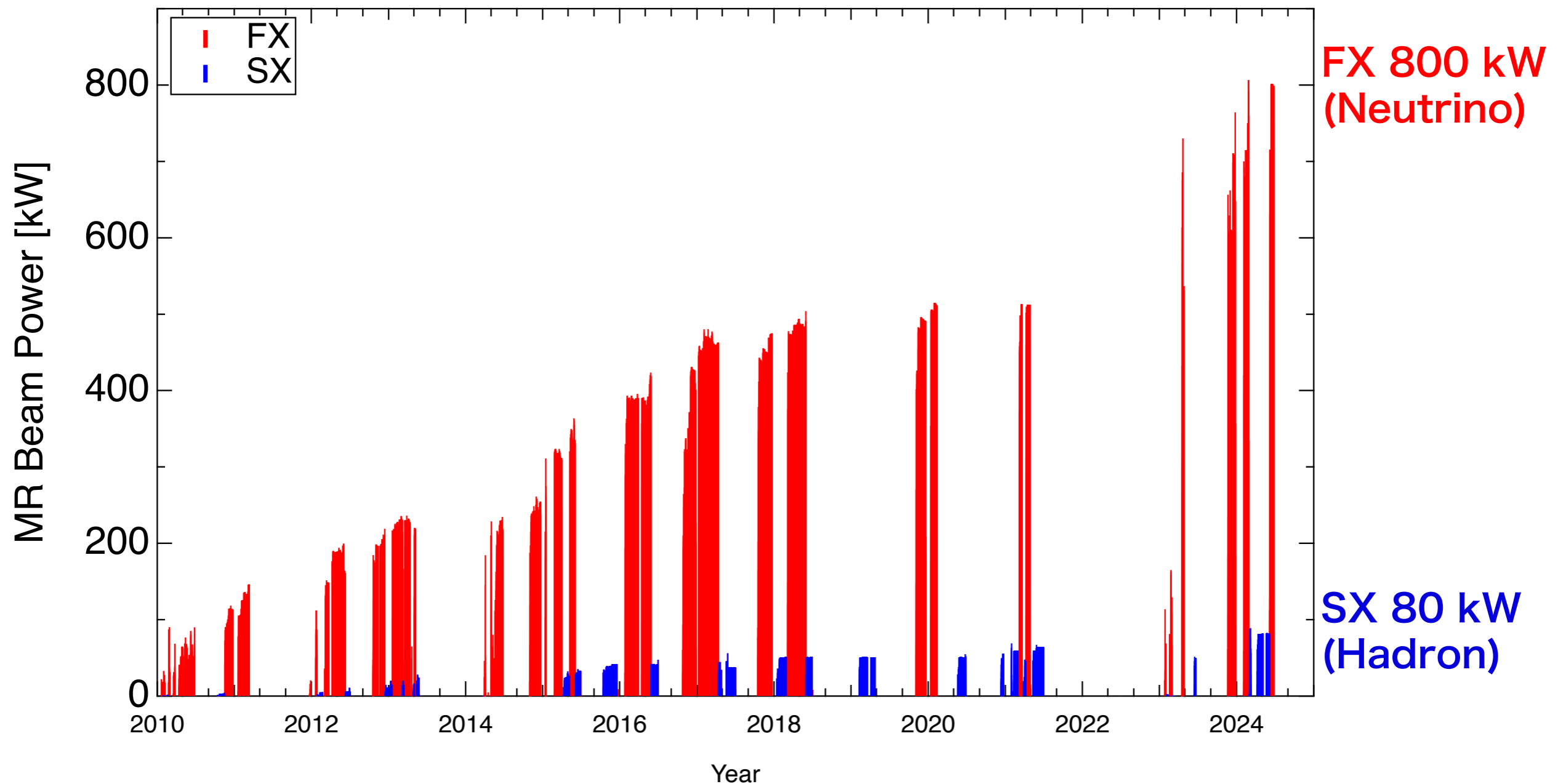
J-PARC MR



The main ring synchrotron (MR) provides high power proton beams for the neutrino and hadron experiments.

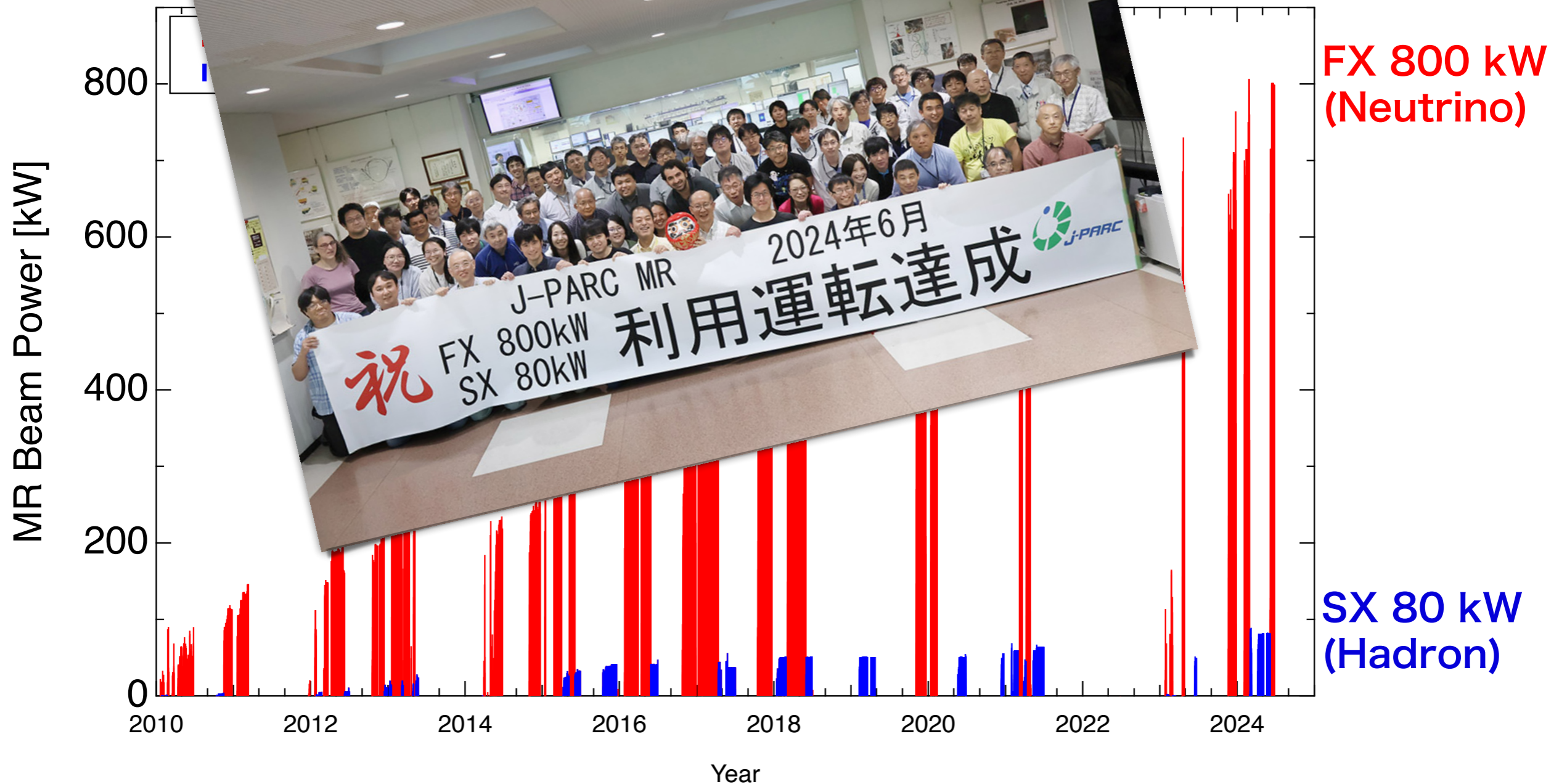
MR beam power history

To accumulate the statistics of neutrinos and hadrons, stable beam operation with higher power is required.



MR beam power history

To accumulate the statistics for neutrino oscillation experiments, a stable beam of 800 kW of muons (hadrons), is required.



FX 1.3 MW upgrade plan

$$\text{Power} = \text{Energy}(30 \text{ GeV}) \times \text{Number of protons} / \text{Cycle time}$$

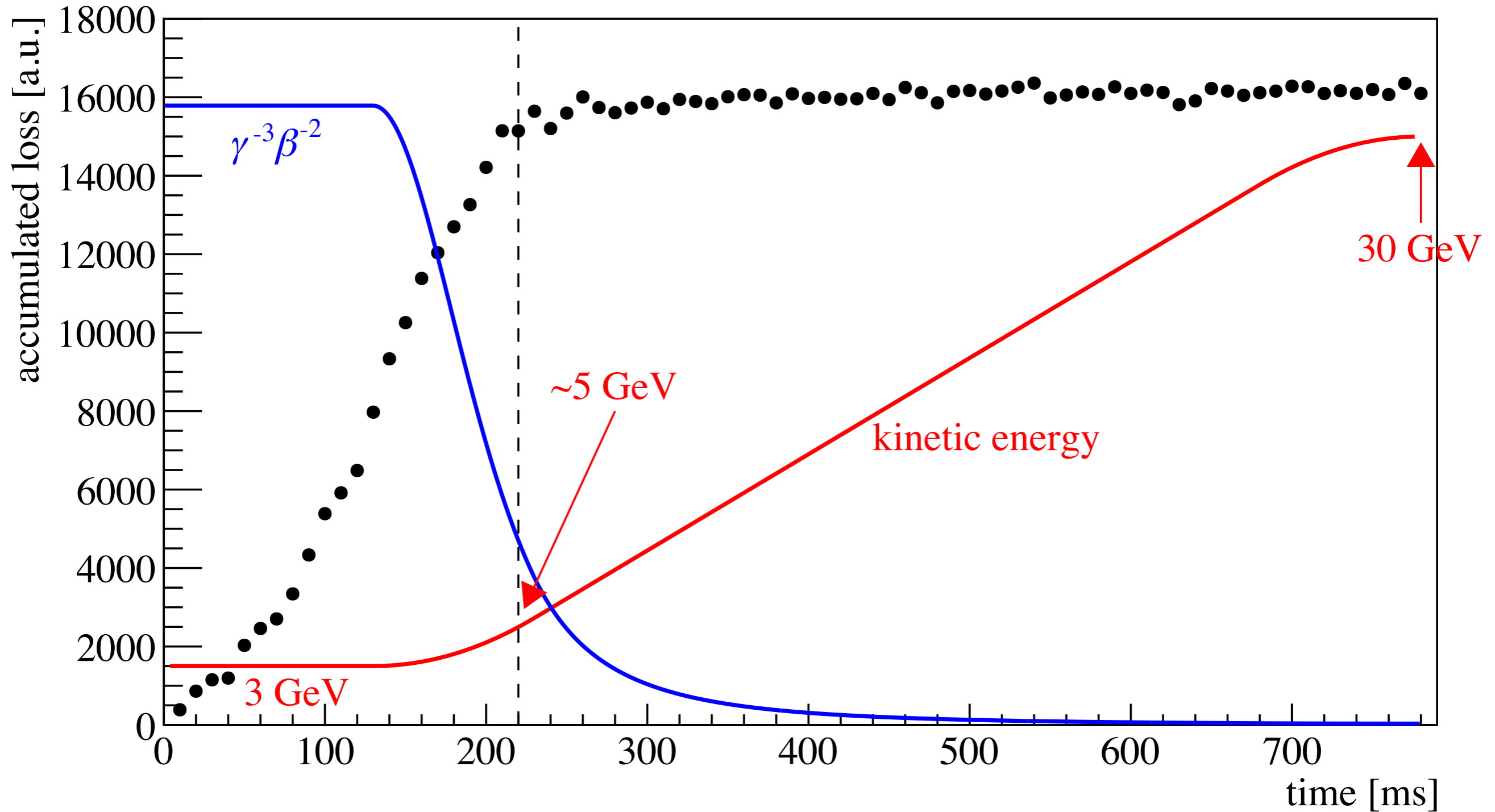
JFY2021	515 kW	2.66×10^{14} ppp	2.48 s
	Long-term shutdown for faster cycling		
Present	800 kW	2.3×10^{14} ppp	1.36 s
Future	1300 kW	3.3×10^{14} ppp	1.16 s

ppp ... protons per pulse

To increase the beam intensity, we should

- Upgrade the RF system
- **Reduce beam loss** ← **today's talk**
- (• Improve the localization quality of beam loss)

Beam loss timing

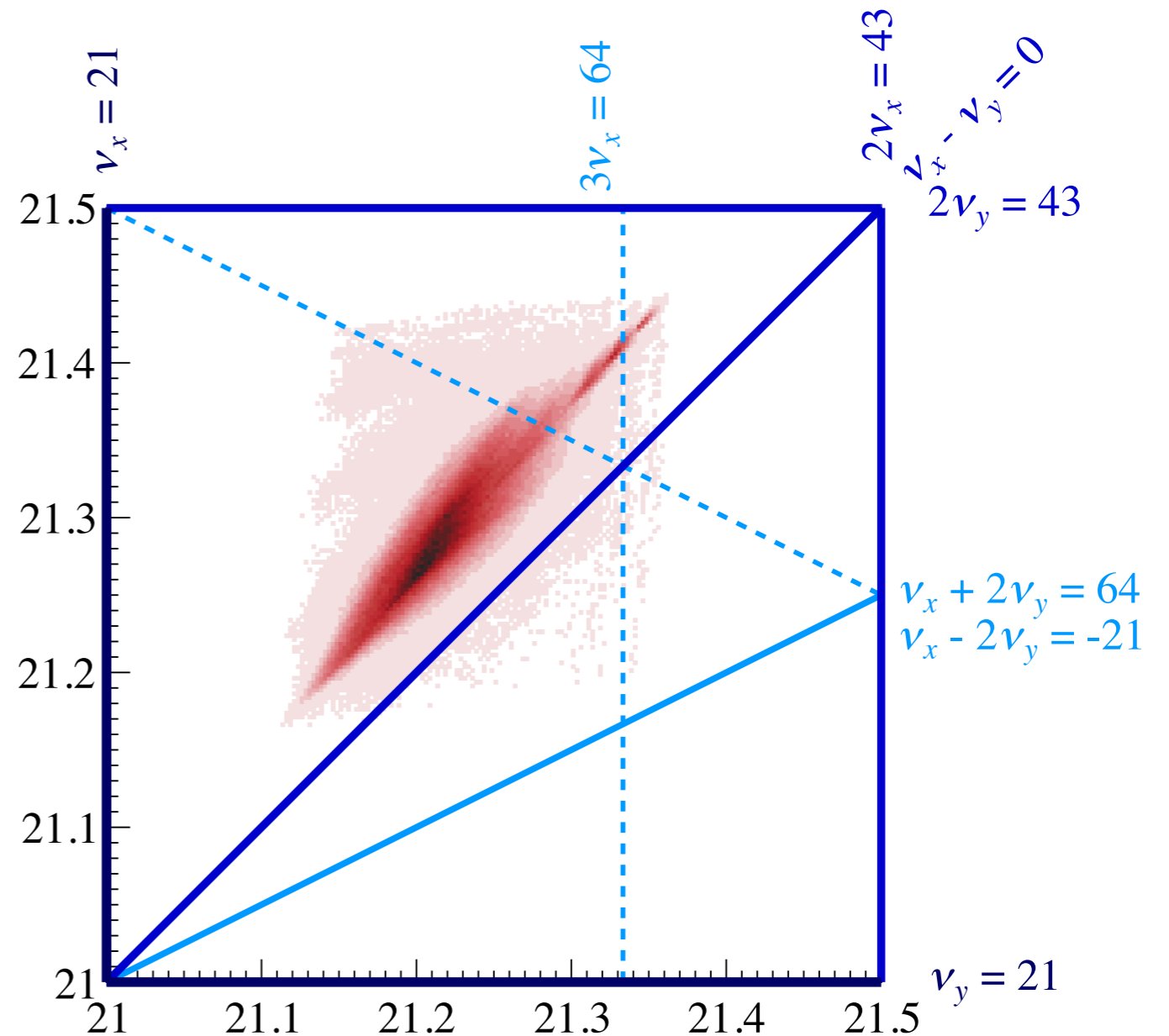


Tune spread and resonances

The working point is set not to cross low order resonances.

Beams are crossing the nonstructure resonances $3\nu_x = 64$ and $\nu_x + 2\nu_y = 64$ driven by sextupole fields.

The tune spread is also close to the differential resonance $\nu_x - \nu_y = 0$.



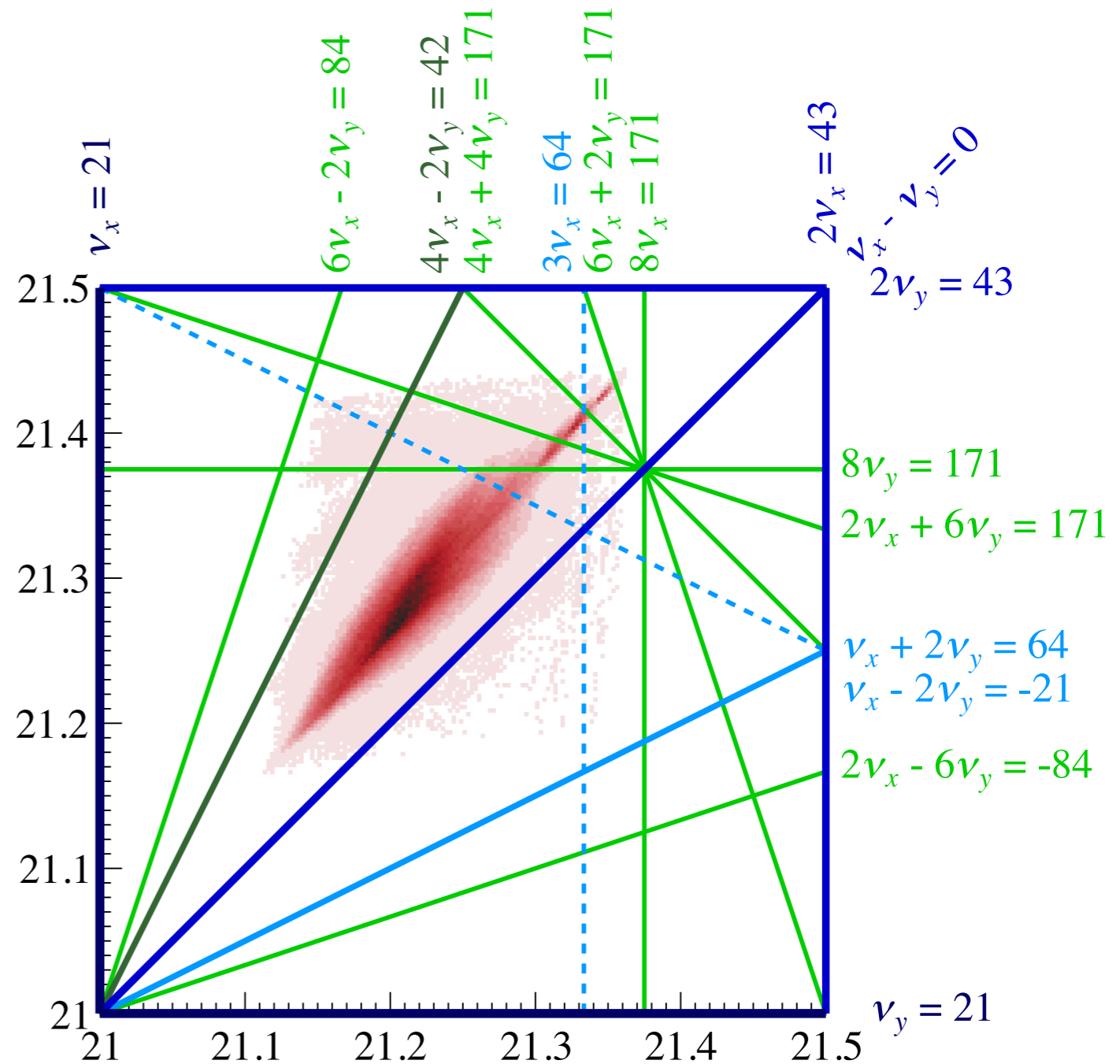
Beam intensity : 2.66×10^{14} ppp

Tune spread and resonances

8th-order structure resonances driven by space charge cross the tune spread.

Space charge enhances the differential resonance as $2\nu_x - 2\nu_y = 0$.

Nonstructure resonances driven by space charge also cross tune spread (not drawn).



Beam intensity : 2.66×10^{14} ppp

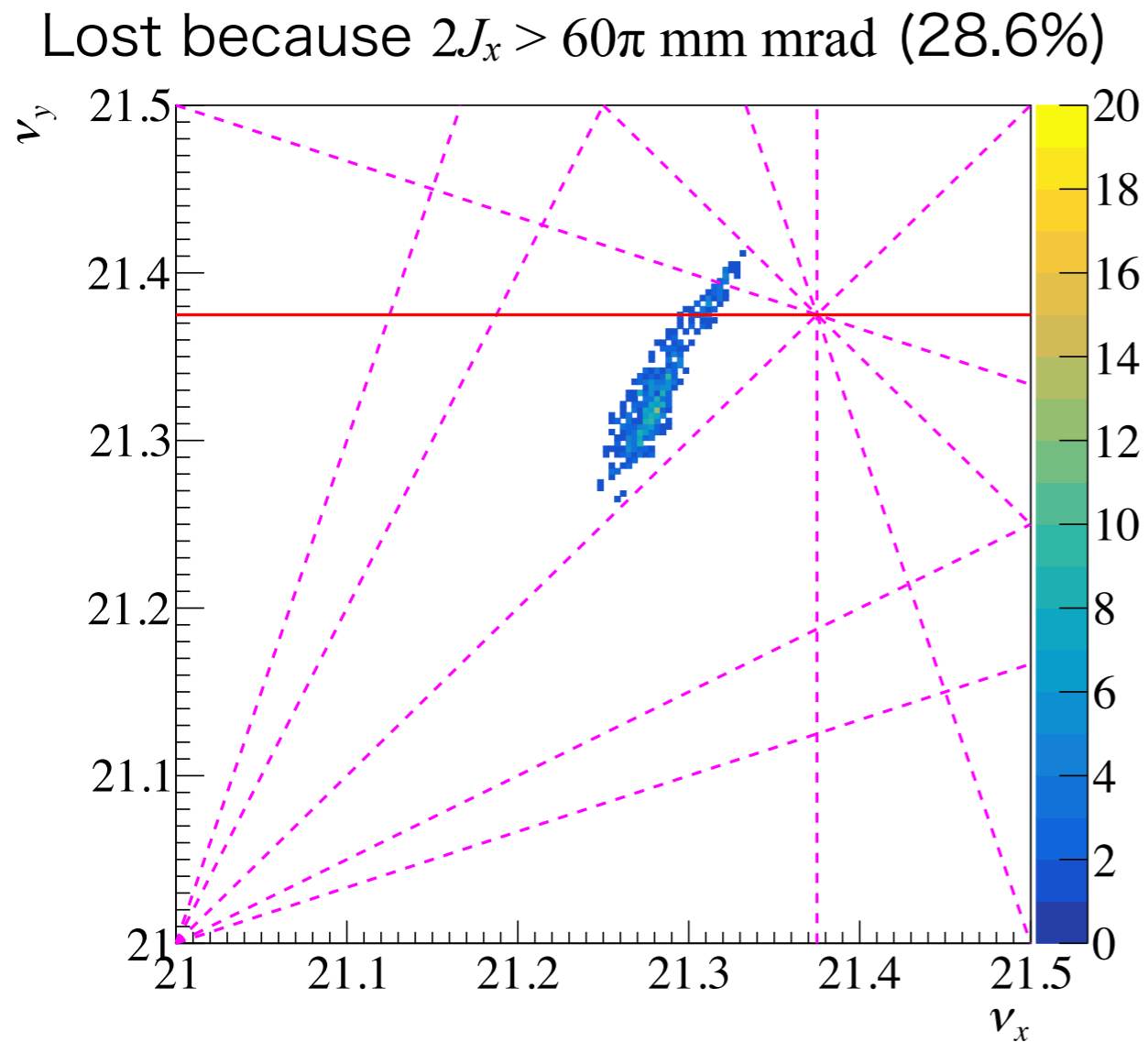
Summary of resonances in FX operation

	Space charge	Magnets
Structure	$8\nu_y = 171, 2\nu_x + 6\nu_y = 171, \dots$ <ul style="list-style-type: none"> • 8th order • cross tune spread $2\nu_x - 2\nu_y = 0$ <ul style="list-style-type: none"> • 4th order 	(far enough)
Nonstructure	$4\nu_y = 85, 2\nu_x + 2\nu_y = 85, \dots$ <ul style="list-style-type: none"> • 4th, 6th, ... order • cross tune spread 	$3\nu_x = 64, \nu_x + 2\nu_y = 64$ <ul style="list-style-type: none"> • 3rd order • cross tune spread $\nu_x - \nu_y = 0$ <ul style="list-style-type: none"> • 2nd order

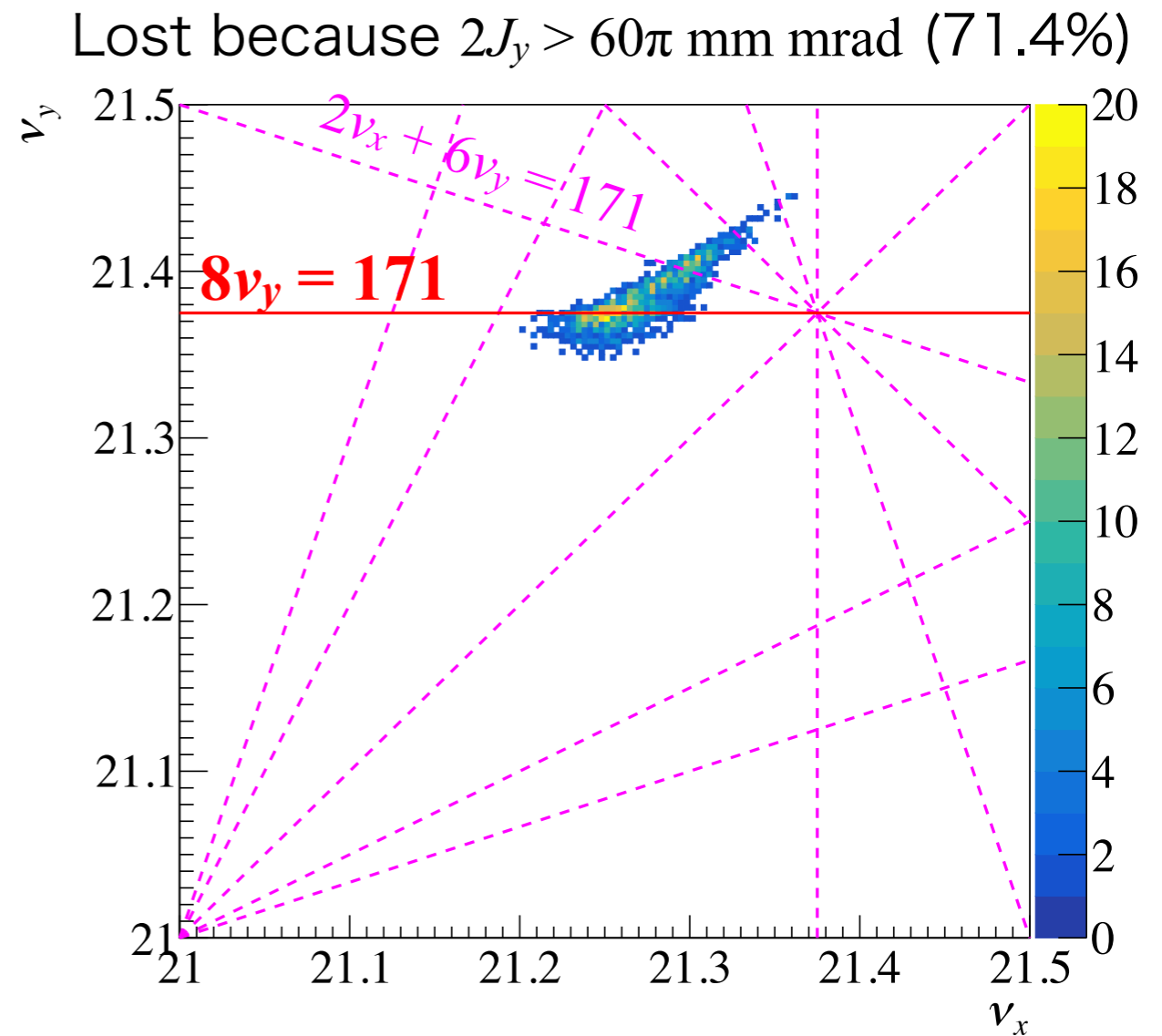
Summary of resonances in FX operation

	Space charge	Magnets
Structure	$8\nu_y = 171, 2\nu_x + 6\nu_y = 171, \dots$ <ul style="list-style-type: none"> • 8th order • cross tune spread <p><u>T. Yasui and Y. Kurimoto, PRAB 25, 121001 (2022)</u></p> $\nu_x - \nu_y = 0$ <ul style="list-style-type: none"> • 4th order 	<p>(far enough)</p>
Nonstructure	$4\nu_y = 85, 2\nu_x + 2\nu_y = 85, \dots$ <ul style="list-style-type: none"> • 4th, 6th, ... order • cross tune spread 	$3\nu_x = 64, \nu_x + 2\nu_y = 64$ <ul style="list-style-type: none"> • 3rd order • cross tune spread $\nu_x - \nu_y = 0$ <ul style="list-style-type: none"> • 2nd order

Tunes of lost particles (2.5D PIC simulation)



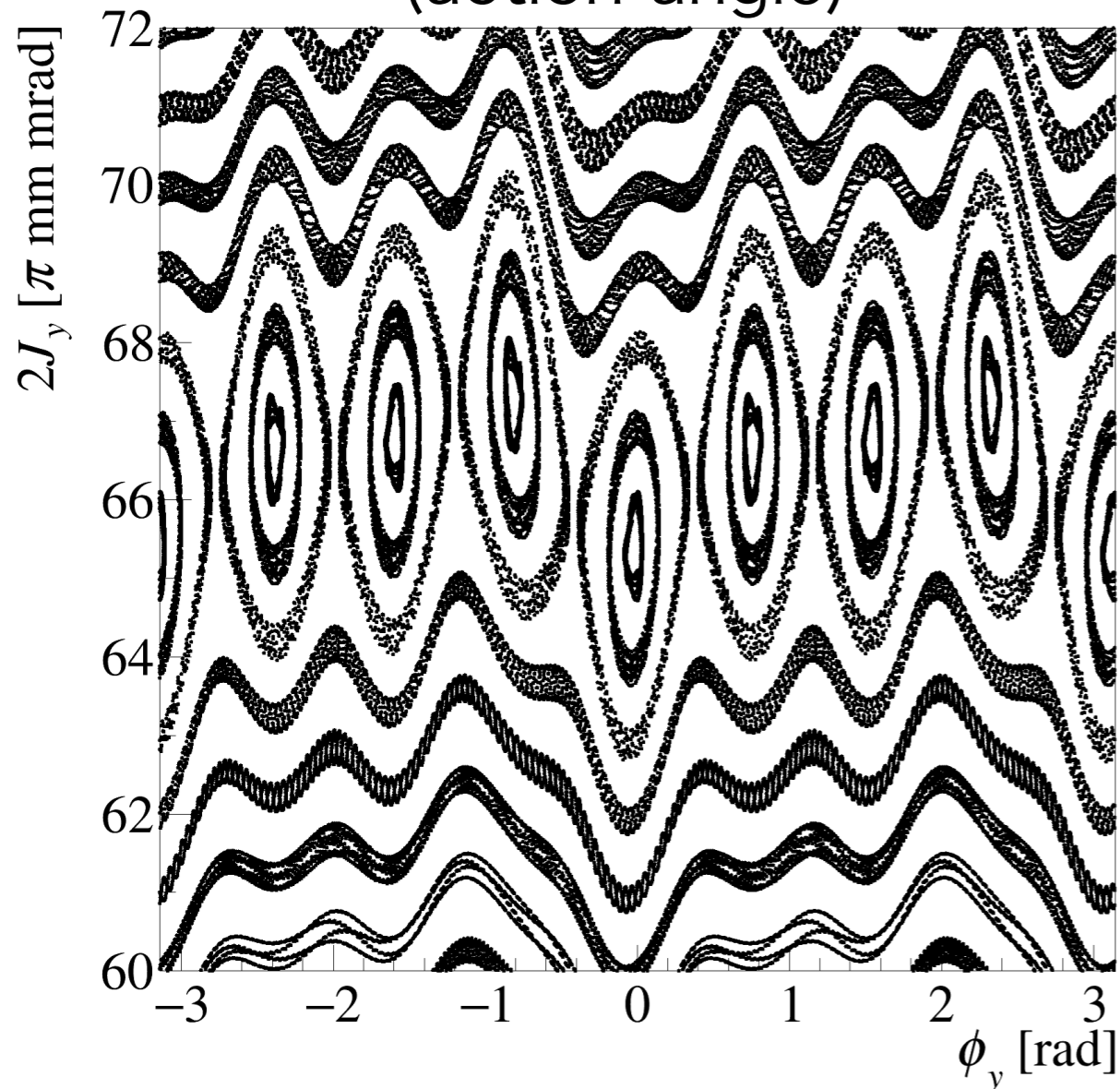
No clear relation
with resonances



Many particles are lost
around the resonance $8v_y = 171$.

Vertical Poincaré map (2D simulation)

Vertical Poincaré map
(action-angle)



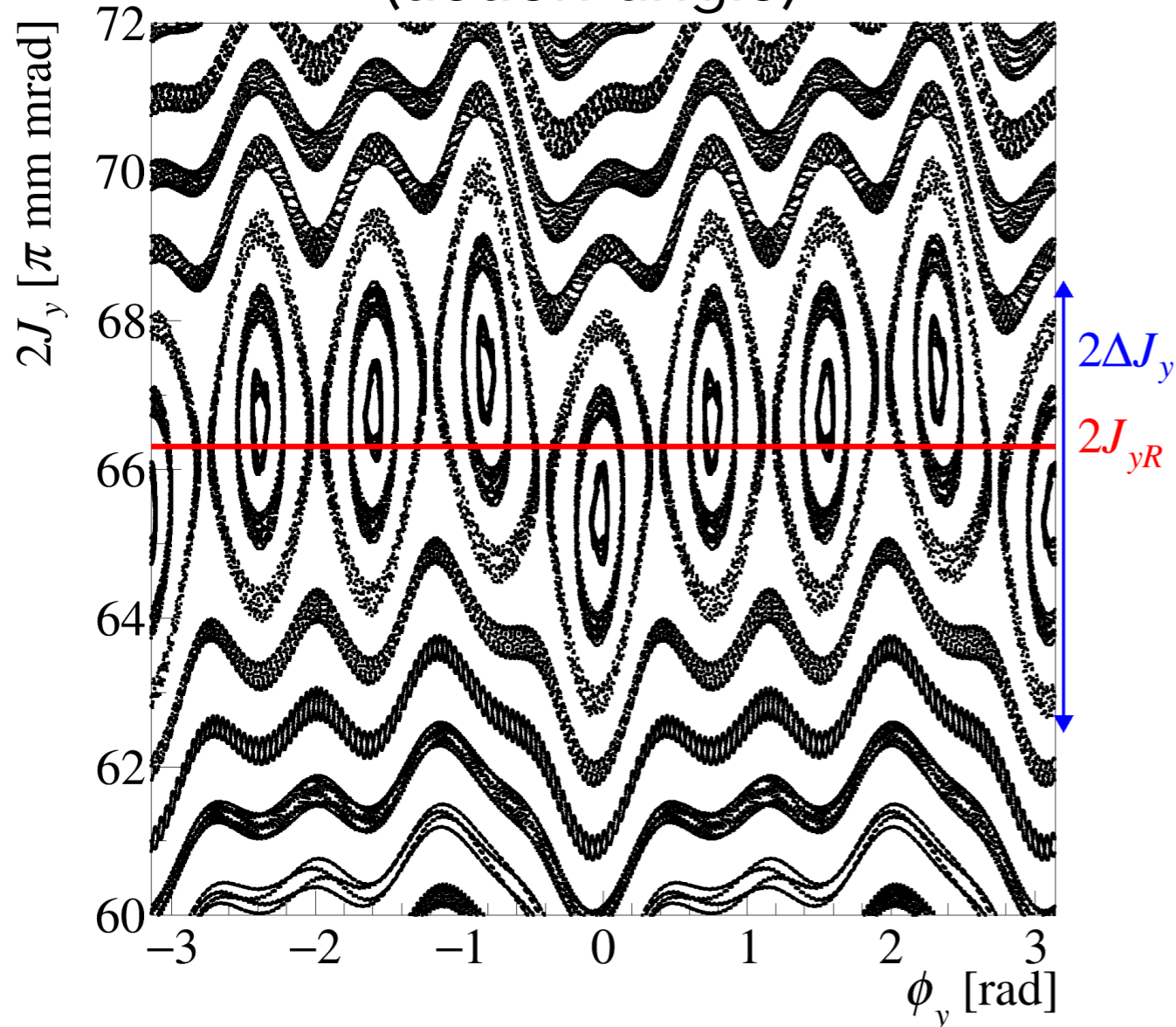
Simulation conditions:

- Bassetti-Erskine formula
(fields of 2D Gaussian beam)
- $\lambda = \lambda_{\max}$
- $z = \delta = 0$
- $J_x = 0$ (initial)

**Clear 8 resonance islands
can be seen.**

Vertical Poincaré map (2D simulation)

Vertical Poincaré map
(action-angle)



Center $2J_{yR}$ and width $2\Delta J_y$ of resonances can be calculated analytically assuming a 2D-Gaussian distribution.

Analytical results:

$$(J_x = 0, z = \delta = 0, \lambda = \lambda_{\max})$$

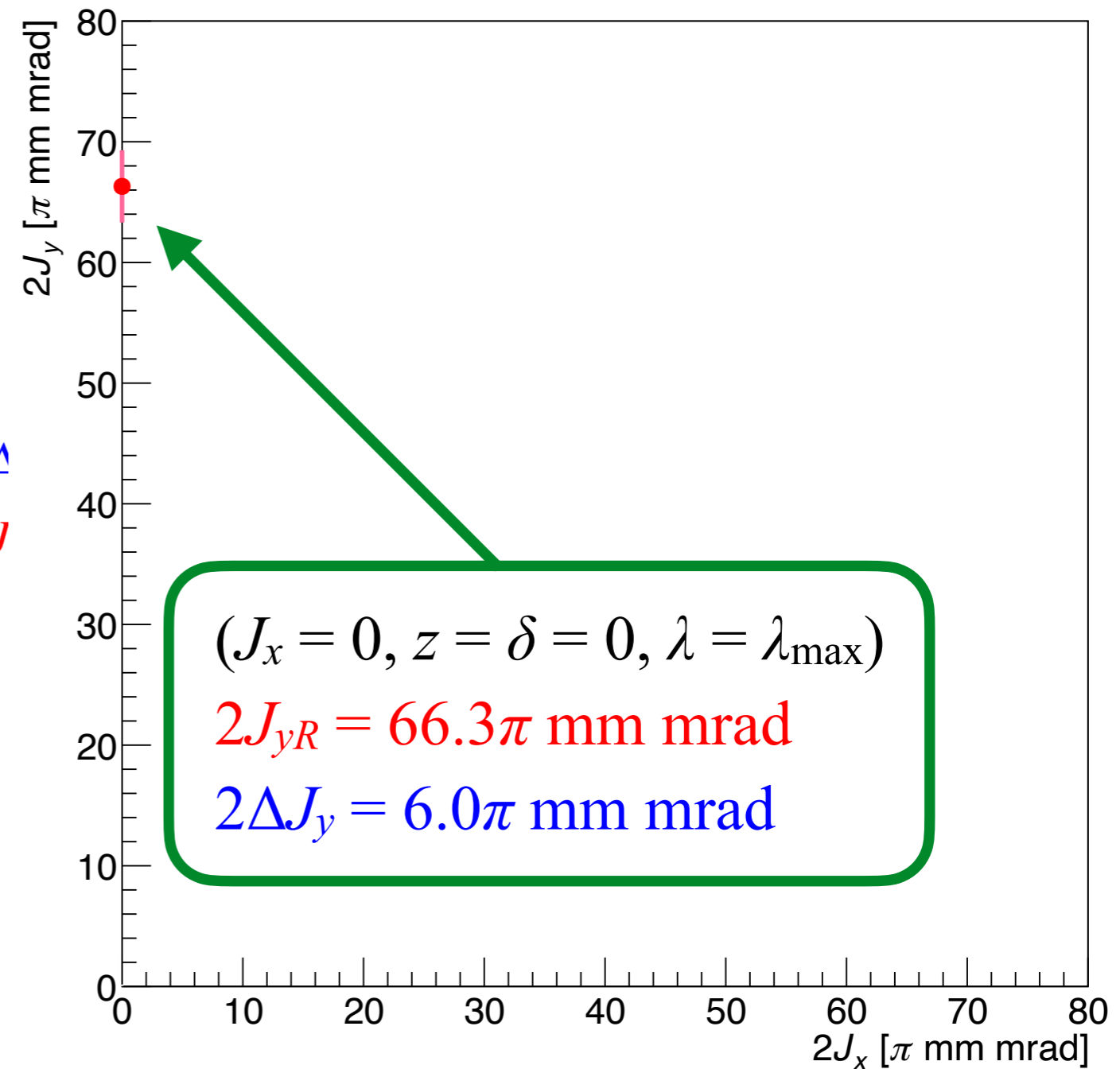
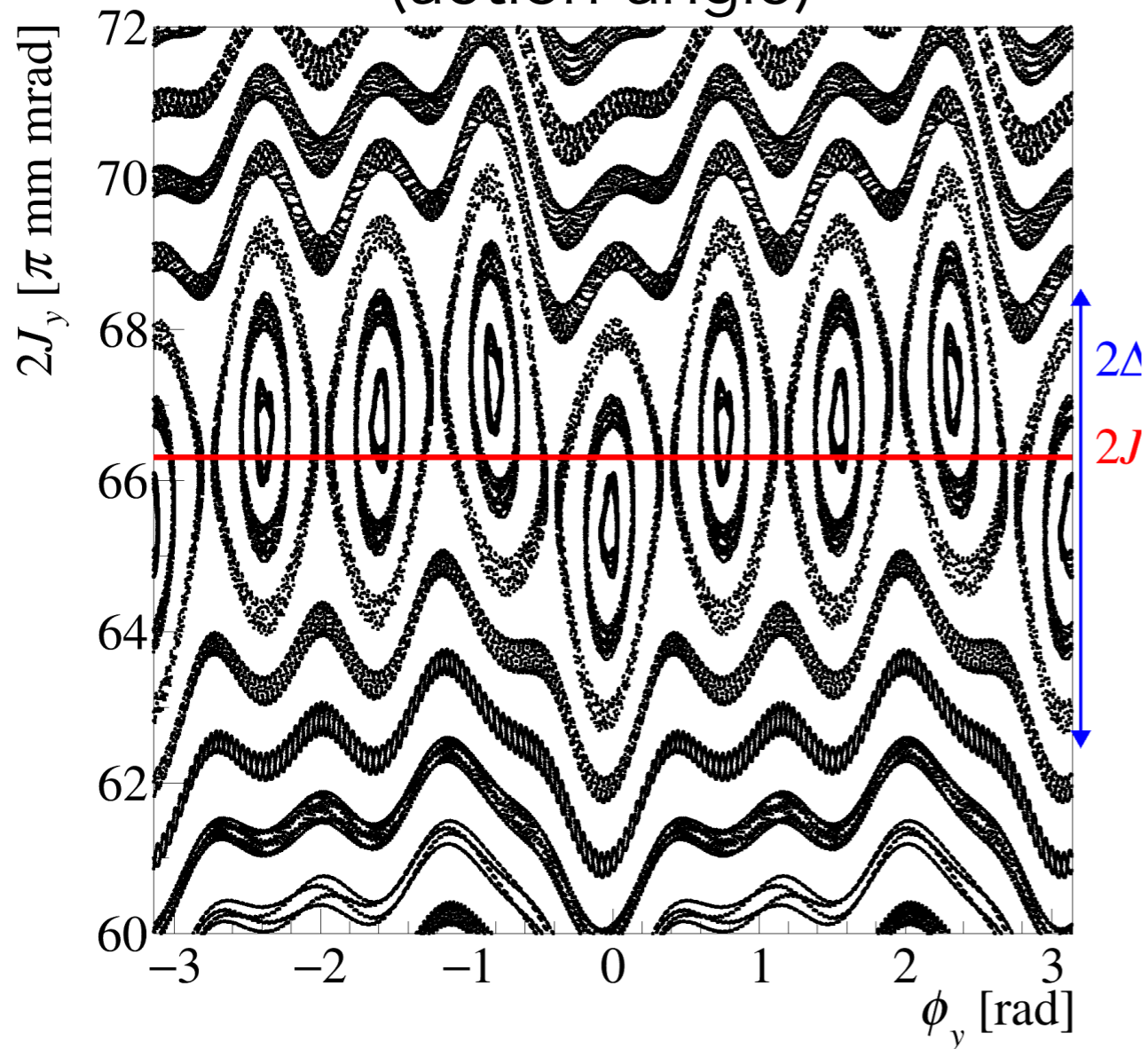
$$2J_{yR} = 66.3\pi \text{ mm mrad}$$

$$2\Delta J_y = 6.0\pi \text{ mm mrad}$$

Well matched!

Resonance region

Vertical Poincaré map
(action-angle)



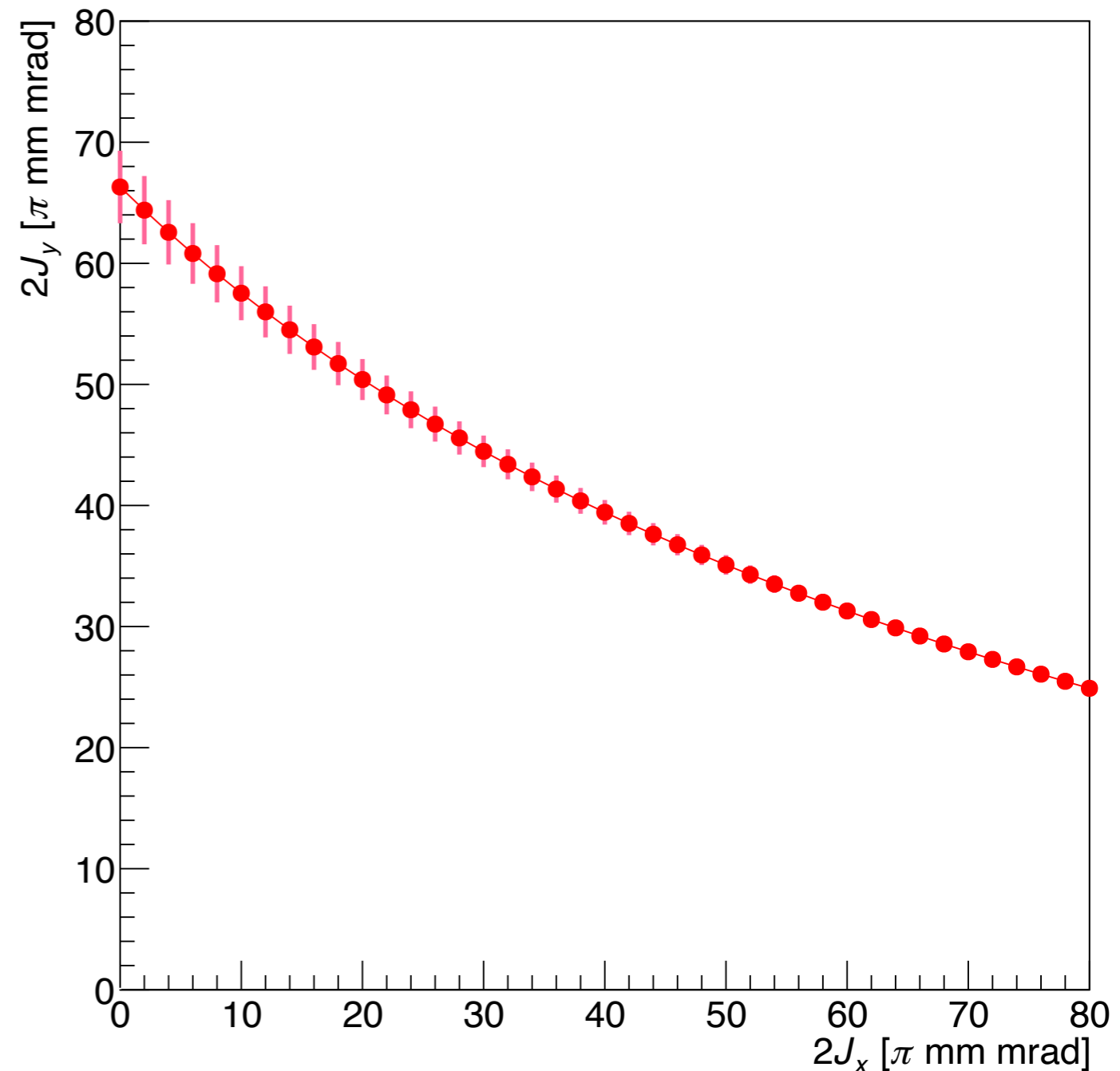
Resonance region

$2J_{yR}$ and $2\Delta J_y$ can also be calculated for $J_x > 0$.

The same process can be applied for $2\nu_x + 6\nu_y = 171$.
($J_y - 3J_x = \text{const.}$)

Solutions of other 8th-order structure resonances were out of plot range.

This is why $8\nu_y = 171$ and $2\nu_x + 6\nu_y = 171$ are loss sources.



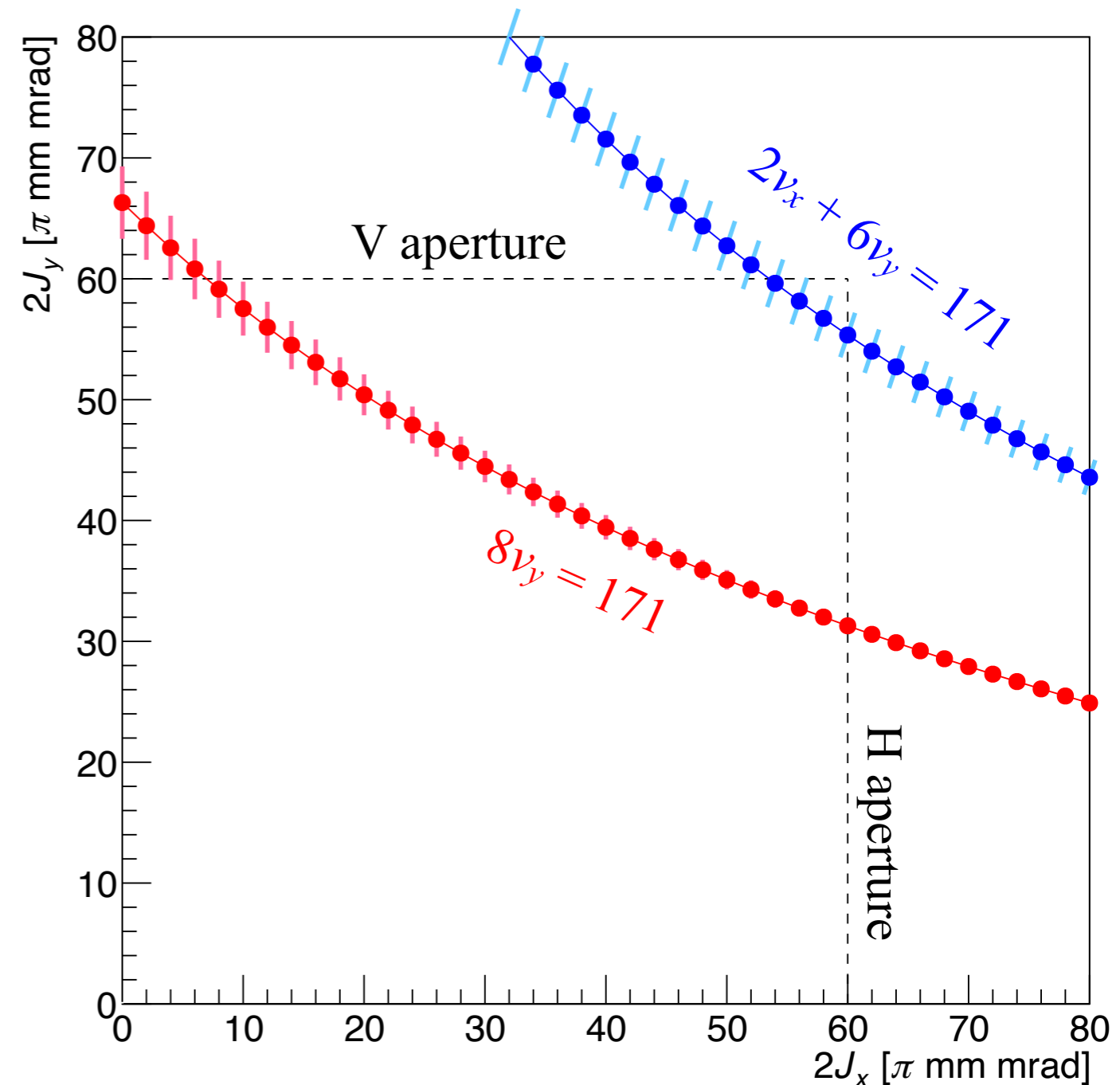
Resonance region

$2J_{yR}$ and $2\Delta J_y$ can also be calculated for $J_x > 0$.

The same process can be applied for $2\nu_x + 6\nu_y = 171$.
($J_y - 3J_x = \text{const.}$)

Solutions of other 8th-order structure resonances were out of plot range.

This is why $8\nu_y = 171$ and $2\nu_x + 6\nu_y = 171$ are loss sources.



Strategy for lower-loss operation

If we change the working point to avoid $\delta\nu_y = 171$, the tune spread will cross other lower-order resonances.

If we use corrector magnets, we need at least six 16-pole magnets.

$$U_{0,8,171} e^{i\xi_{0,8,171}} = \frac{\lambda r_0}{\pi \gamma^3 \beta^2} \oint ds e^{i[8\chi_y - \underbrace{(8\nu_y - 171)}_{\text{fixed}}]\theta} \int_0^\infty dq \frac{e^{-\frac{J_x \beta_x}{2\sigma_x^2 + q} - \frac{J_y \beta_y}{2\sigma_y^2 + q}} I_0\left(\frac{J_x \beta_x}{2\sigma_x^2 + q}\right) I_4\left(\frac{J_y \beta_y}{2\sigma_y^2 + q}\right)}{\sqrt{2\sigma_x^2 + q} \sqrt{2\sigma_y^2 + q}}$$

phase advance

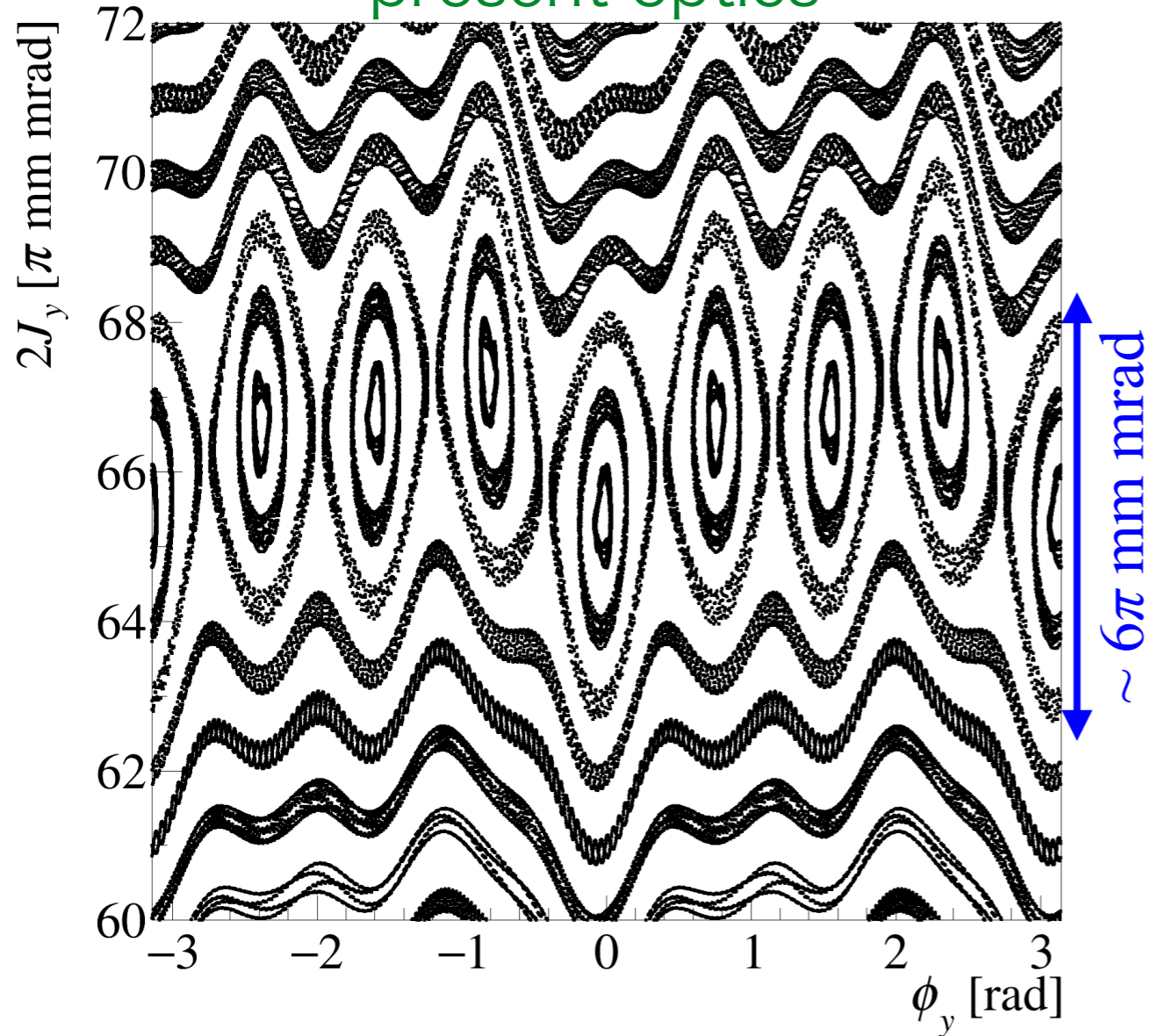
$$\chi_y(s) = \int_0^s \frac{ds}{\beta_y} \quad \dots \text{changeable}$$

$$\chi_y(C) = 2\pi\nu_y \quad \dots \text{fixed}$$

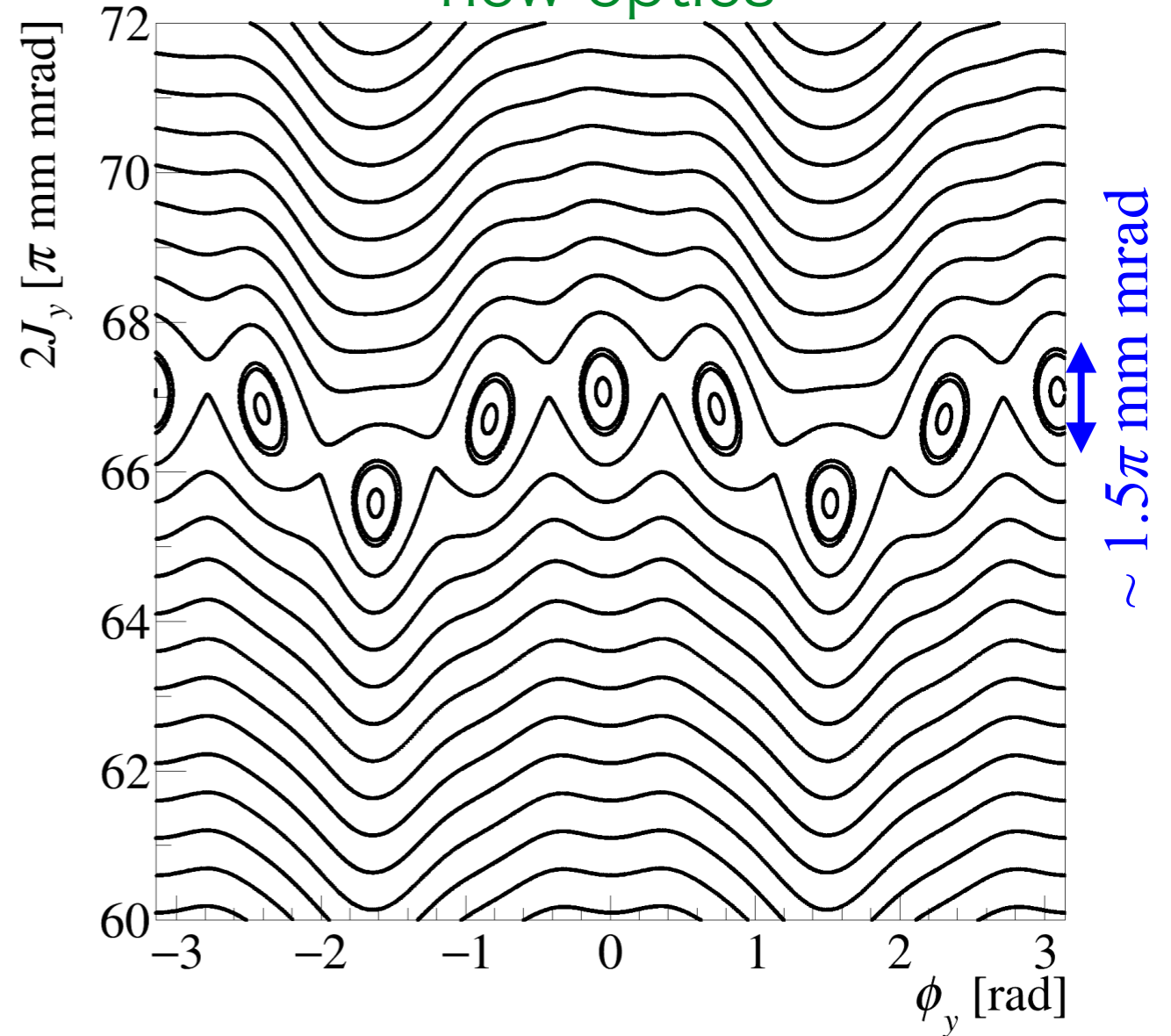
We consider a new beam optics to suppress $\delta\nu_y = 171$, but maintaining the working point.

Vertical Poincaré map (2D simulation)

present optics



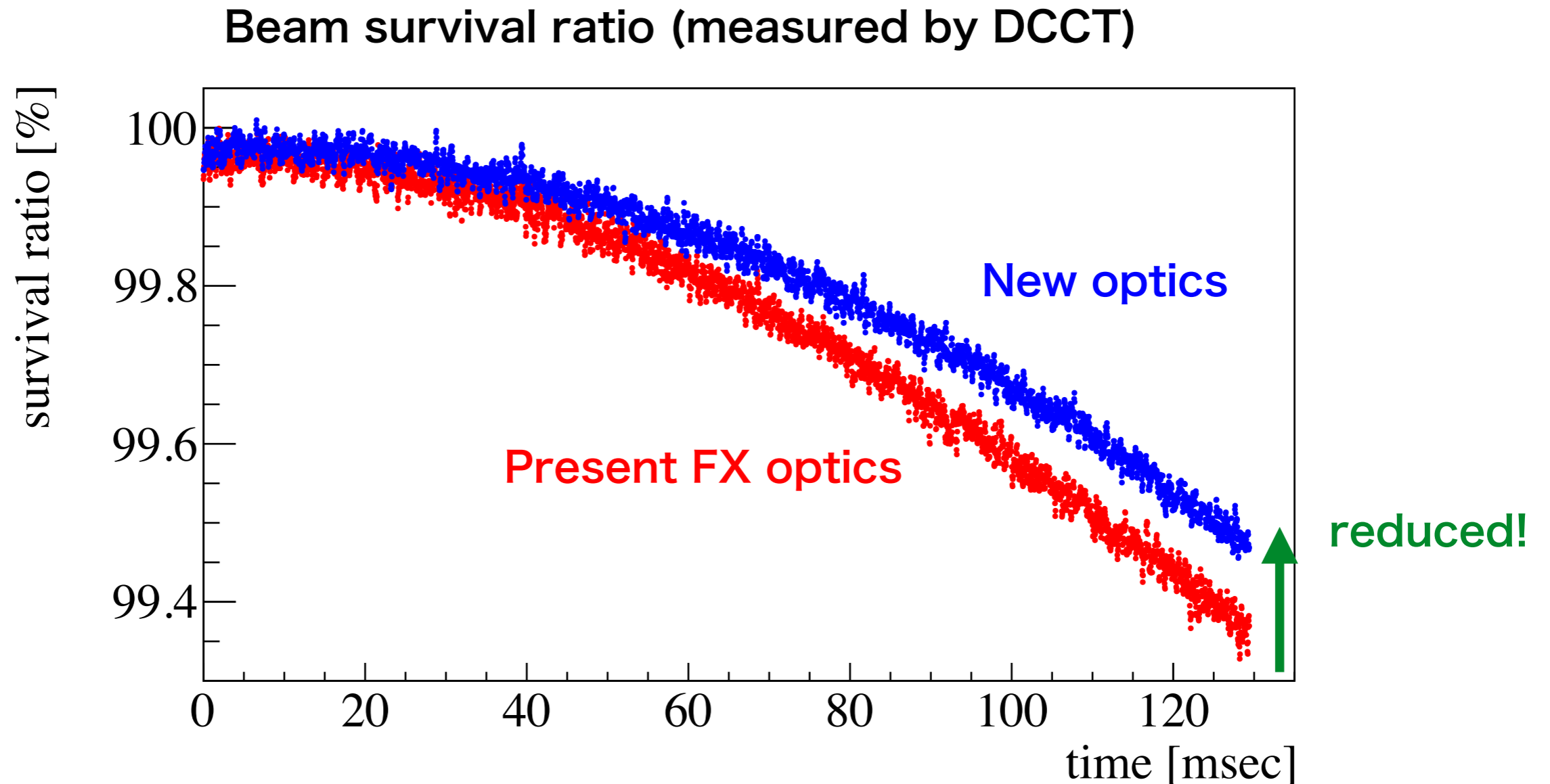
new optics



The resonance $8\nu_y = 171$ is weakened!

Beam loss measurement

We measured beam losses with the present and new optics.

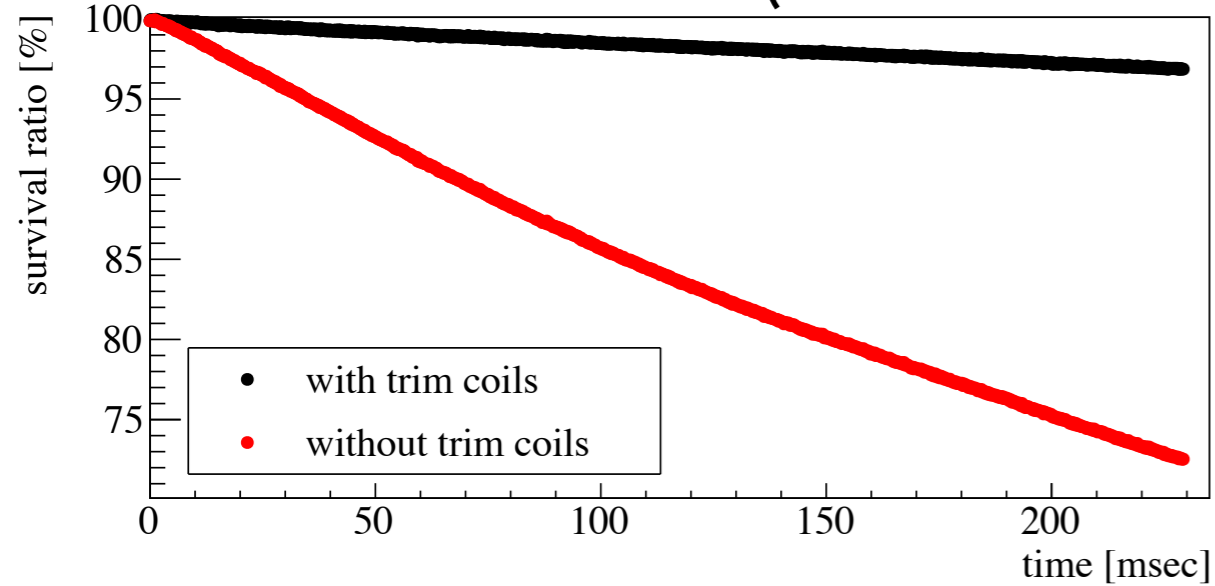


Summary of resonances in FX operation

	Space charge	Magnets
Structure	$8\nu_y = 171, 2\nu_x + 6\nu_y = 171, \dots$ <ul style="list-style-type: none"> • 8th order • cross tune spread $2\nu_x - 2\nu_y = 0$ <ul style="list-style-type: none"> • 4th order 	(far enough)
Nonstructure	$4\nu_y = 85, 2\nu_x + 2\nu_y = 85, \dots$ <ul style="list-style-type: none"> • 4th, 6th, ... order • cross tune spread 	$3\nu_x = 64, \nu_x + 2\nu_y = 64$ <ul style="list-style-type: none"> • 3rd order • cross tune spread $\nu_x - \nu_y = 0$ <ul style="list-style-type: none"> • 2nd order

3rd order nonstr. resonances

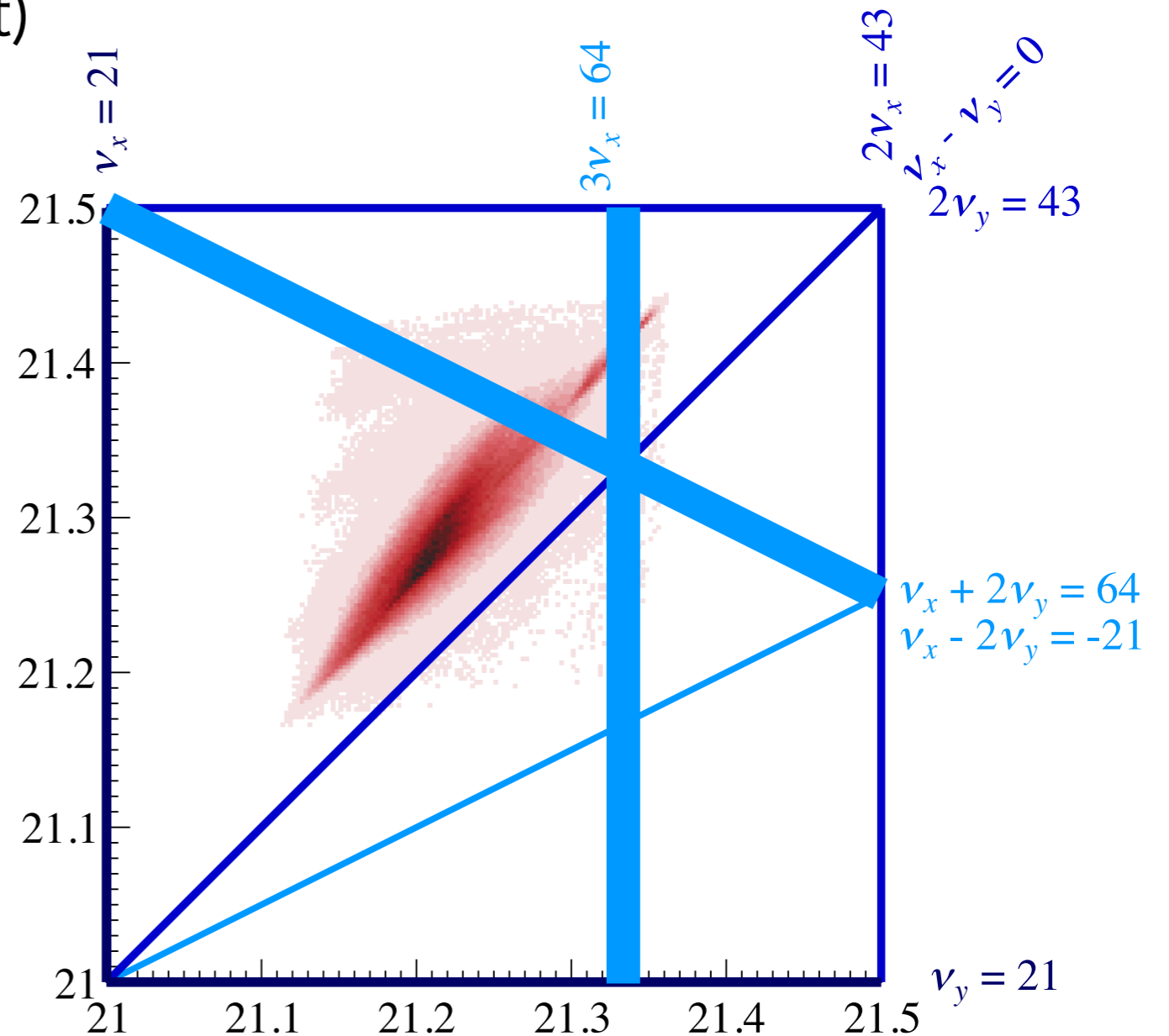
Beam survival ratio (measurement)



Nonstructure resonances

$$3\nu_x = 64 \text{ and } \nu_x + 2\nu_y = 64$$

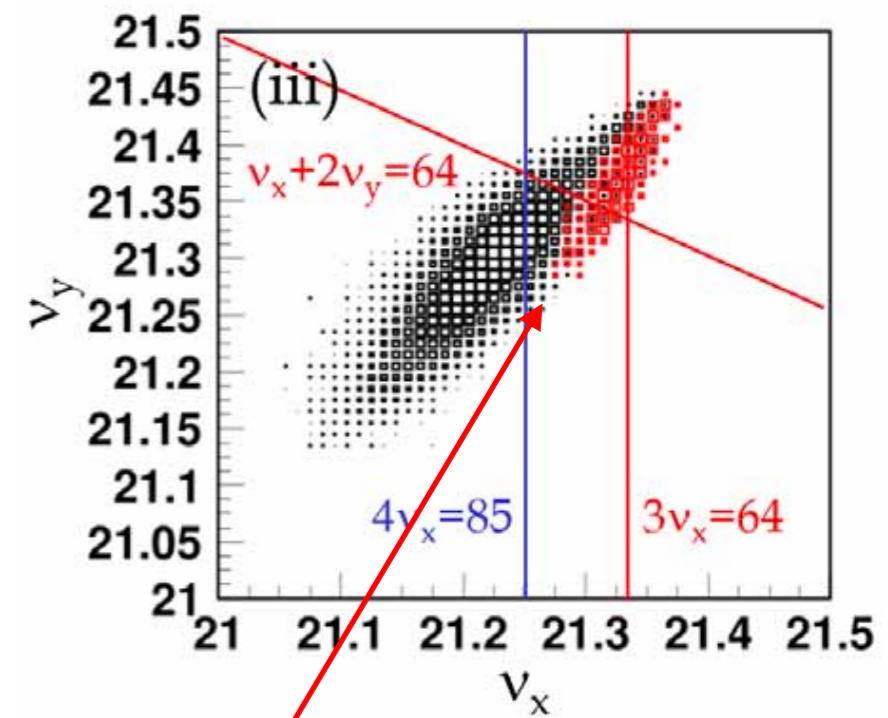
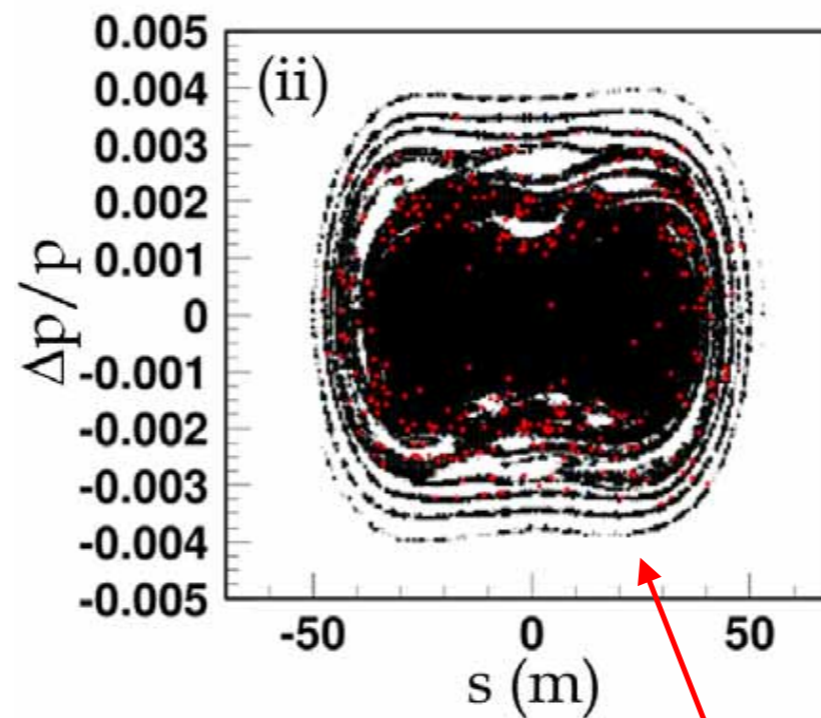
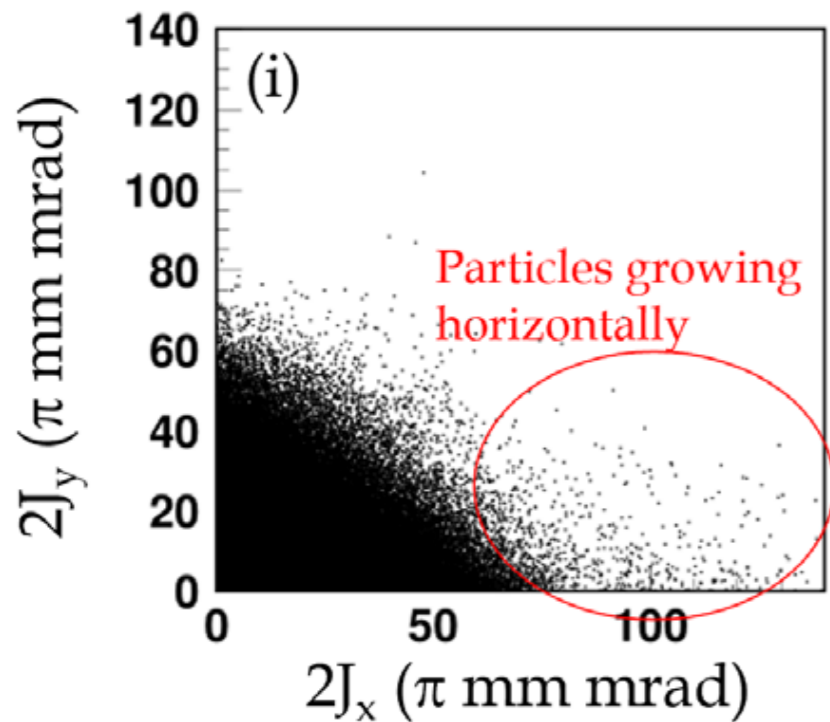
are simultaneously “corrected”
by using 4 trim coils of the
sextupole magnets.



Status of lost particles

Tracking simulation including magnet imperfections suggest that off-momentum particles grow horizontally and are lost.

Even after applying trim coils, the resonances $3\nu_x = 64$ and $\nu_x + 2\nu_y = 64$ affect off-momentum particles.



Red: high horizontal action

Resonance width of

$$3\nu_x = 64, \nu_x + 2\nu_y = 64$$

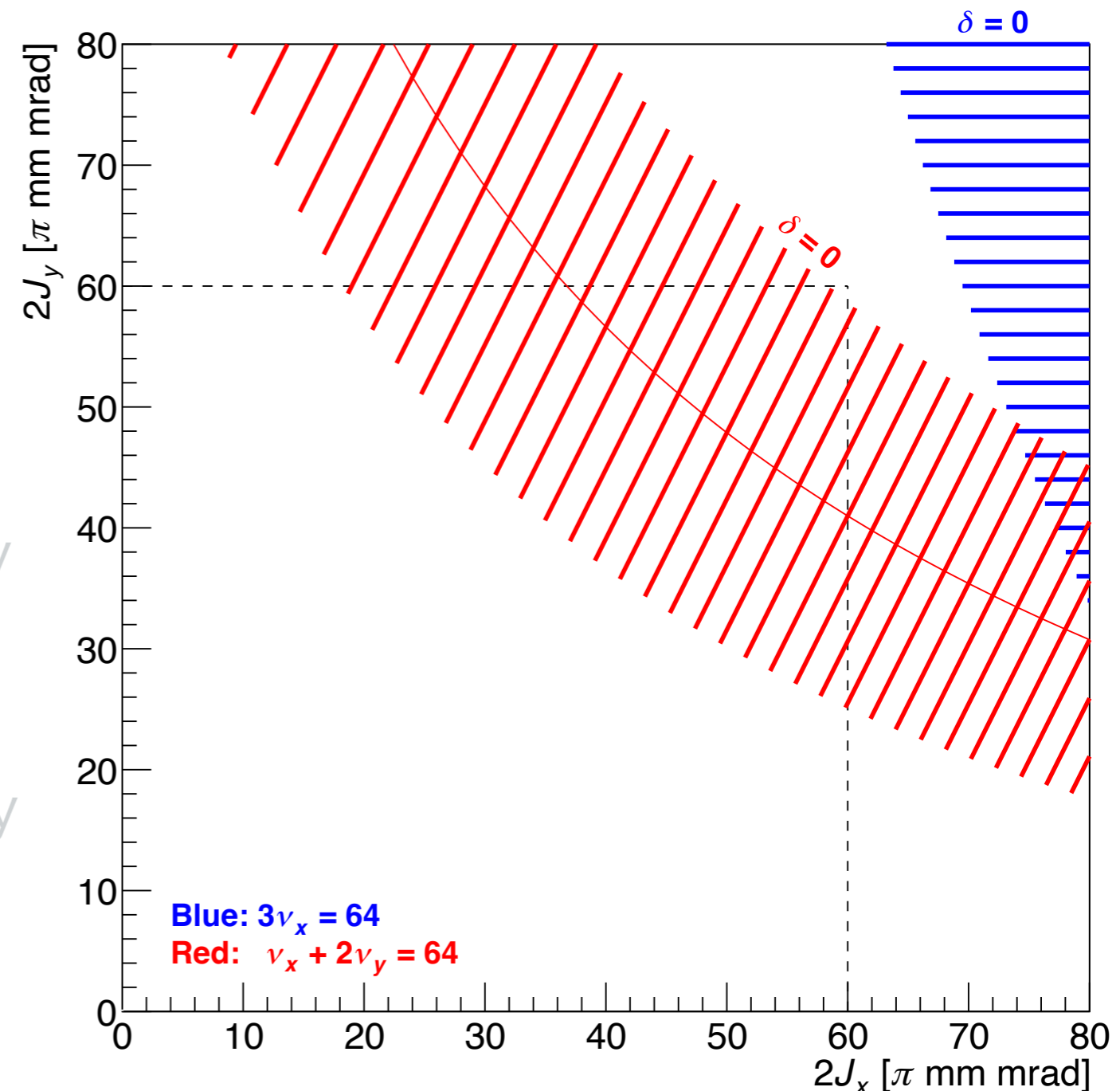
without trim coils

We estimated the resonance widths by the current applying to the 4 trim coils.

In MR, $|\delta| \leq 0.004$.

Negative- δ particles are strongly affected by the resonances.

The resonances are successfully suppressed by the trim coils, but their effects remain for negative- δ particles.



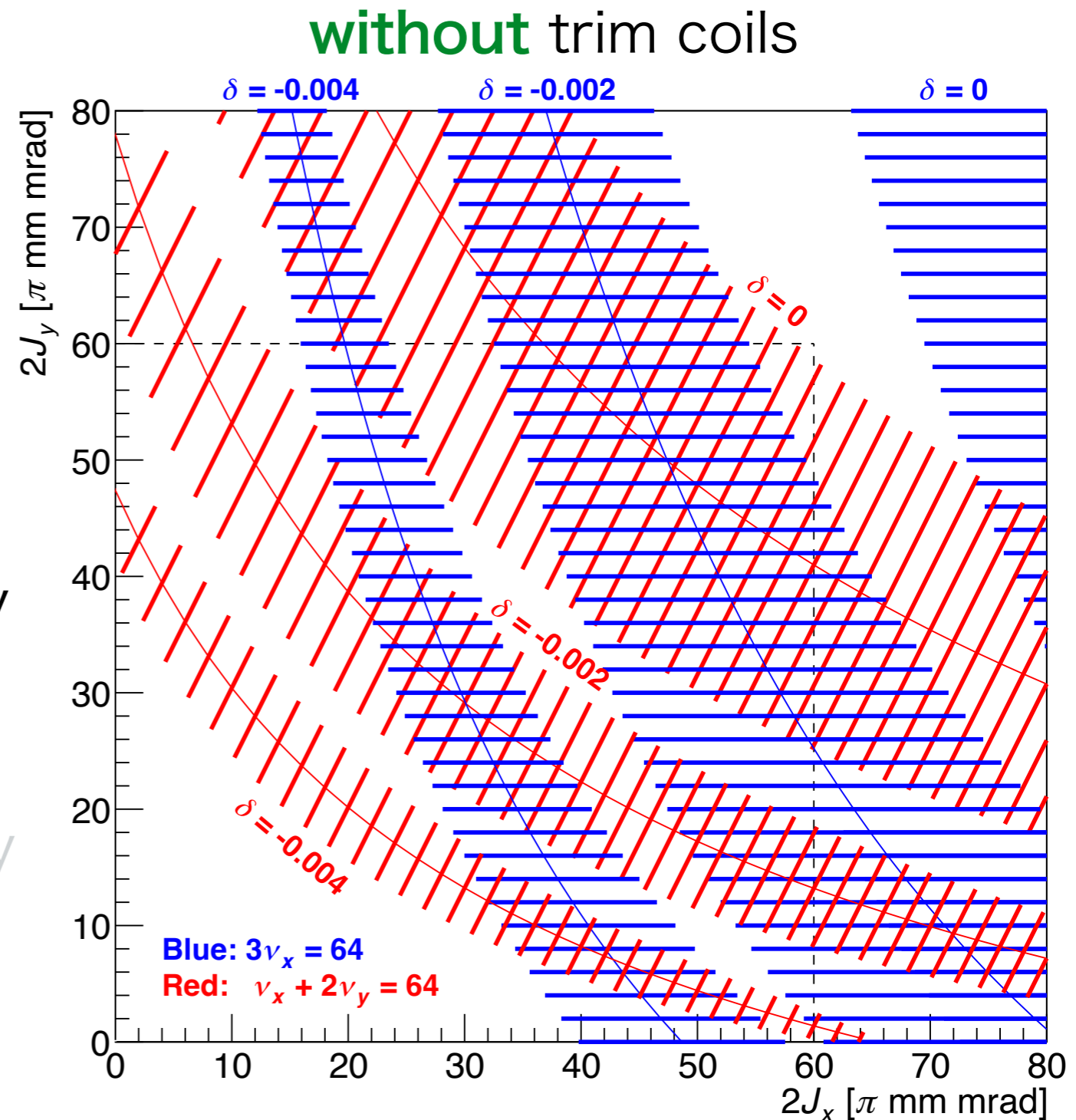
Resonance width of $3\nu_x = 64, \nu_x + 2\nu_y = 64$

We estimated the resonance widths by the current applying to the 4 trim coils.

In MR, $|\delta| \leq 0.004$.

Negative- δ particles are strongly affected by the resonances.

The resonances are successfully suppressed by the trim coils, but their effects remain for negative- δ particles.



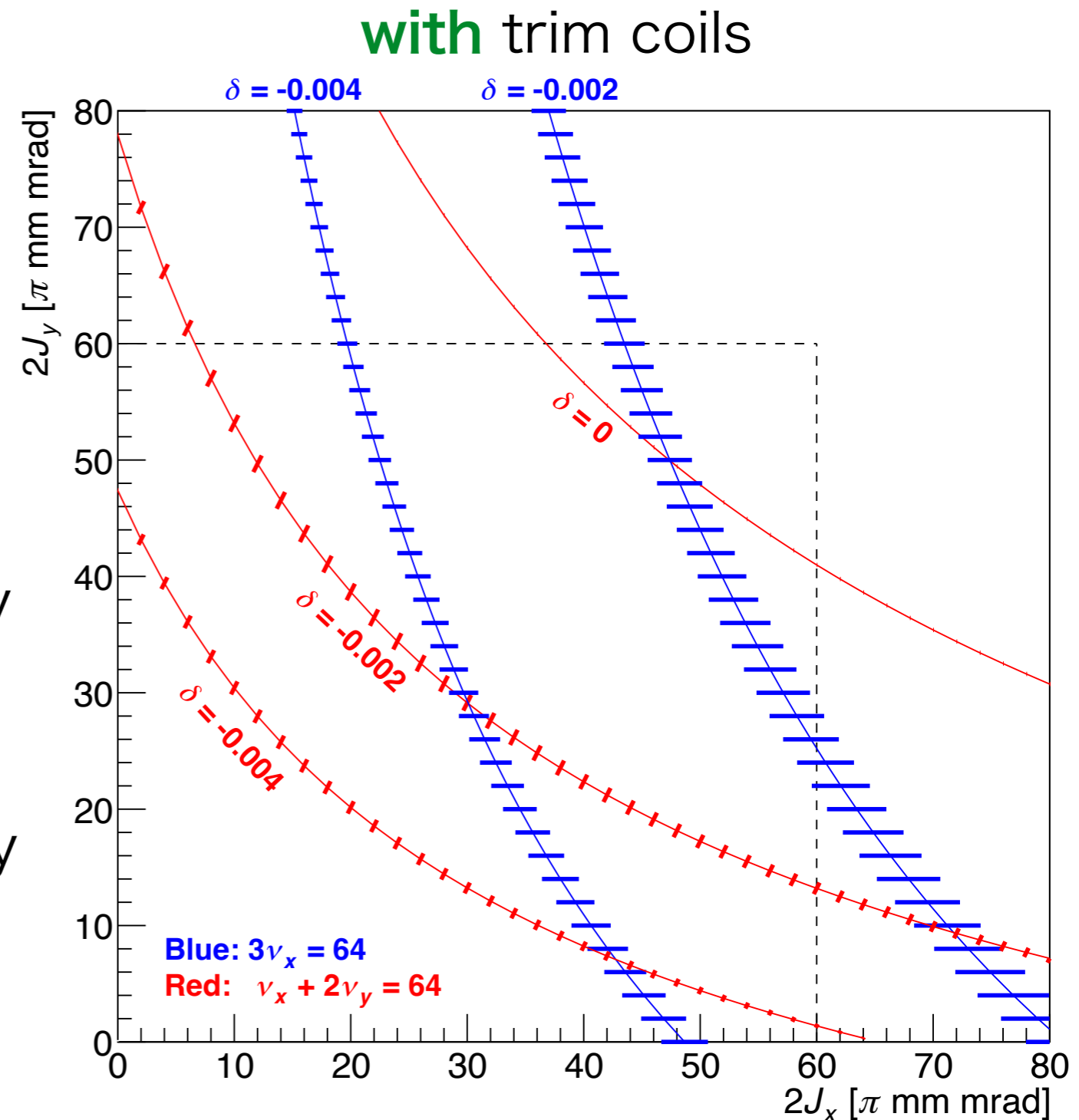
Resonance width of $3\nu_x = 64, \nu_x + 2\nu_y = 64$

We estimated the resonance widths by the current applying to the 4 trim coils.

In MR, $|\delta| \leq 0.004$.

Negative- δ particles are strongly affected by the resonances.

The resonances are successfully suppressed by the trim coils, but their effects remain for negative- δ particles.

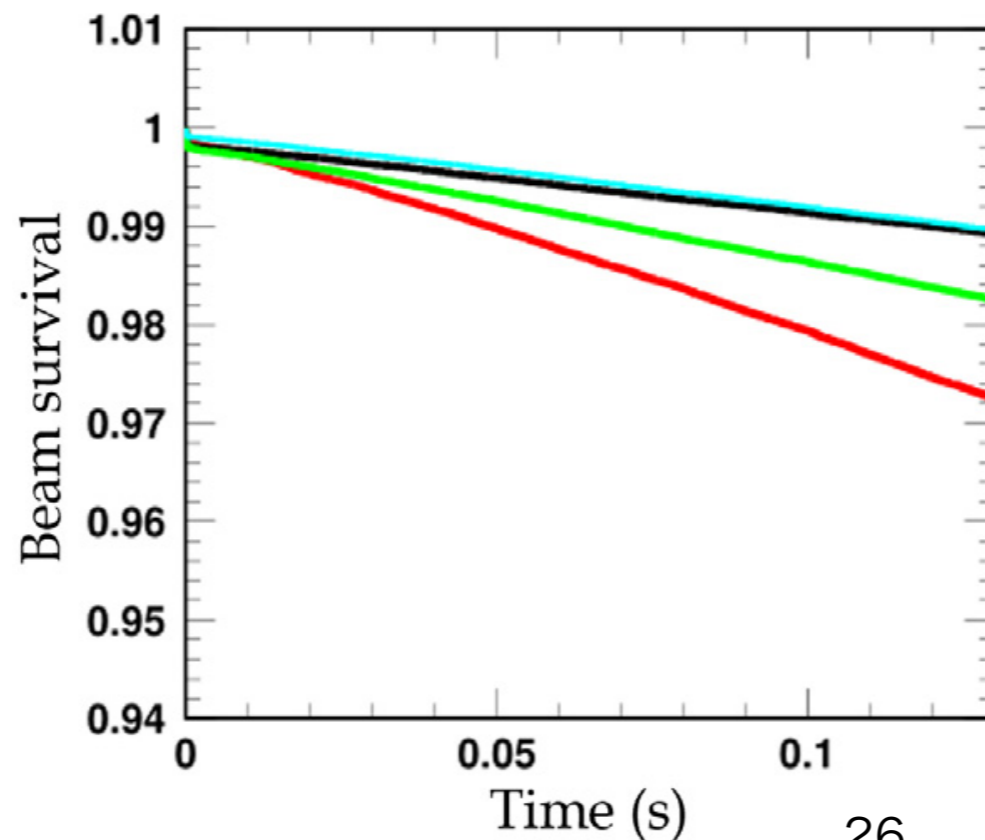


Countermeasure for

$$3\nu_x = 64, \nu_x + 2\nu_y = 64$$

Tracking simulations suggest that we can compensate resonances for off-momentum particles by increasing the number of trim coils to 24.

As a first step, we will increase the number 4 \rightarrow 8 this summer.



Beam survival ratio
(2.5D tracking simulation)

- Ideal (no errors)
- TrimSx24
- TrimSx12
- TrimSx4 (present)

H. Hotchi *et al.*, IPAC2023, TUPM055

Summary of resonances in FX operation

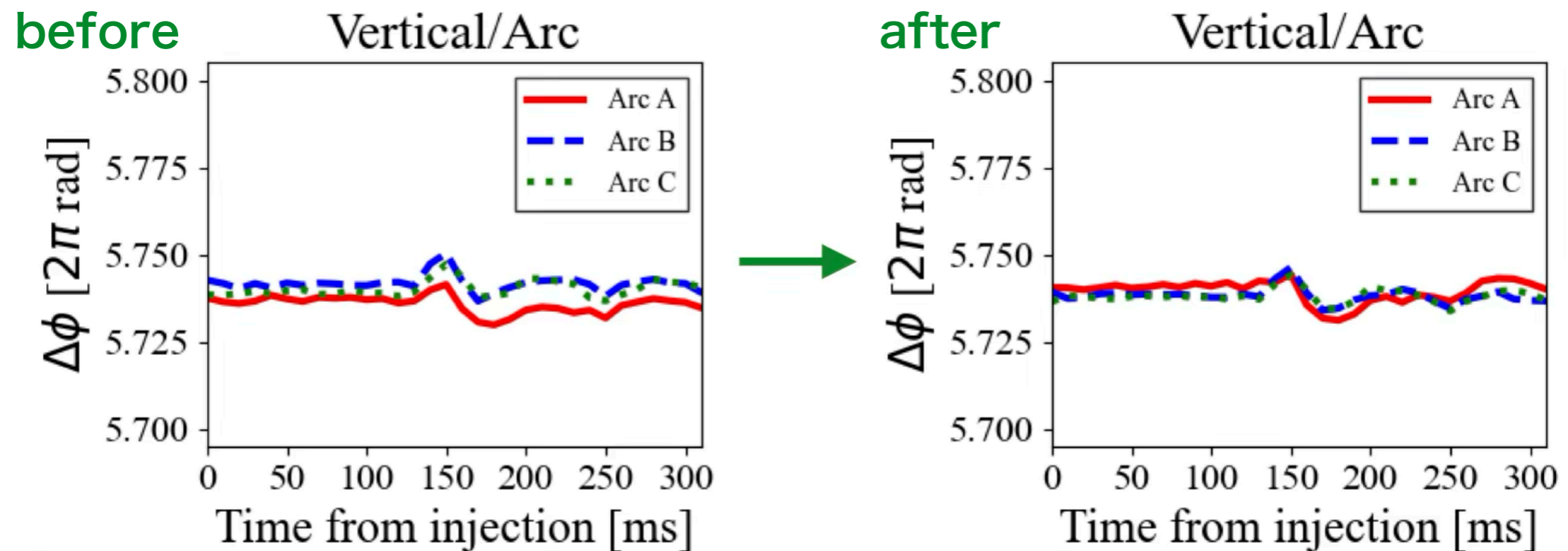
	Space charge	Magnets
Structure	$8\nu_y = 171, 2\nu_x + 6\nu_y = 171, \dots$ <ul style="list-style-type: none"> • 8th order • cross tune spread $2\nu_x - 2\nu_y = 0$ <ul style="list-style-type: none"> • 4th order 	(far enough)
Nonstructure	$4\nu_y = 85, 2\nu_x + 2\nu_y = 85, \dots$ <ul style="list-style-type: none"> • 4th, 6th, ... order • cross tune spread 	$3\nu_x = 64, \nu_x + 2\nu_y = 64$ <ul style="list-style-type: none"> • 3rd order • cross tune spread $\nu_x - \nu_y = 0$ <ul style="list-style-type: none"> • 2nd order

Optics correction

Even after applying trim coils of sextupole magnets, optics correction contributed to beam loss reduction.

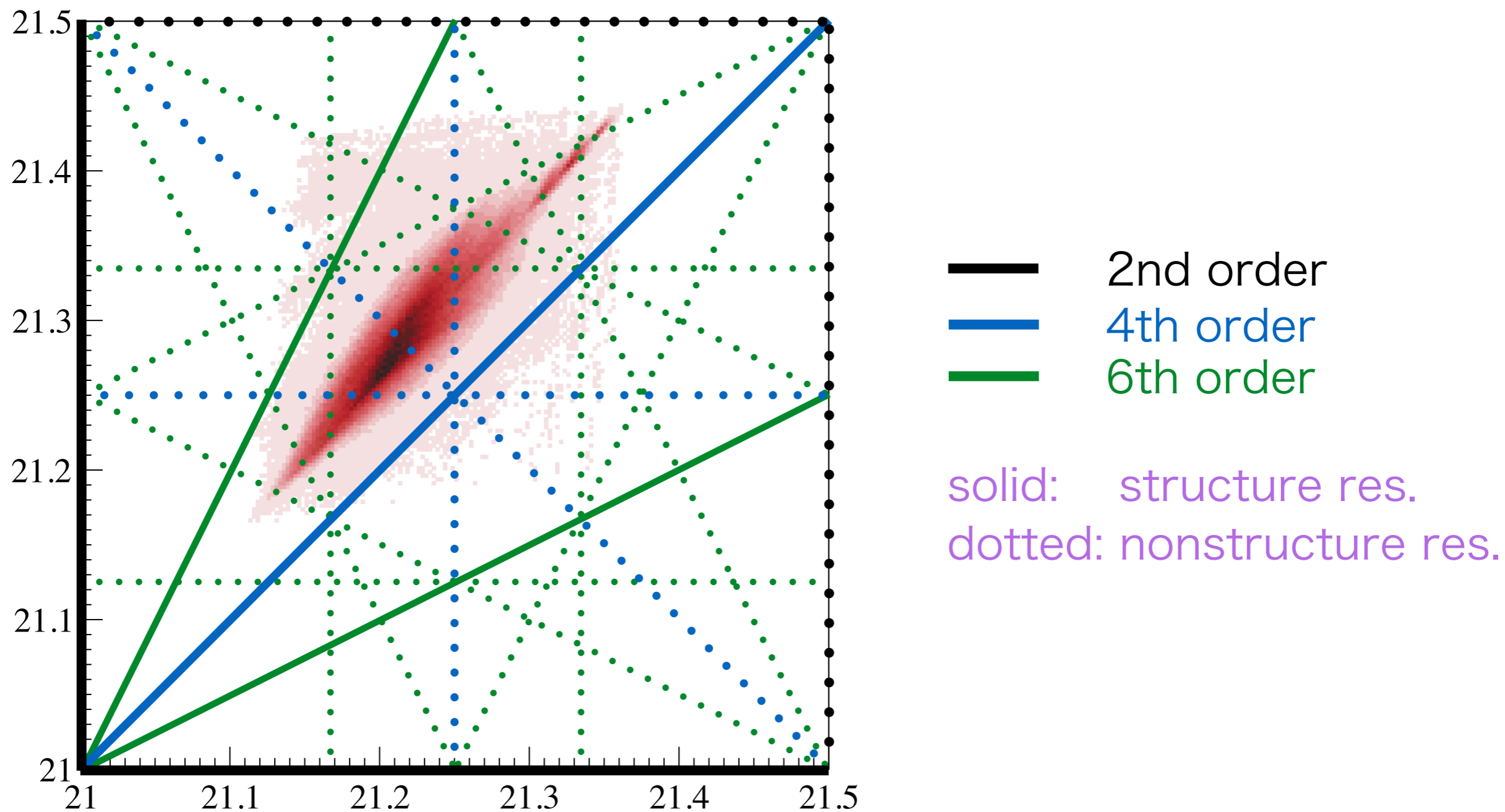
Space-charge-driven nonstructure resonances were weakened?

Example of optics correction (measurement)



Beam loss was reduced ~20% by this optics correction!
(with 2.3×10^{13} -ppb beams)

Resonances driven by space charge



Resonance width of SC nonstructure res.

before optics correction

Space-charge-driven nonstructure resonances appear to be weak overall.

Resonances affecting particles close to the aperture can be source of the beam loss.

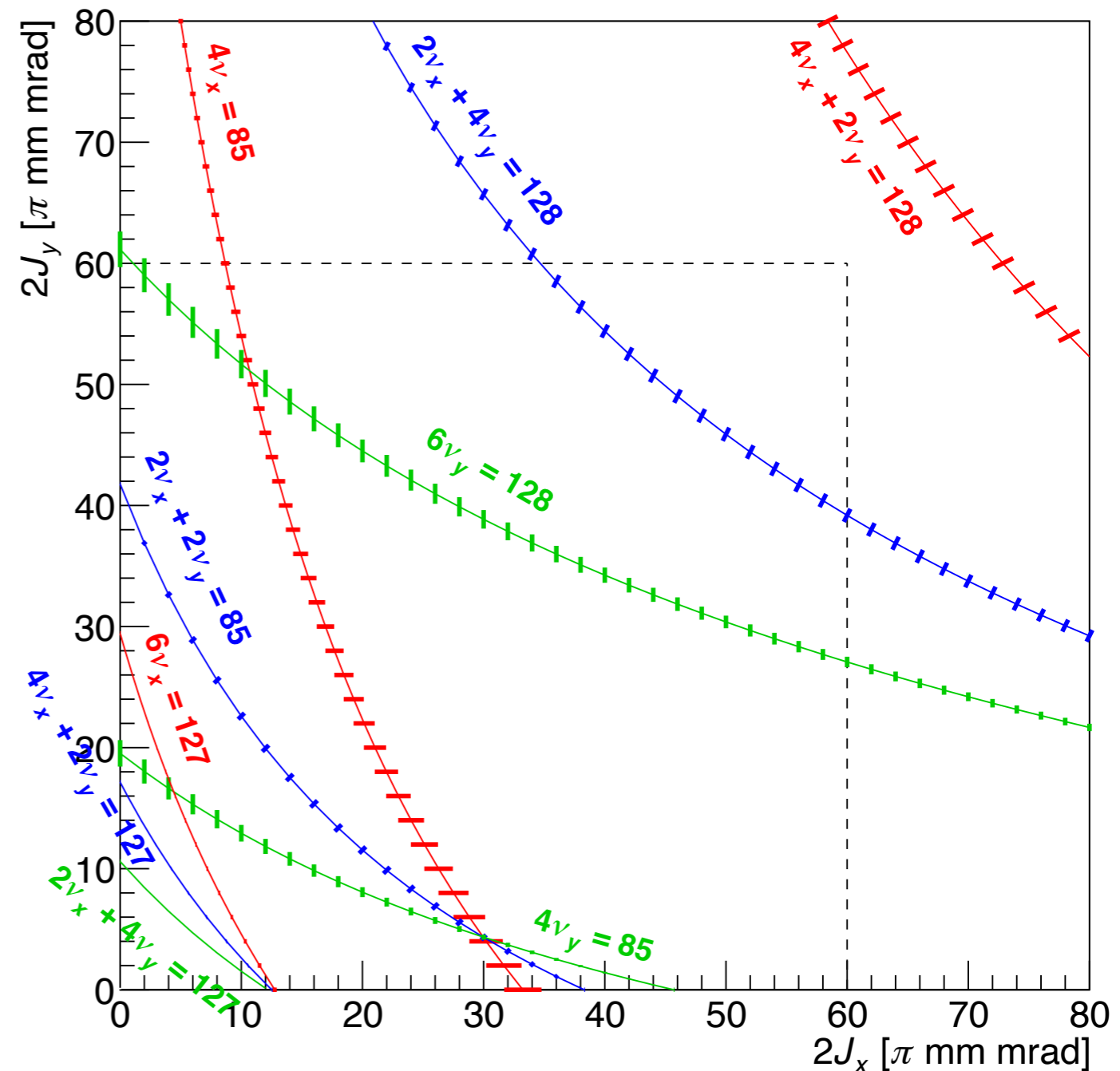
$$\rightarrow 6\nu_y = 128 ?$$

Resonance width of $6\nu_y = 128$:

$$2\Delta J_y = 2.9\pi \rightarrow 2.0\pi \text{ mm mrad}$$

$$(J_x = 0, \delta = 0)$$

by optics correction.



Summary of resonances in FX operation

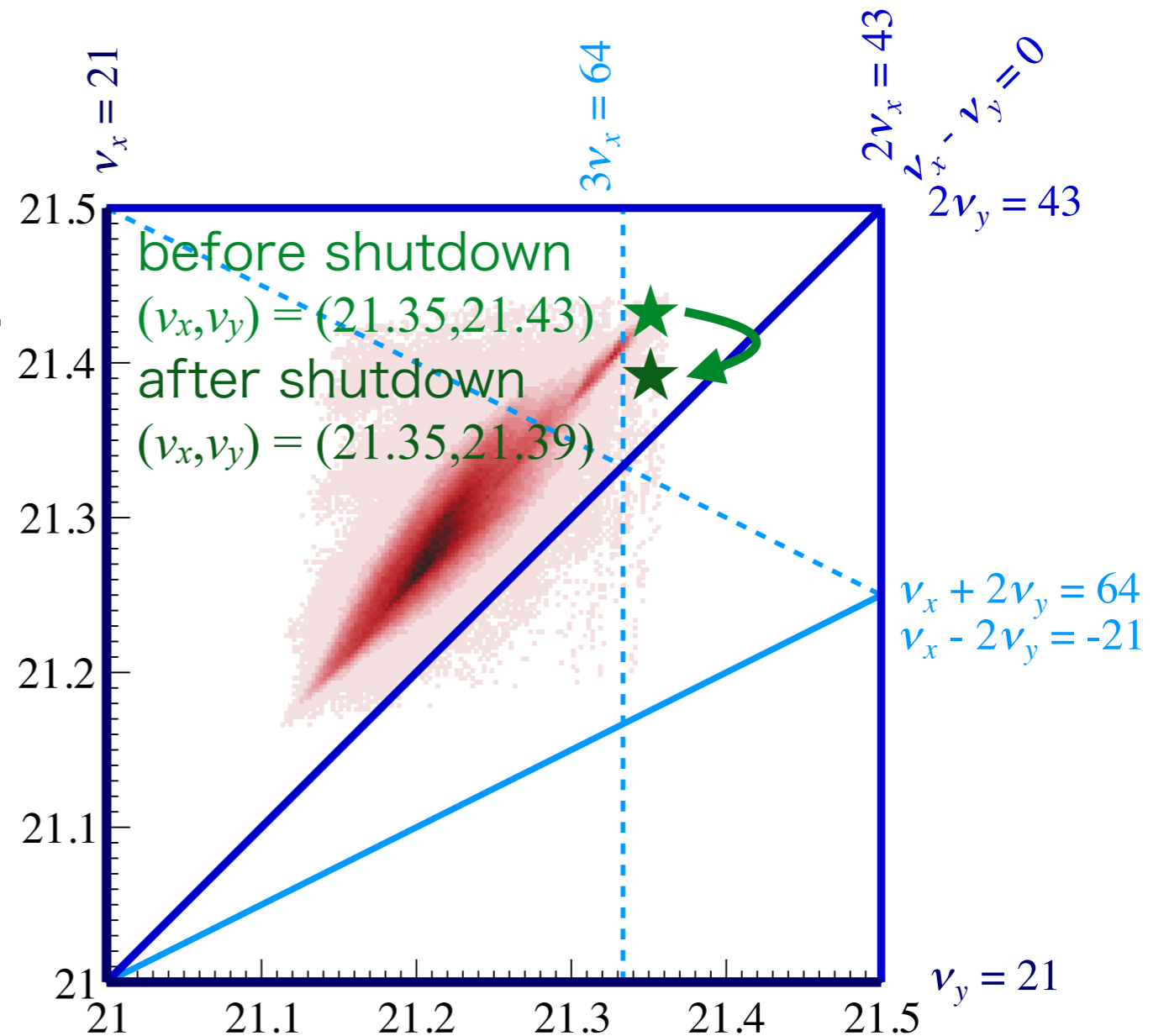
	Space charge	Magnets
Structure	$8\nu_y = 171, 2\nu_x + 6\nu_y = 171, \dots$ <ul style="list-style-type: none"> • 8th order • cross tune spread $2\nu_x - 2\nu_y = 0$ <ul style="list-style-type: none"> • 4th order 	(far enough)
Nonstructure	$4\nu_y = 85, 2\nu_x + 2\nu_y = 85, \dots$ <ul style="list-style-type: none"> • 4th, 6th, ... order • cross tune spread 	$3\nu_x = 64, \nu_x + 2\nu_y = 64$ <ul style="list-style-type: none"> • 3rd order • cross tune spread $\nu_x - \nu_y = 0$ <ul style="list-style-type: none"> • 2nd order

Recent working point

After the long-term shutdown, the beam loss scan results showed that the optimal working point moved vertically down 0.04.

The optimal DC currents of the trim coils did not change. Some AC components arose?

After the shutdown, the differential resonance became more important.



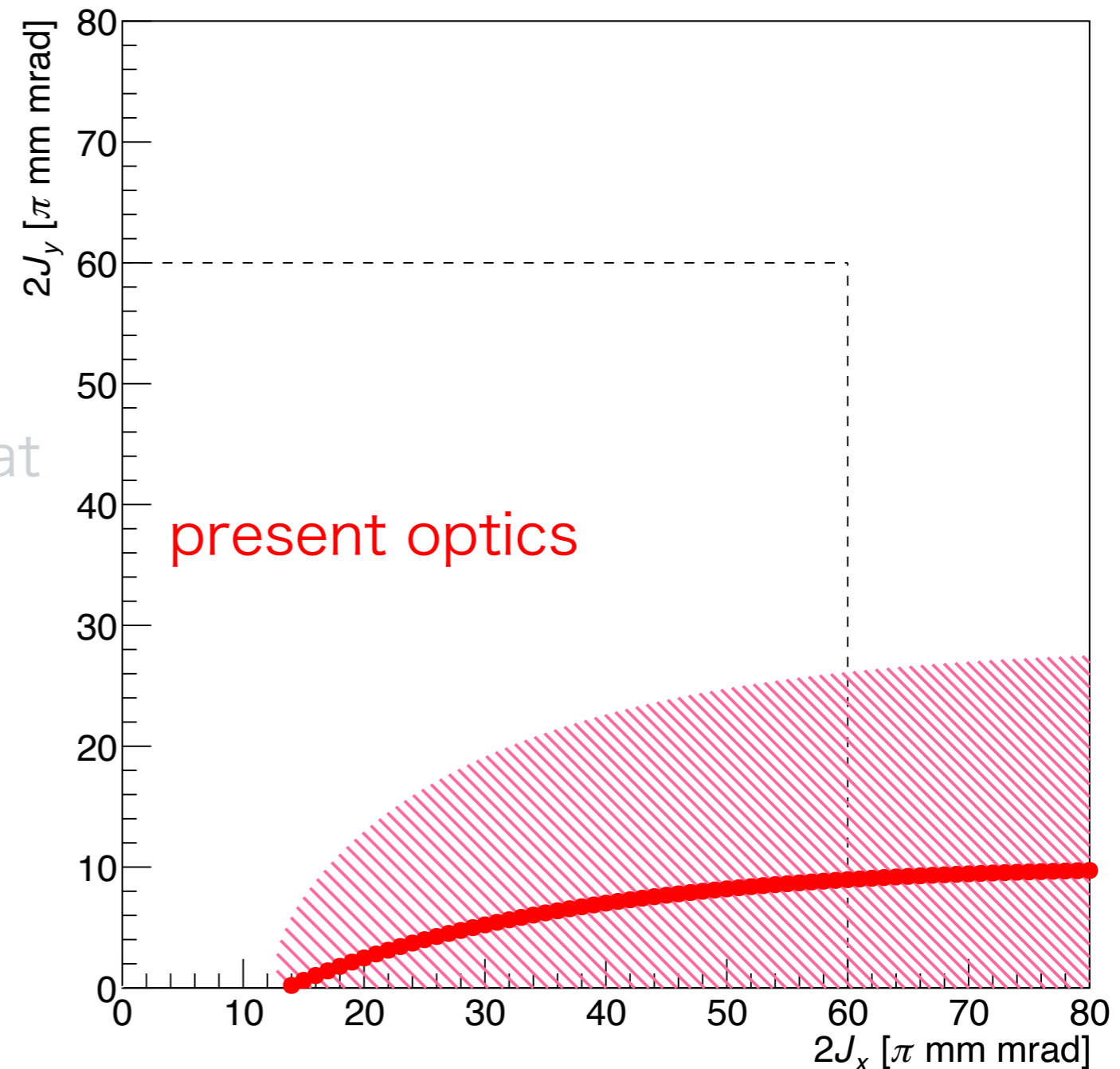
Resonance width of

$$2\nu_x - 2\nu_y = 0$$

The resonance $2\nu_x - 2\nu_y = 0$ affects wide area.

The new optics is effective not only for $8\nu_y = 171$ but also for $2\nu_x - 2\nu_y = 0$.

Tracking simulation suggests that applying the new optics will reduce the beam loss.



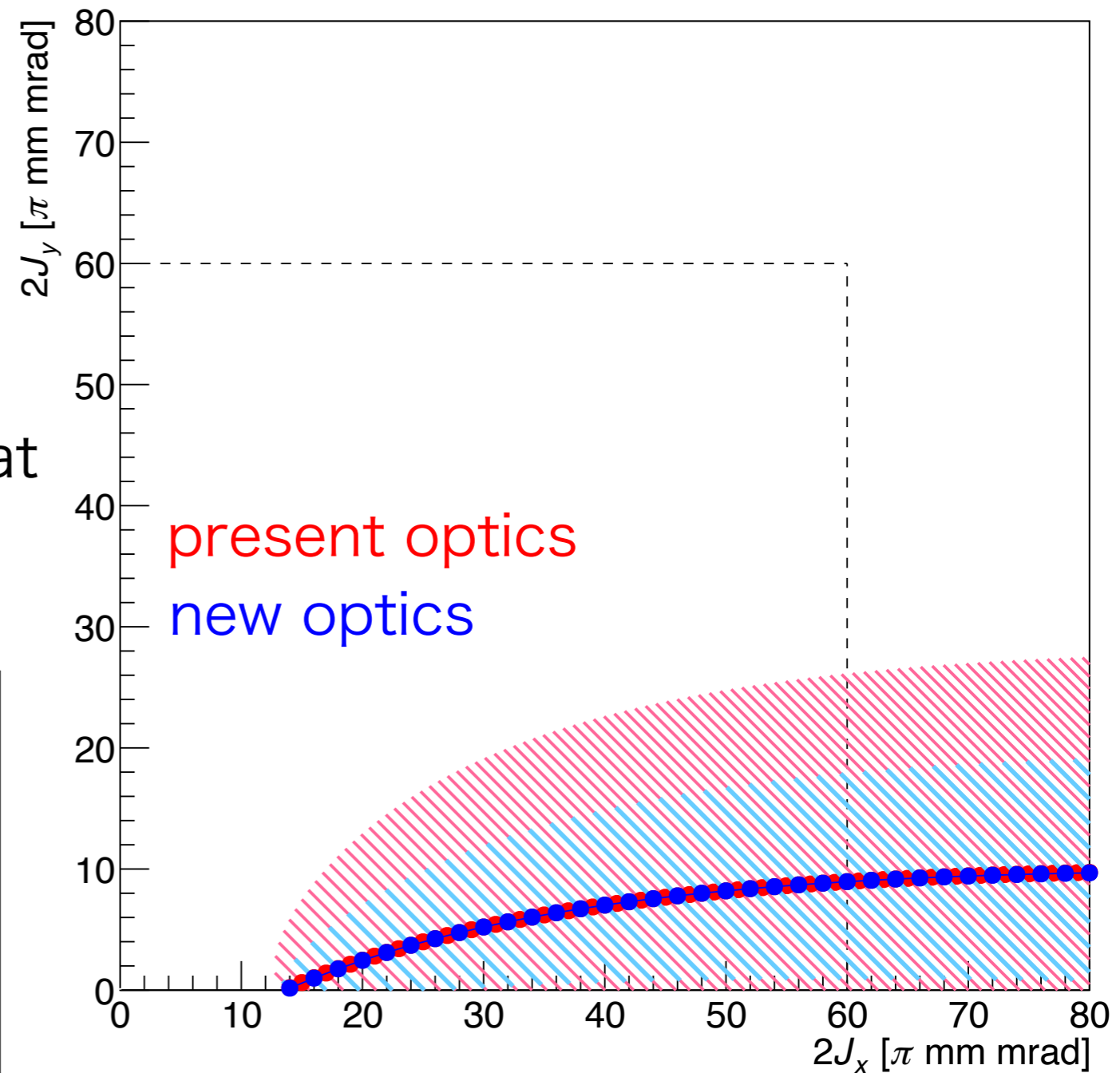
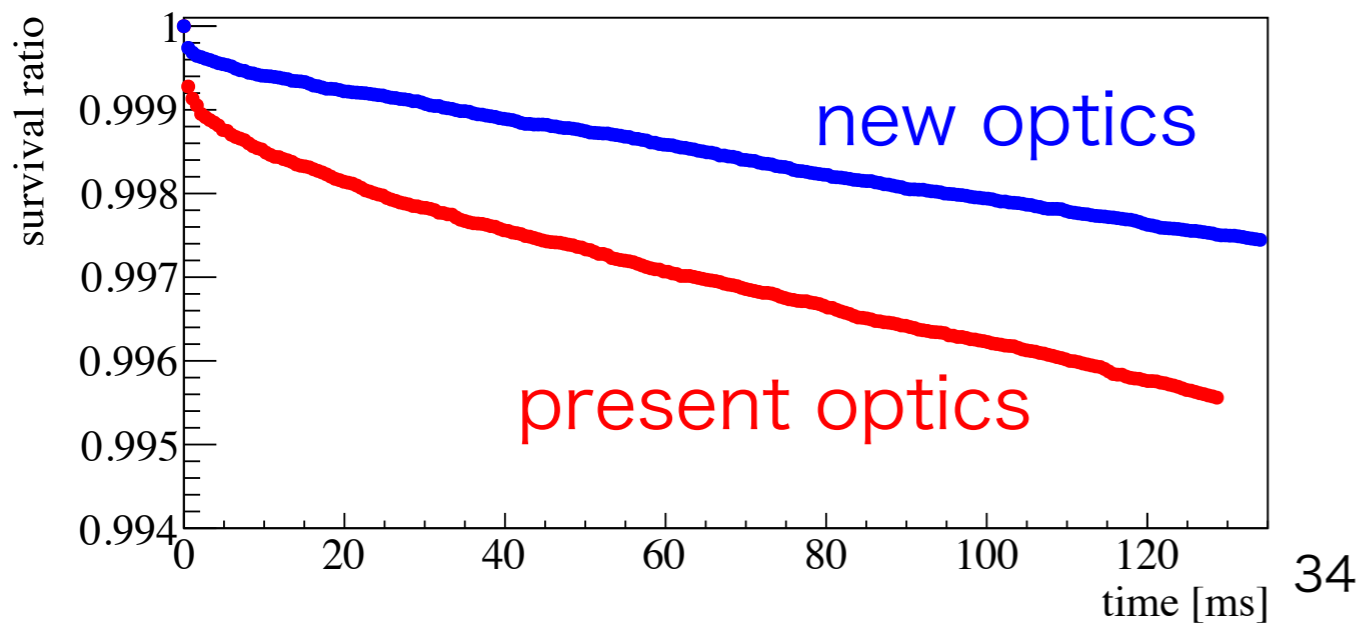
Resonance width of

$$2\nu_x - 2\nu_y = 0$$

The resonance $2\nu_x - 2\nu_y = 0$ affects wide area.

The new optics is effective not only for $8\nu_y = 171$ but also for $2\nu_x - 2\nu_y = 0$.

Tracking simulation suggests that applying the new optics will reduce the beam loss.



Summary of resonances in FX operation

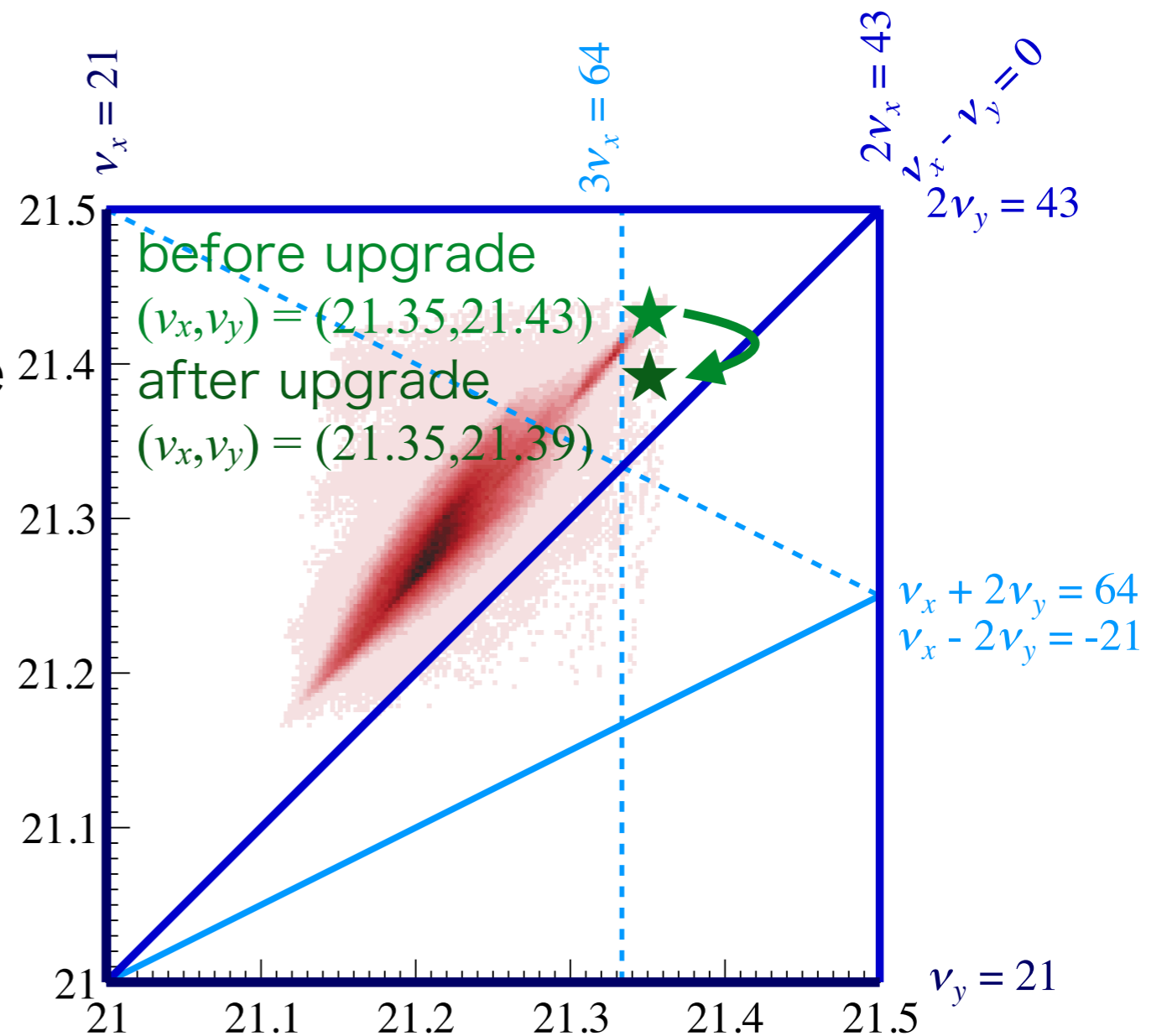
	Space charge	Magnets
Structure	$8\nu_y = 171, 2\nu_x + 6\nu_y = 171, \dots$ <ul style="list-style-type: none"> • 8th order • cross tune spread $2\nu_x - 2\nu_y = 0$ <ul style="list-style-type: none"> • 4th order 	(far enough)
Nonstructure	$4\nu_y = 85, 2\nu_x + 2\nu_y = 85, \dots$ <ul style="list-style-type: none"> • 4th, 6th, ... order • cross tune spread 	$3\nu_x = 64, \nu_x + 2\nu_y = 64$ <ul style="list-style-type: none"> • 3rd order • cross tune spread $\nu_x - \nu_y = 0$ <ul style="list-style-type: none"> • 2nd order

Differential resonance

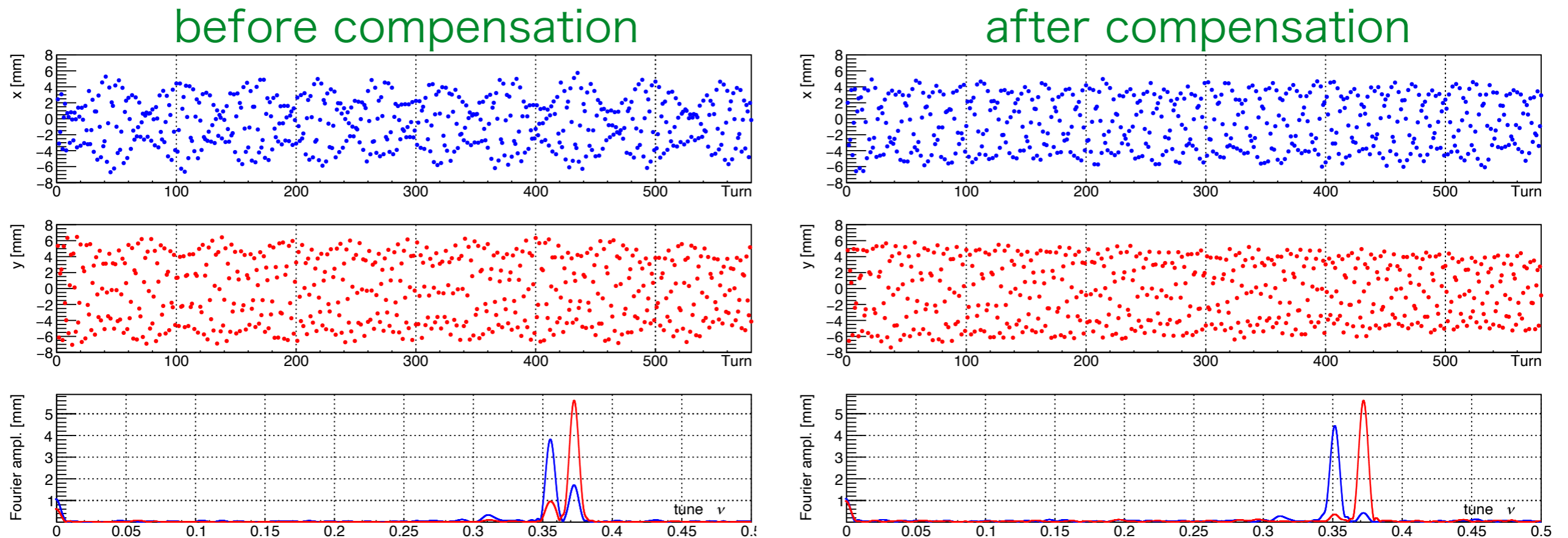
We did not use to compensate for the differential resonance $\nu_x - \nu_y = 0$.

Since the working point became close to this resonance, we attempted to compensate for this resonance using two skew quadrupoles.

We measured turn-by-turn transverse beam positions using low-intensity beams.



Result of compensation



The differential resonance $\nu_x - \nu_y = 0$ was successfully compensated in low-intensity beams.

However, when we apply skew quadrupoles in high-intensity beams, the beam loss worsened.

Anyone have ideas?

Summary

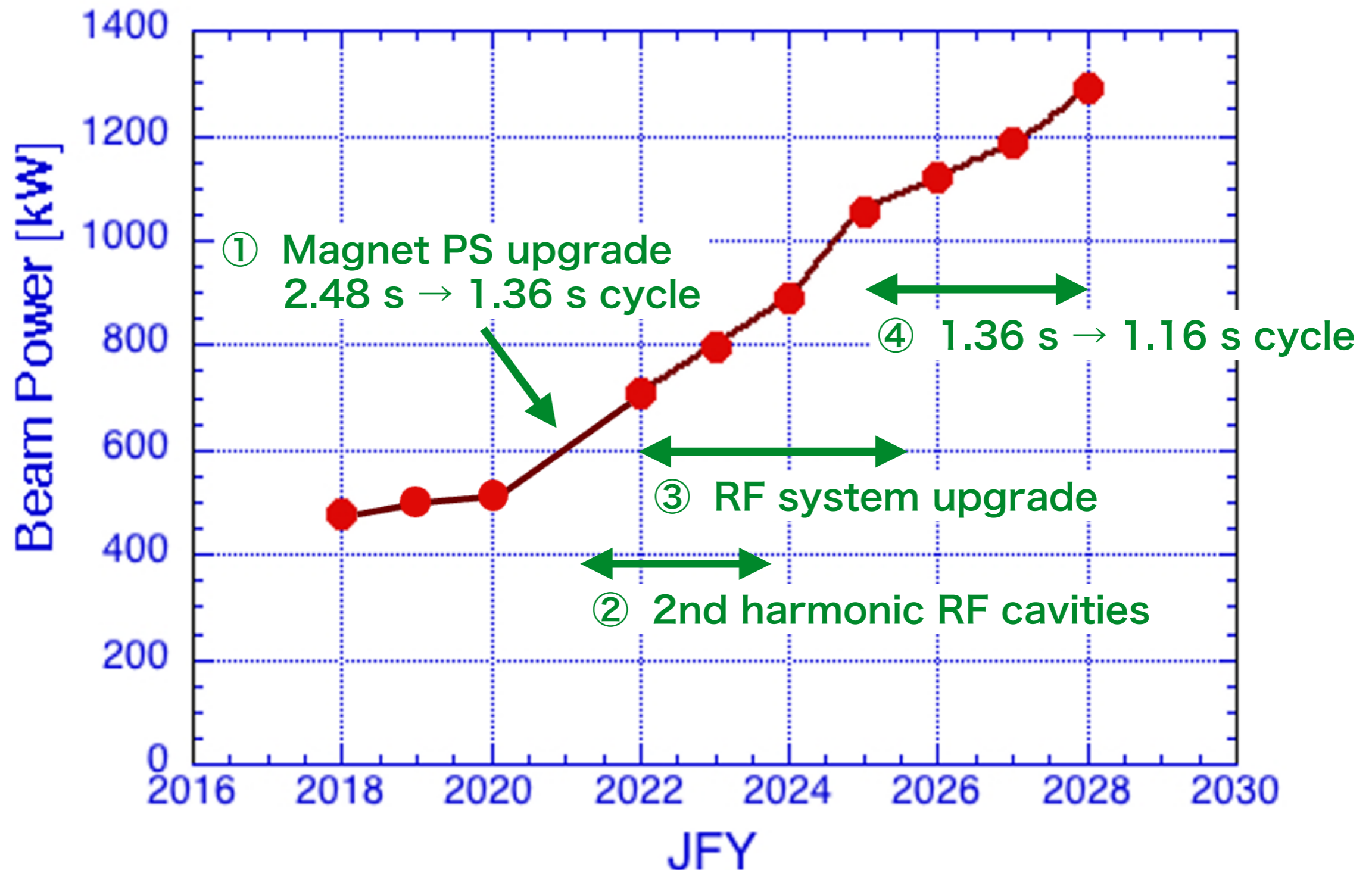
To realize FX 1.3 MW operation, we need to compensate for resonances and reduce beam loss.

Countermeasures

	Space charge	Magnets
Structure	$8\nu_y = 171$ <ul style="list-style-type: none"> • apply the new optics $2\nu_x - 2\nu_y = 0$ <ul style="list-style-type: none"> • apply the new optics 	(far enough)
Nonstructure	$4\nu_y = 85, 2\nu_x + 2\nu_y = 85, \dots$ <ul style="list-style-type: none"> • fine optics correction 	$3\nu_x = 64, \nu_x + 2\nu_y = 64$ <ul style="list-style-type: none"> • increase the number of trim coils $\nu_x - \nu_y = 0$ <ul style="list-style-type: none"> • skew quadrupole?

Backup

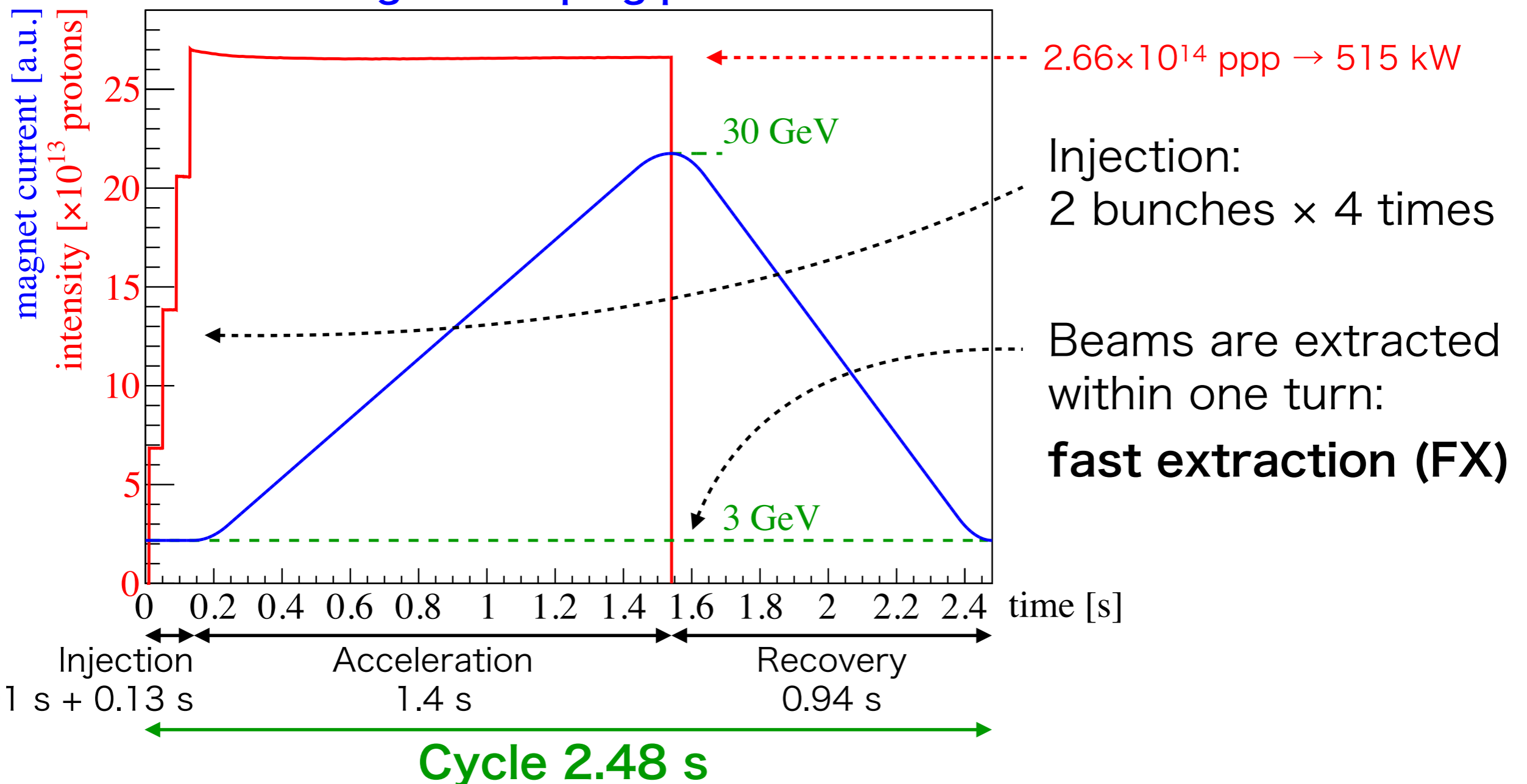
Beam power upgrade plan of the MR



FX operation status by 2021

Beam intensity (measured by DCCT)

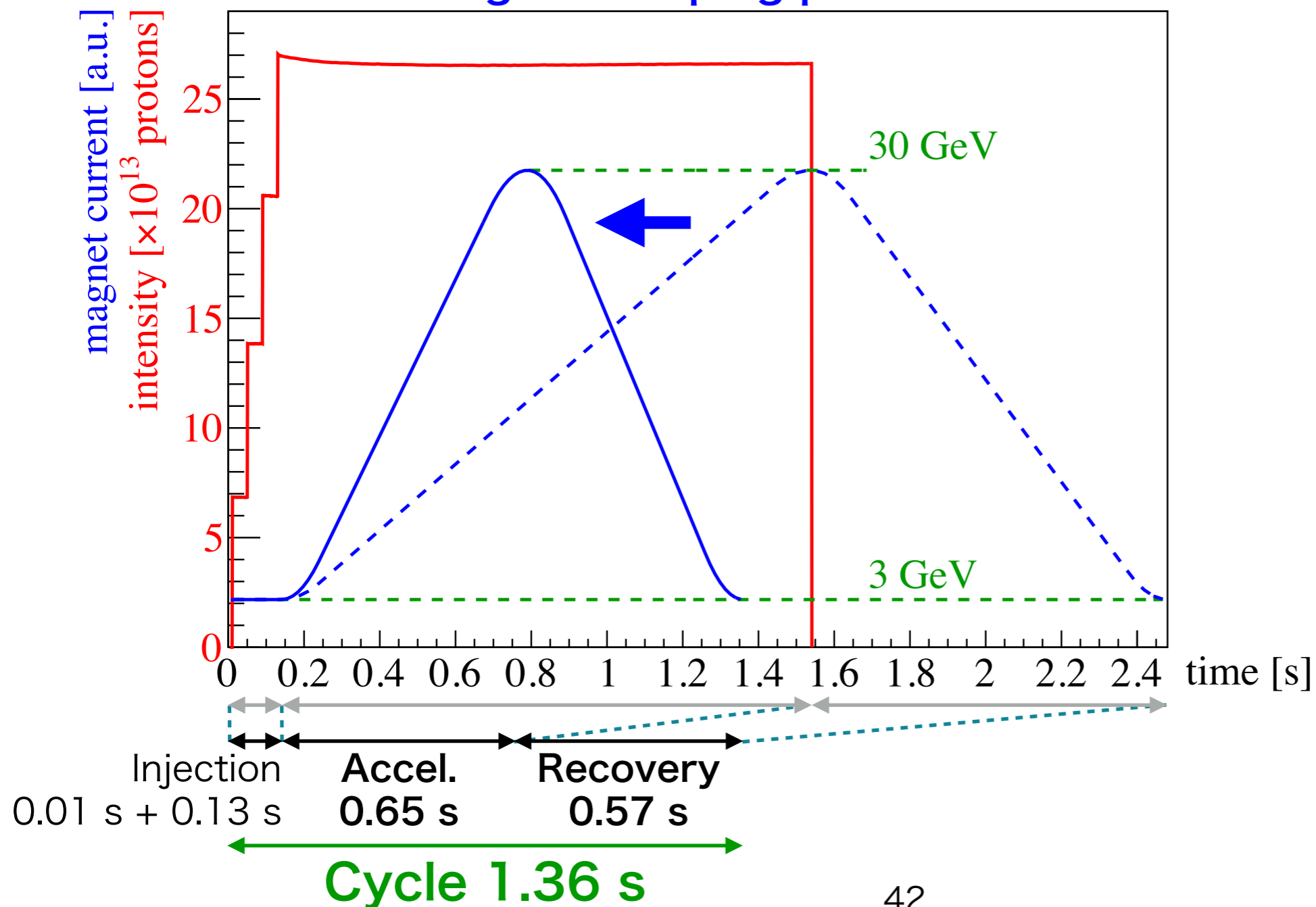
Magnet ramping pattern



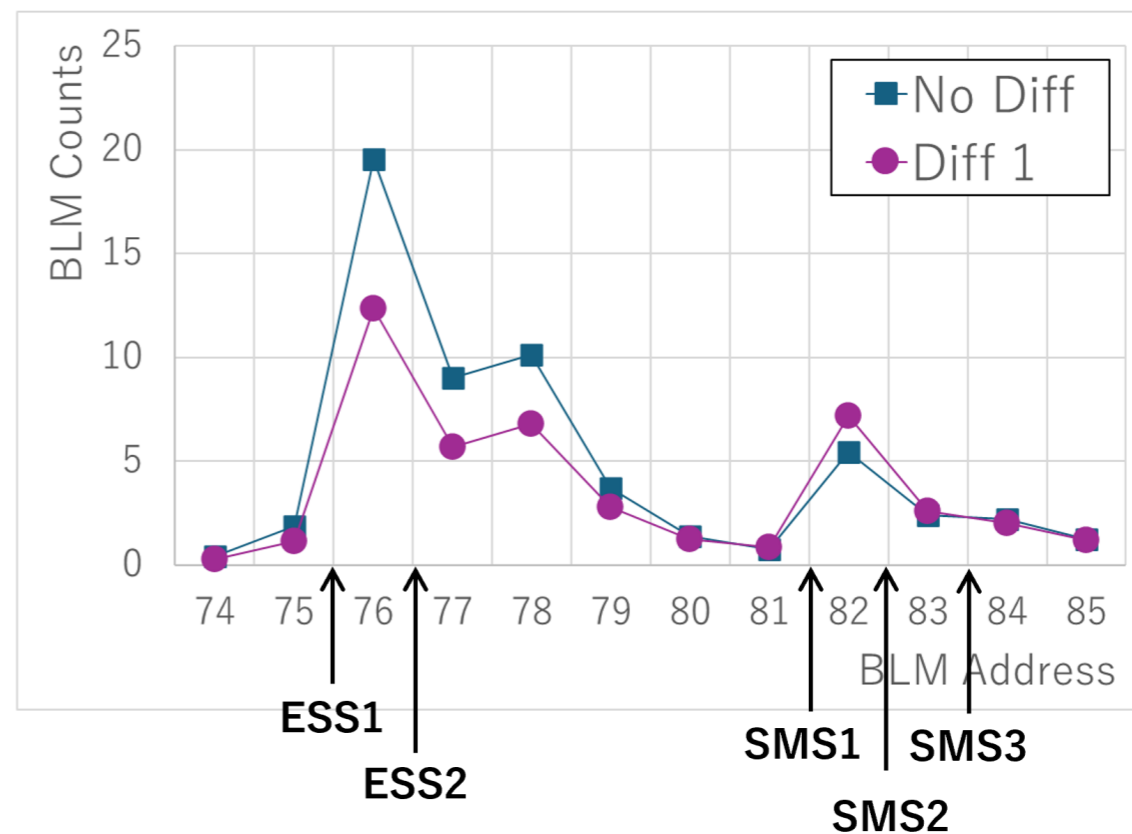
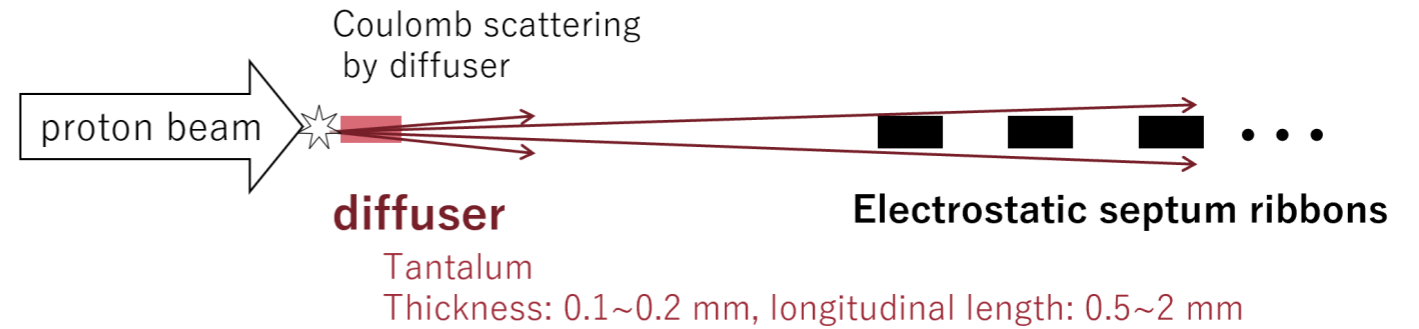
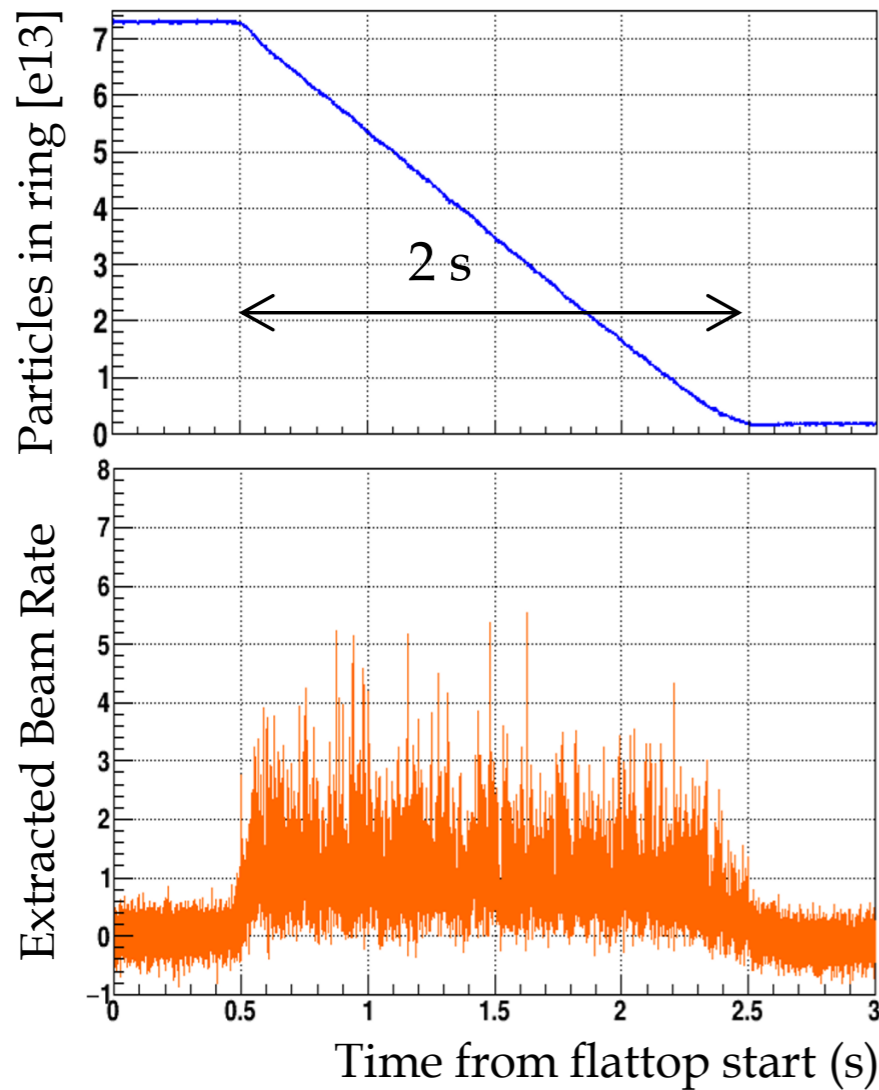
FX operation status from 2023

Beam intensity by 2021 (measured by DCCT)

Magnet ramping pattern



SX 80-kW beam operation



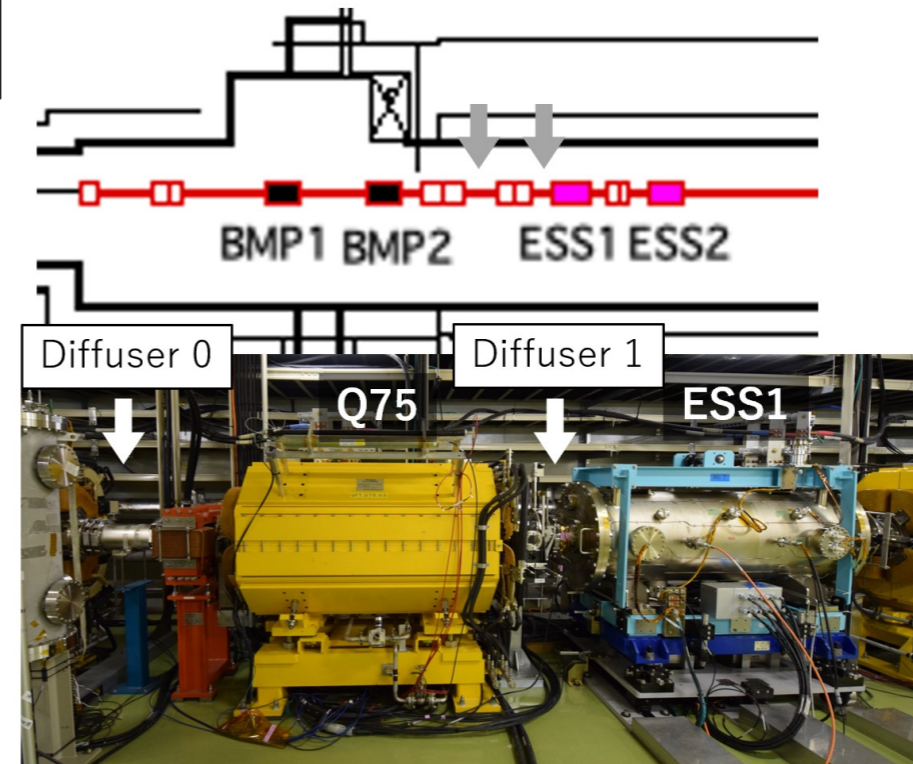
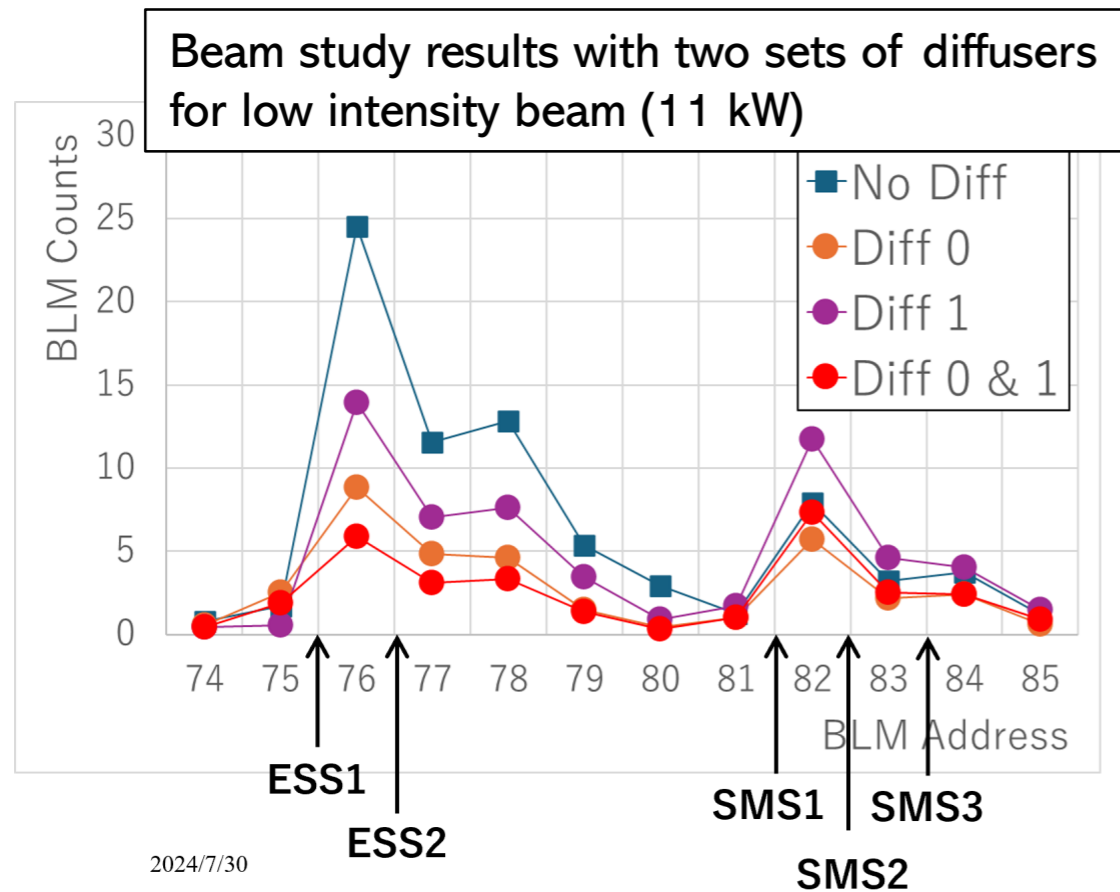
● We preformed:

- Optics tuning
- Dynamic RF manipulation to suppress beam instability during the de-bunching process at flattop
- Introduction of a diffuser to reduce beam loss at ESS during SX
- Spill feedback tuning ...



Extraction efficiency 99.6%
Spill duty factor 72%

Perspective of the SX operation



- The beam power will be increased to 100 kW in stages
 - while further reducing beam loss
 - while further improving spill duty factor
 by
 - improving configuration of diffusers
 - introducing new optics with large slippage factor
 - improving spill feedback system
 - reducing current ripple of main magnet PS
 - introducing VHF cavity, etc.
- We aim to achieve this by 2026.

Strategy for beam loss reduction

Presently, beam loss is caused by

1. Current ripples of bend power supplies

- $\Delta x = \eta_x \frac{\Delta B}{B}$, $|\Delta K_1| = |K_2 \Delta x|$ T. Yasui, IPAC2023, TUXG1
Y. Sato, this meeting, MOA2I1

- We are going to reduce ripples within a year.

2. Nonstructure resonances induced by magnet imperfections

- We plan to add correction sextupole fields

H. Hotchi *et al.*, IPAC2023, TUPM055

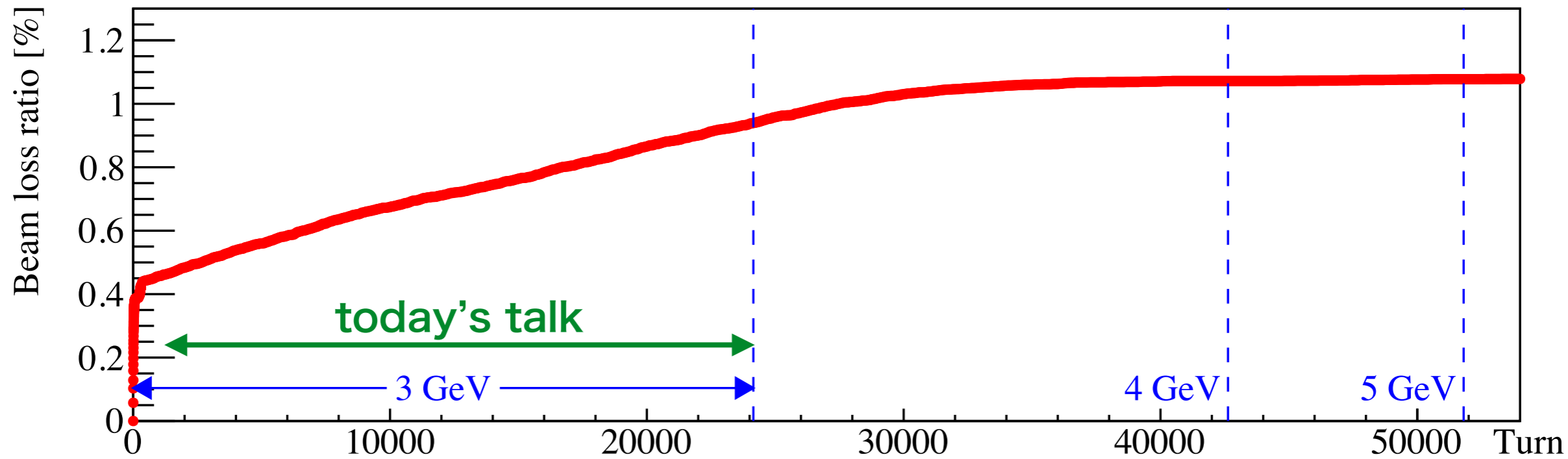
3. Structure resonances induced by space charge effects

- Today's talk

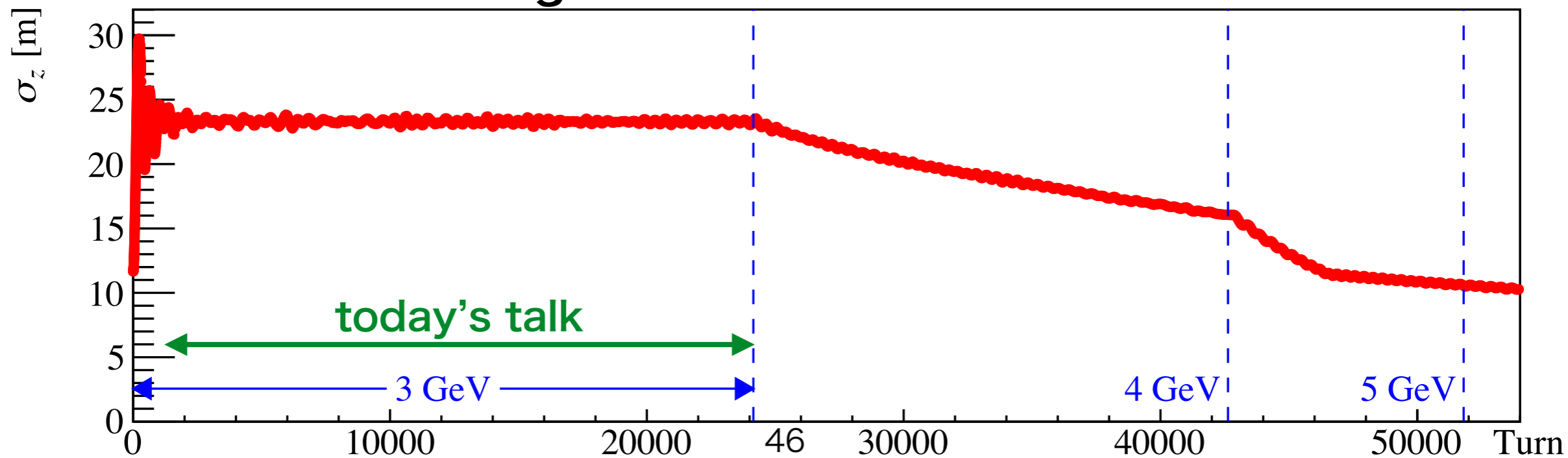
(T. Yasui and Y. Kurimoto, PRAB **25**, 121001 (2022) + some FMA results)

Beam loss & beam size (simulation)

Beam loss



Longitudinal rms beam size



Longitudinal distribution

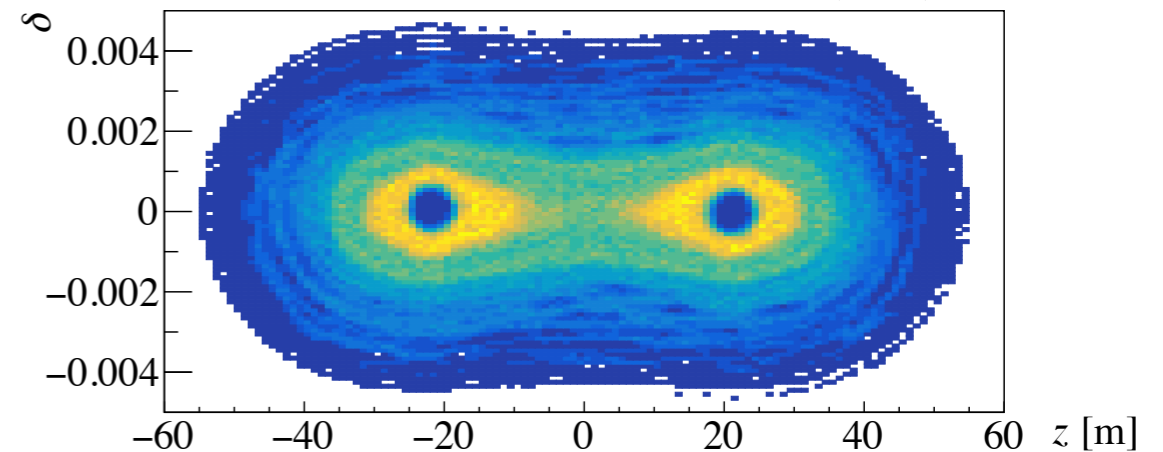
2nd harmonic RF cavities are used for peak suppression.

Most of the lost particles are found at locations of high line densities.

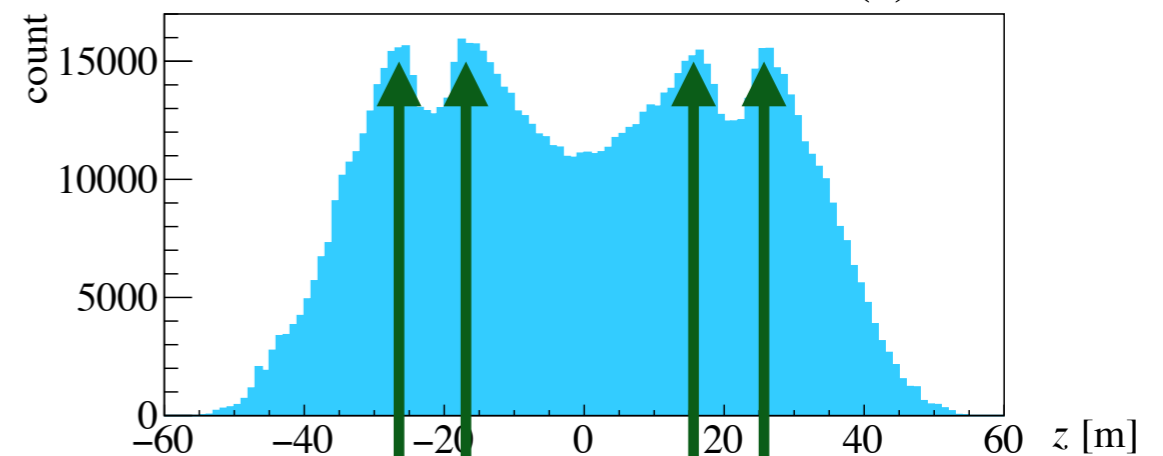
Beam loss is caused by space charge effect.

Peak suppression by the 2nd harmonic RF cavities are very important.

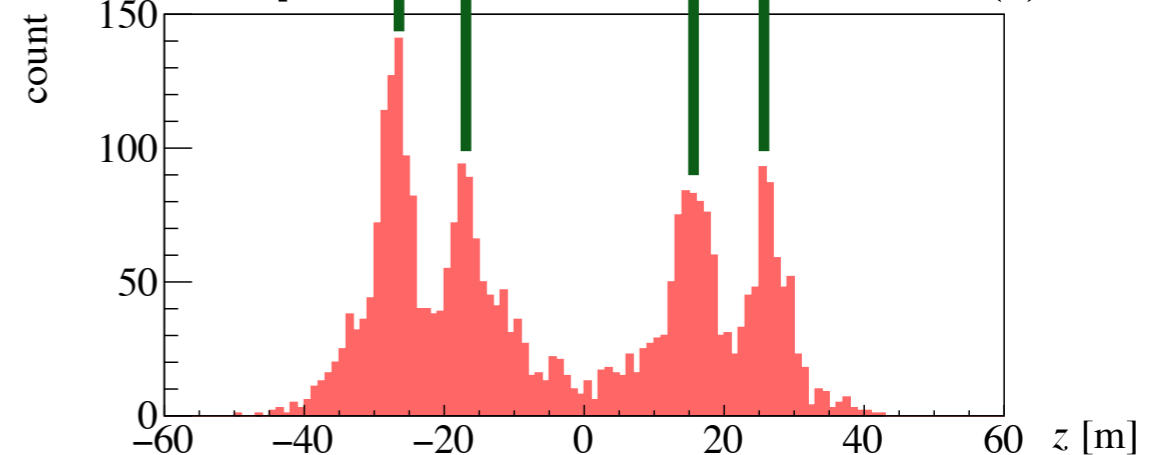
Beam distribution (z, δ)



Beam distribution (z)



Lost particles distribution (z)

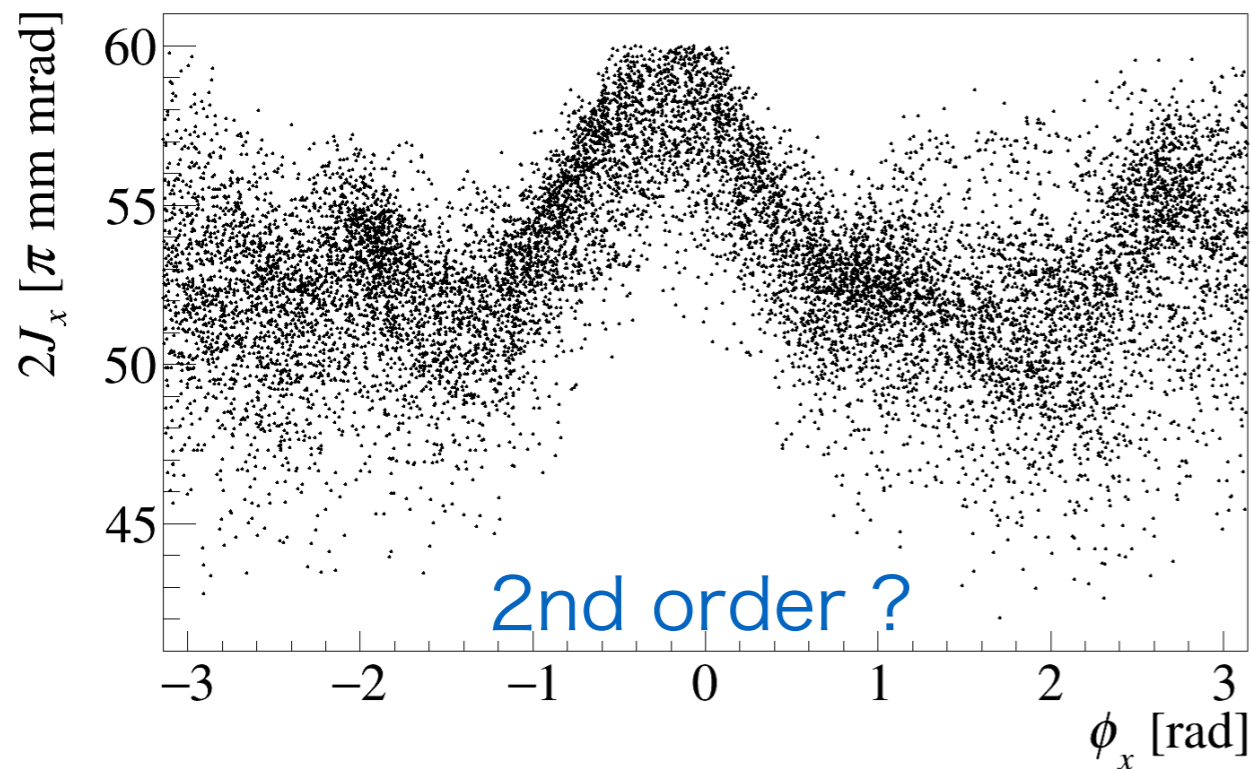


Transverse distribution

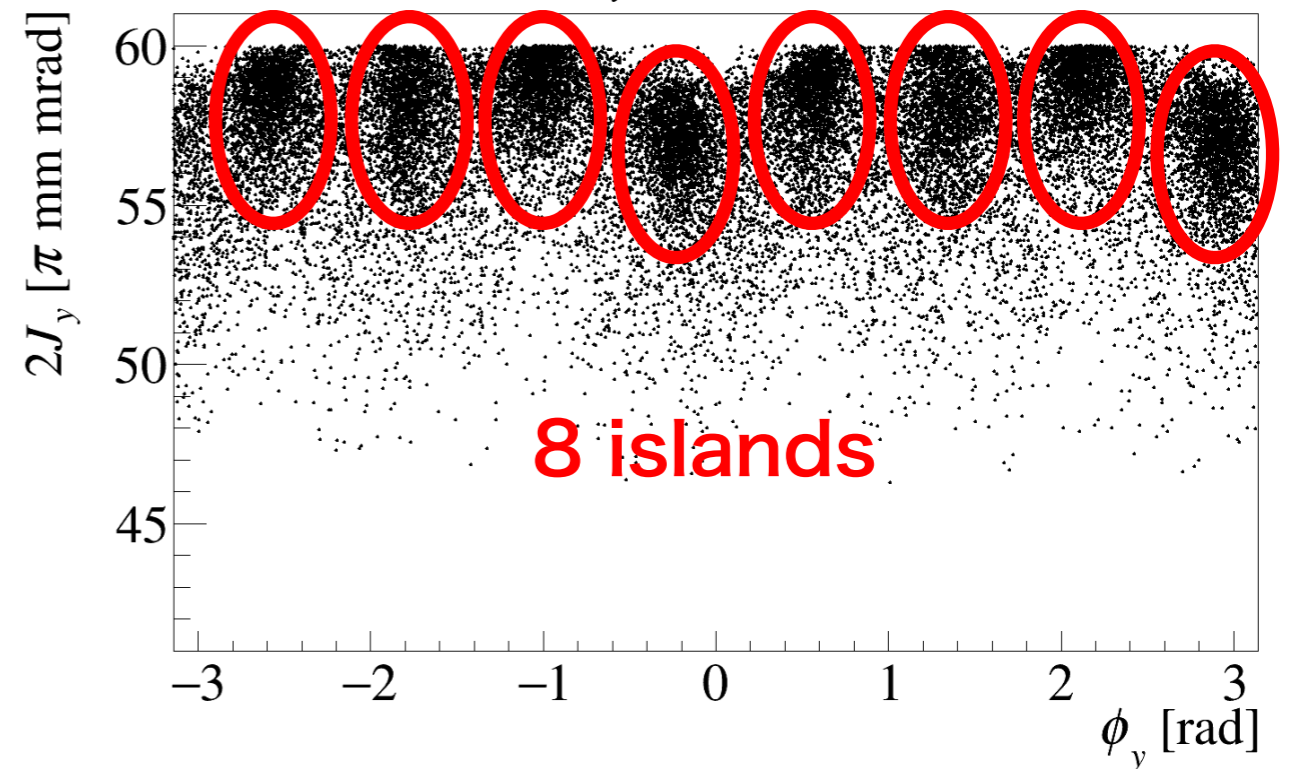
The collimators were set to $(2J_x, 2J_y) = (60\pi, 60\pi)$ mm mrad.

Phase-space (action-angle) distribution of lost particles

Lost because $2J_x > 60\pi$ mm mrad (28.6%)



Lost because $2J_y > 60\pi$ mm mrad (71.4%)



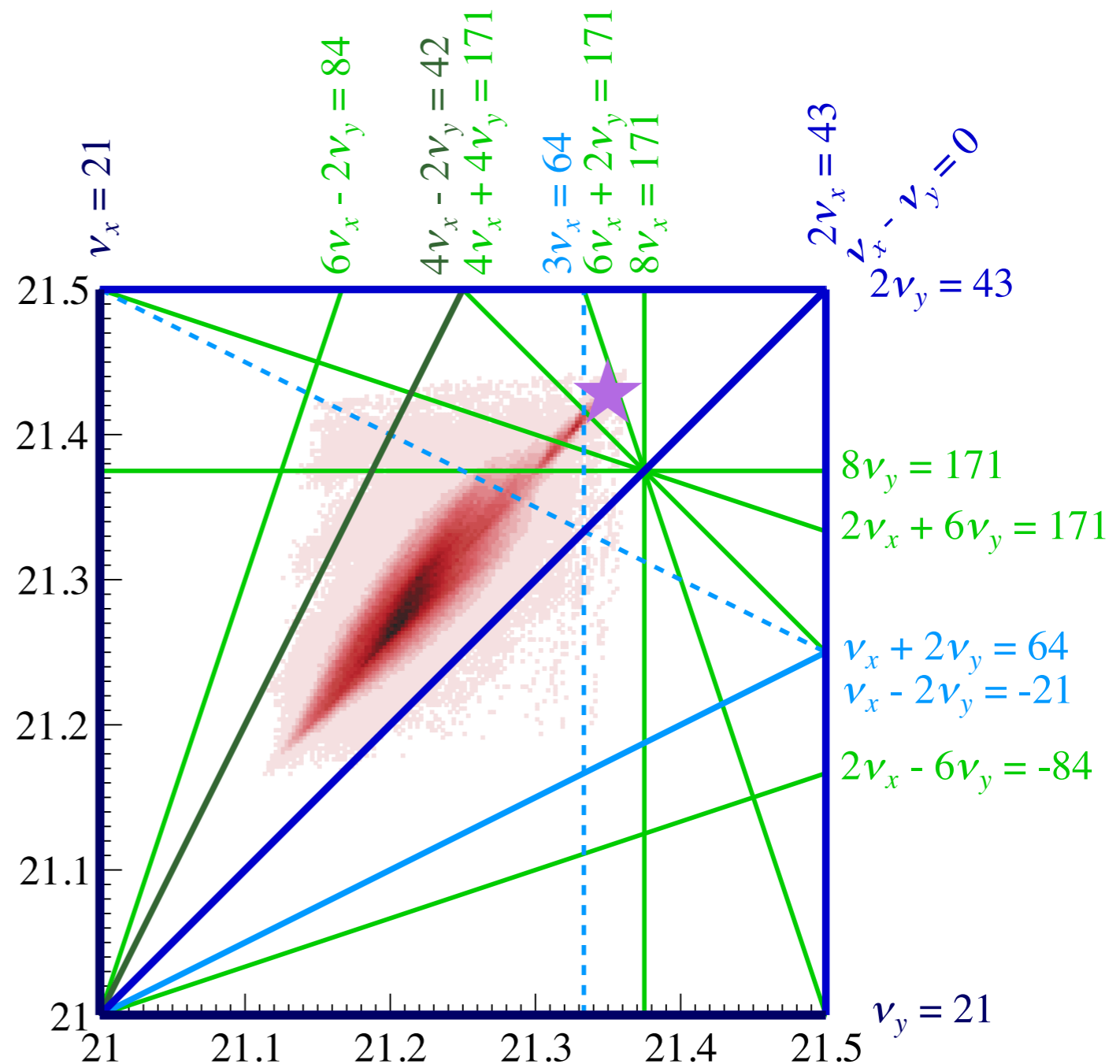
The distribution of the lost particles suggest effects of the resonance $8\nu_y = n$.

Interpretation for $8\nu_y = 171$?

The working point is at $(\nu_x, \nu_y) = (21.35, 21.43)$.

The resonance $8\nu_y = 171$ is neither strong nor close to the working point.

Why $8\nu_y = 171$?

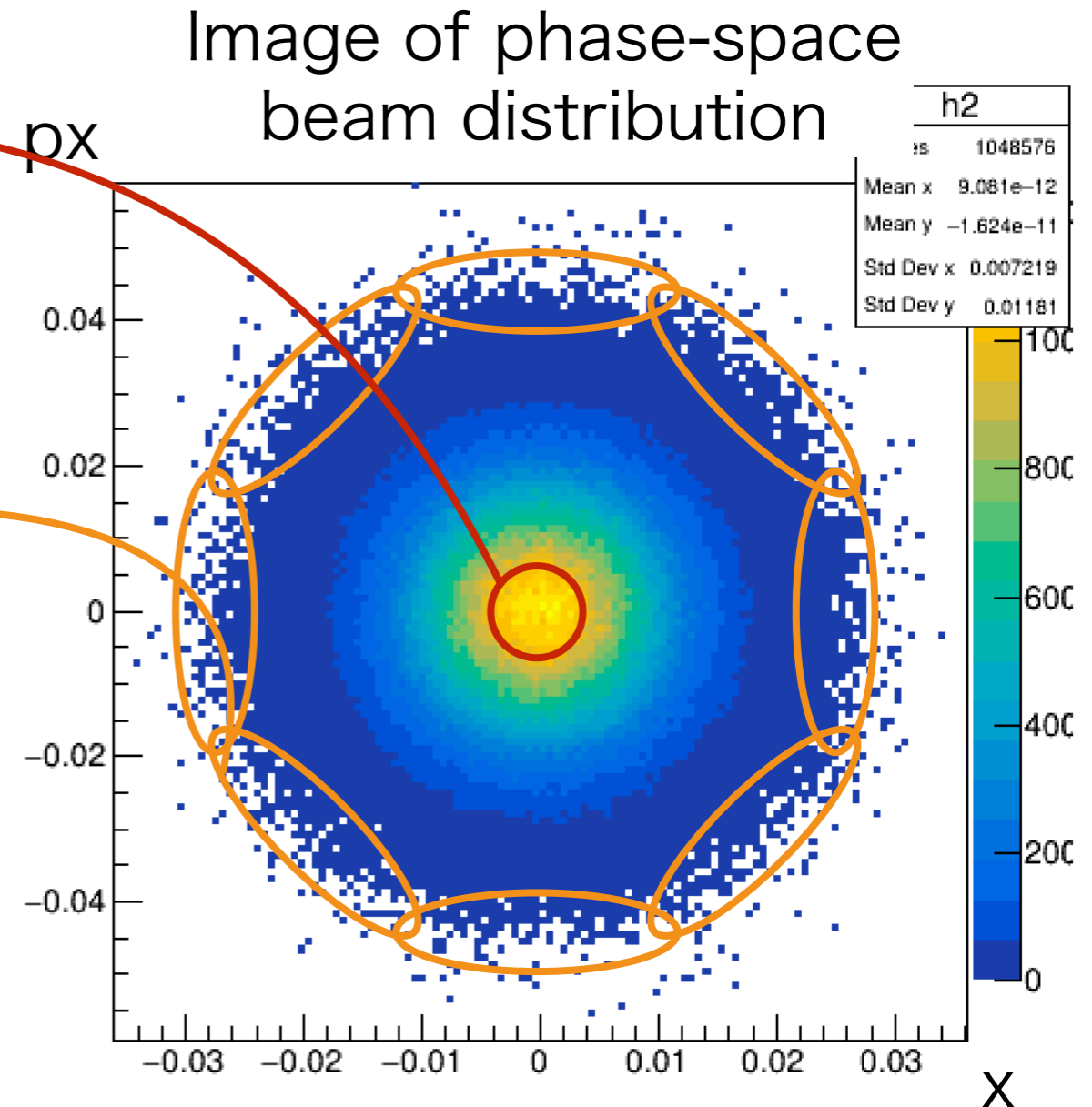


Positions of lost particles

Particles at the center of 6D phase space.
Basically they survive.

Particles at the beam halo of 6D phase space.
These particles may be lost due to resonances.

Beam loss is caused by the resonances which affect particles at beam halo.



Calculations of incoherent tunes

A particle is affected by a resonance $m_x \nu_x + m_y \nu_y = n$
 when its **incoherent tune** satisfies $m_x \nu_{x,\text{incoh.}} + m_y \nu_{y,\text{incoh.}} = n$.

Incoherent tunes can be calculated analytically by setting the **line density** λ and assuming a Gaussian distribution.

$$\nu_{\text{incoh.}} = \nu_{\text{working point}} + \underbrace{\Delta\nu_{\text{space charge}}}_{\text{space charge tune shift}} + \underbrace{\Delta\nu_{\text{sext.}}}_{\text{amplitude dependent tune shift by sextupole fields}} + \underbrace{\xi\delta}_{\text{chromaticity}}$$

$$\Delta\nu_{\text{space charge},u} = \frac{1}{2\pi} \oint d\theta \frac{\partial}{\partial J_u} \frac{C}{(2\pi)^3} \iint d\phi_x d\phi_y U_{\text{space charge}}$$

$$U_{\text{space charge}} = \frac{\lambda r_0}{\gamma^3 \beta^2} \int_0^\infty dq \frac{\exp\left[-\frac{x^2}{2\sigma_x^2+q} - \frac{y^2}{2\sigma_y^2+q}\right]}{\sqrt{2\sigma_x^2+q} \sqrt{2\sigma_y^2+q}} \quad (2\text{D Gaussian})$$

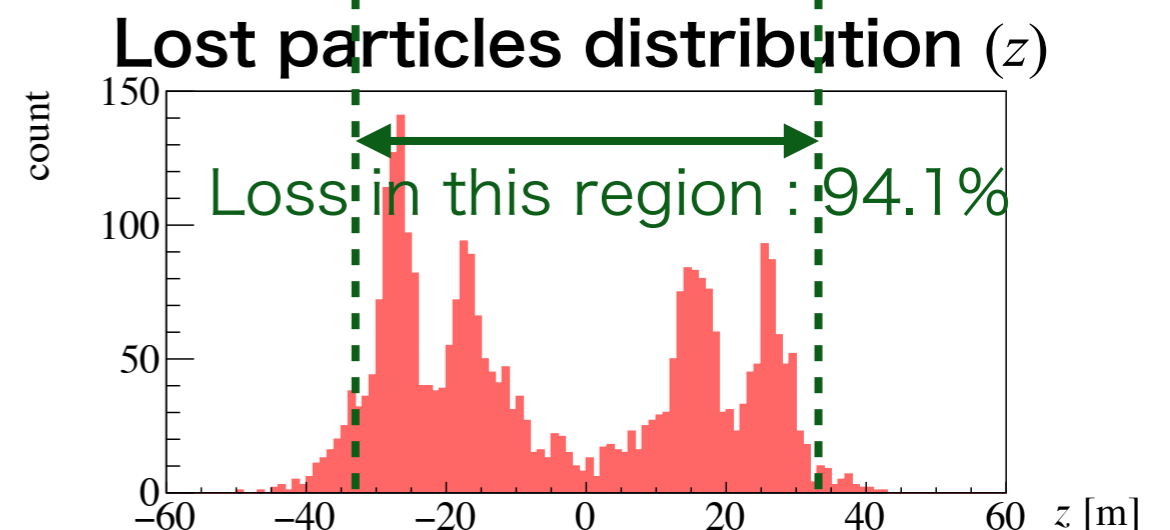
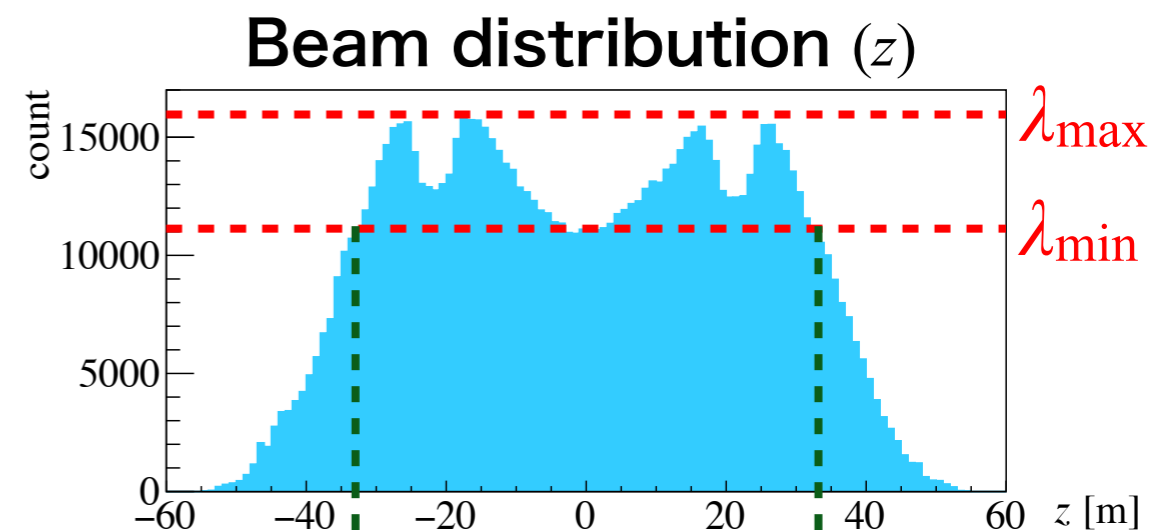
Calculations of incoherent tunes

A particle is affected by a resonance $m_x \nu_x + m_y \nu_y = n$ when its **incoherent tune** satisfies $m_x \nu_{x,\text{incoh.}} + m_y \nu_{y,\text{incoh.}} = n$.

Incoherent tunes can be calculated analytically by setting the **line density** λ and assuming a Gaussian distribution.

Calculations were performed using λ_{max} , λ_{min} .

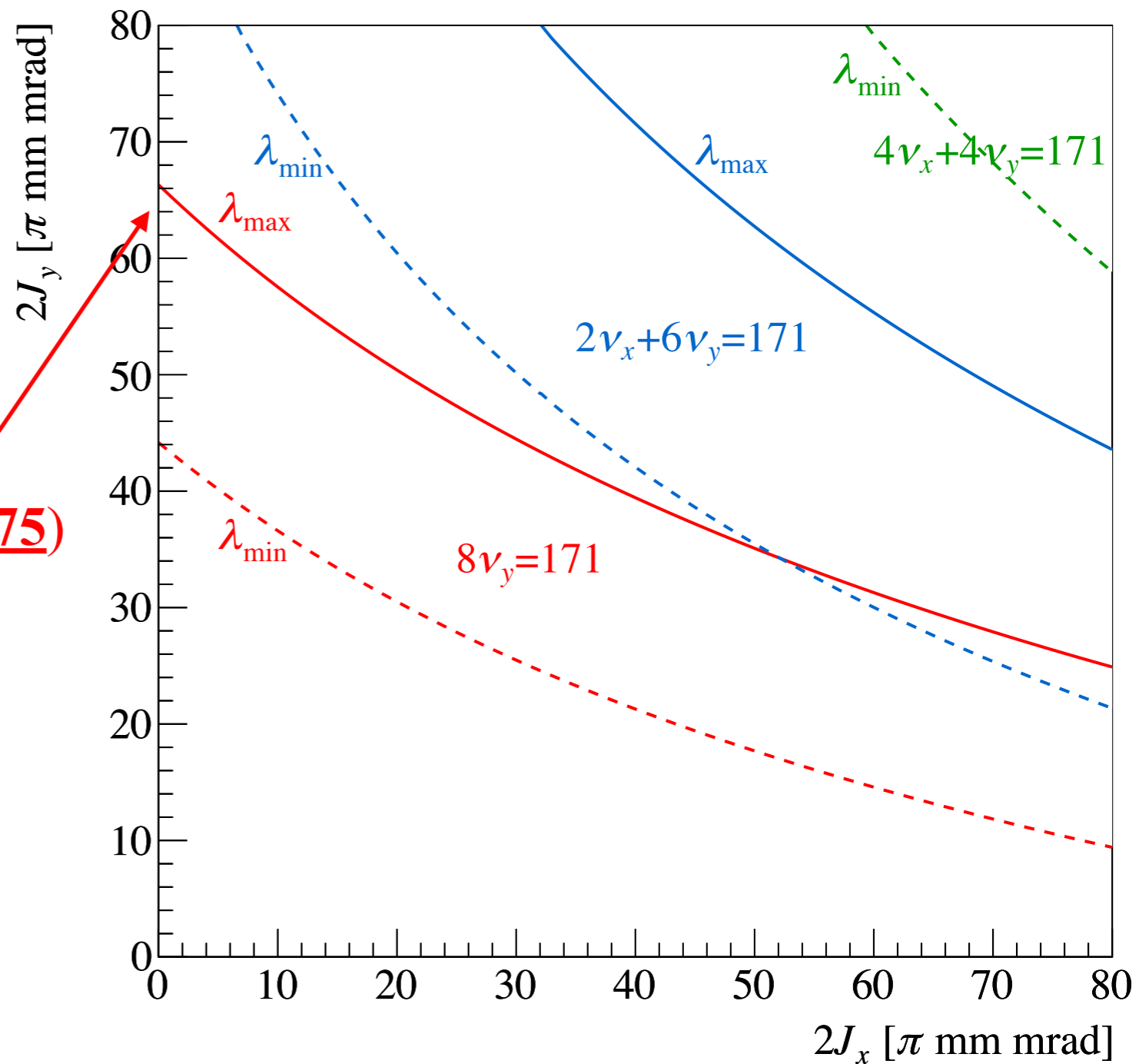
The region $\lambda_{\text{min}} < \lambda < \lambda_{\text{max}}$ ($|z| < 33$ m) covers 94.1% of beam losses.



Where resonances affect

The region covered by the two solutions ($\lambda = \lambda_{\min}, \lambda_{\max}$) can be considered as where the resonance affects.

$$(\nu_{\text{incoh.}, x}, \underline{\nu_{\text{incoh.}, y}}) = (21.258, \underline{21.375})$$



Where resonances affect

The region covered by the two solutions ($\lambda = \lambda_{\min}, \lambda_{\max}$) can be considered as where the resonance affects.

Collimator settings:

$$2J_x = 2J_y = 60\pi \text{ mm mrad}$$



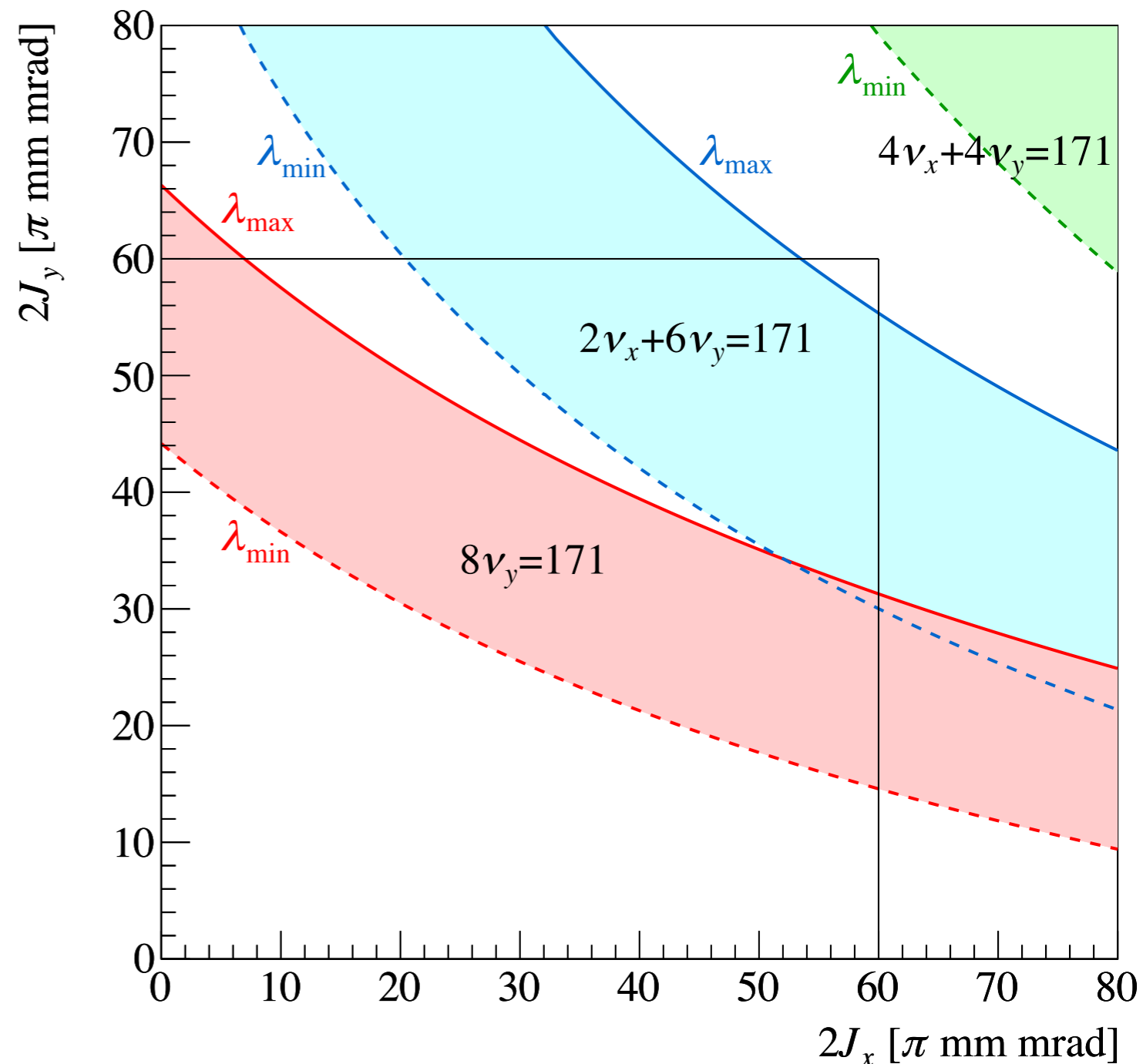
“The beam halo” is also

$$2J_x = 2J_y = 60\pi \text{ mm mrad.}$$

The resonances

$$8\nu_y = 171 \text{ and } 2\nu_y + 6\nu_x = 171$$

affect $2J_x \sim 2J_y \sim 60\pi \text{ mm mrad}$.



Resonance potential

Let us define the resonance potential $U_{m_x, m_y, n}$ as

$$U_{\text{space charge}} = \sum_{m_x, m_y, n} U_{m_x, m_y, n} \cos(m_x \phi_x + m_y \phi_y - n\theta + \xi_{m_x, m_y, n}).$$

It can be derived as

$$U_{m_x, m_y, n} e^{i\xi_{m_x, m_y, n}} = 2 \frac{1}{(2\pi)^3} \oint d\theta \iint d\phi_x d\phi_y U_{\text{space charge}} e^{-i[m_x \phi_x + m_y \phi_y - n\theta]}.$$

Assuming a Gaussian distribution, the potential of $8\nu_y = 171$ is

$$U_{0,8,171} e^{i\xi_{0,8,171}} = \frac{\lambda r_0}{\pi \gamma^3 \beta^2} \oint ds e^{i[8\underbrace{\chi_y}_{\text{fixed}} - (8\nu_y - 171)\theta]} \int_0^\infty dq \frac{e^{-\frac{J_x \beta_x}{2\sigma_x^2 + q} - \frac{J_y \beta_y}{2\sigma_y^2 + q}} I_0\left(\frac{J_x \beta_x}{2\sigma_x^2 + q}\right) I_4\left(\frac{J_y \beta_y}{2\sigma_y^2 + q}\right)}{\sqrt{2\sigma_x^2 + q} \sqrt{2\sigma_y^2 + q}}.$$

phase advance

$$\chi_y(s) = \int_0^s \frac{ds}{\beta_y} \dots \text{changeable}$$

$$\chi_y(C) = 2\pi\nu_y \dots \text{fixed}$$

$U_{0,8,171}$ is changeable maintaining the working point.

How to change $U_{0,8,171}$

Even with the restriction of the working point, there are a lot of solutions for the beam optics.

Other restrictions/suggestions

- Keep achromat lattice ($\Delta\Psi_{\text{arc},x} = 6 \times 2\pi$)
- Better to change globally than locally.

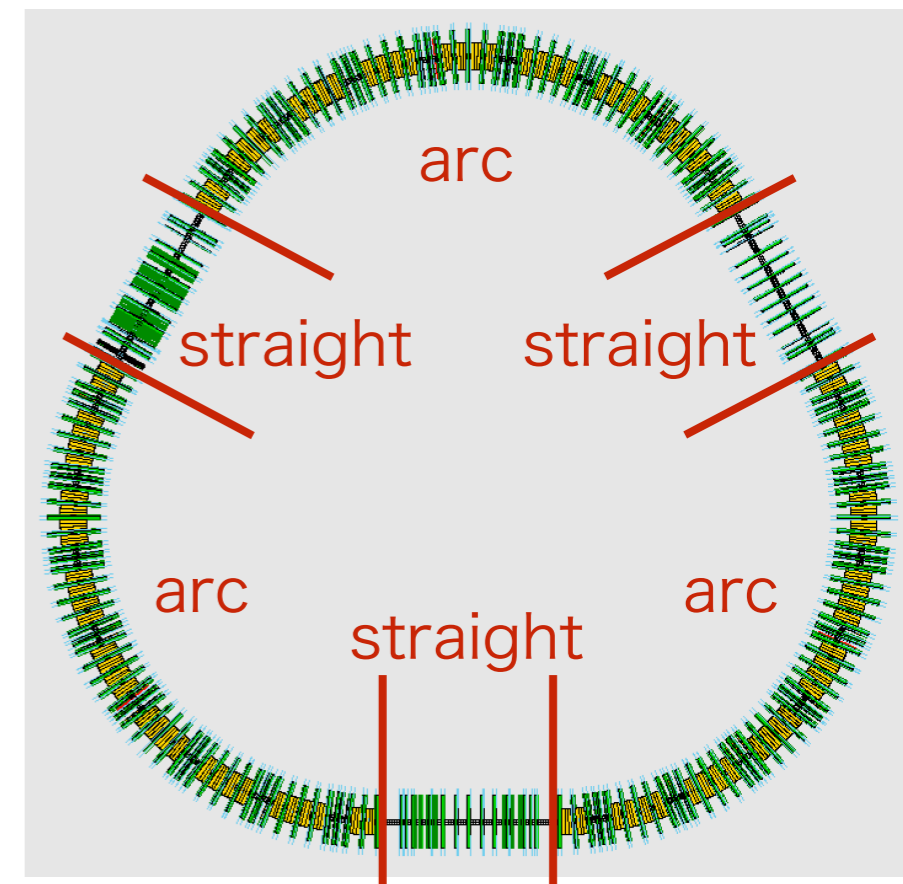


We chose $\Delta\Psi_{\text{arc},y}$ as a scanning knob.

$$\Delta\Psi_{\text{straight},y} = (2\pi\nu_y - 3\Delta\Psi_{\text{arc},y})/3$$

$$\Delta\Psi_{\text{arc},x} = 6 \times 2\pi \quad (\text{fixed})$$

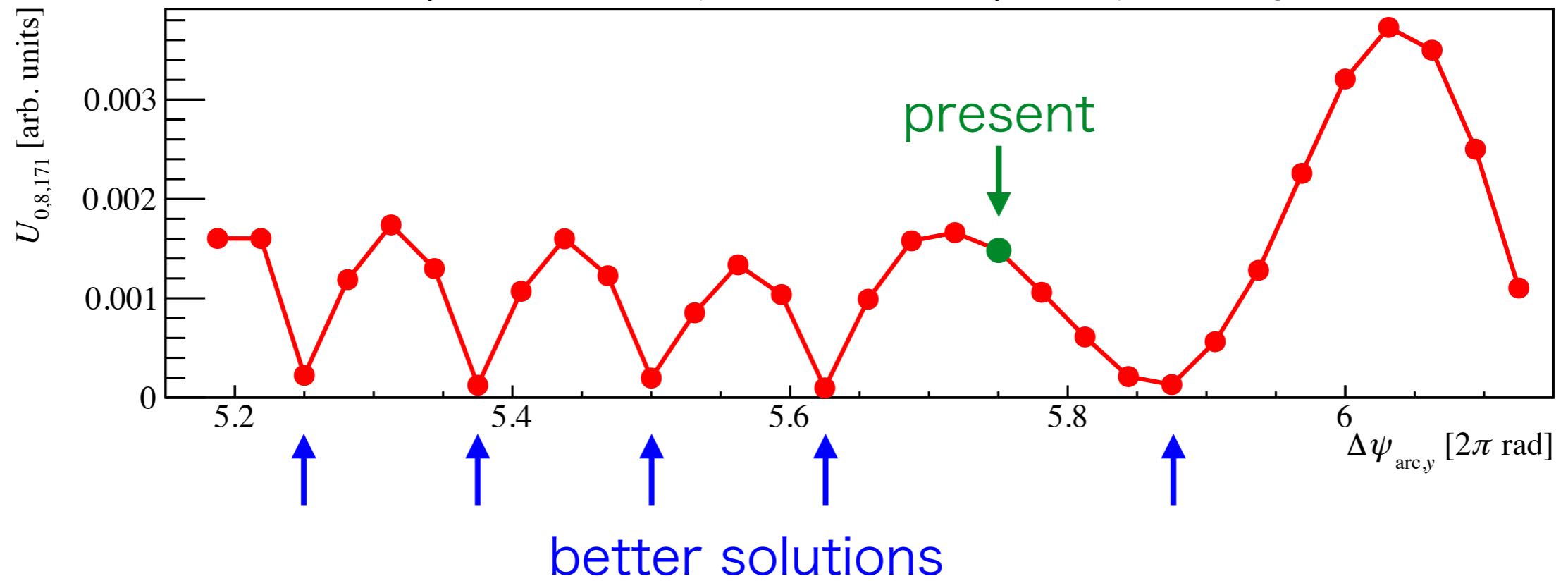
$$\Delta\Psi_{\text{straight},x} = (2\pi\nu_x - 3\Delta\Psi_{\text{arc},x})/3 \quad (\text{fixed})$$



$$3\Delta\Psi_{\text{straight}} + 3\Delta\Psi_{\text{arc}} = 2\pi\nu$$

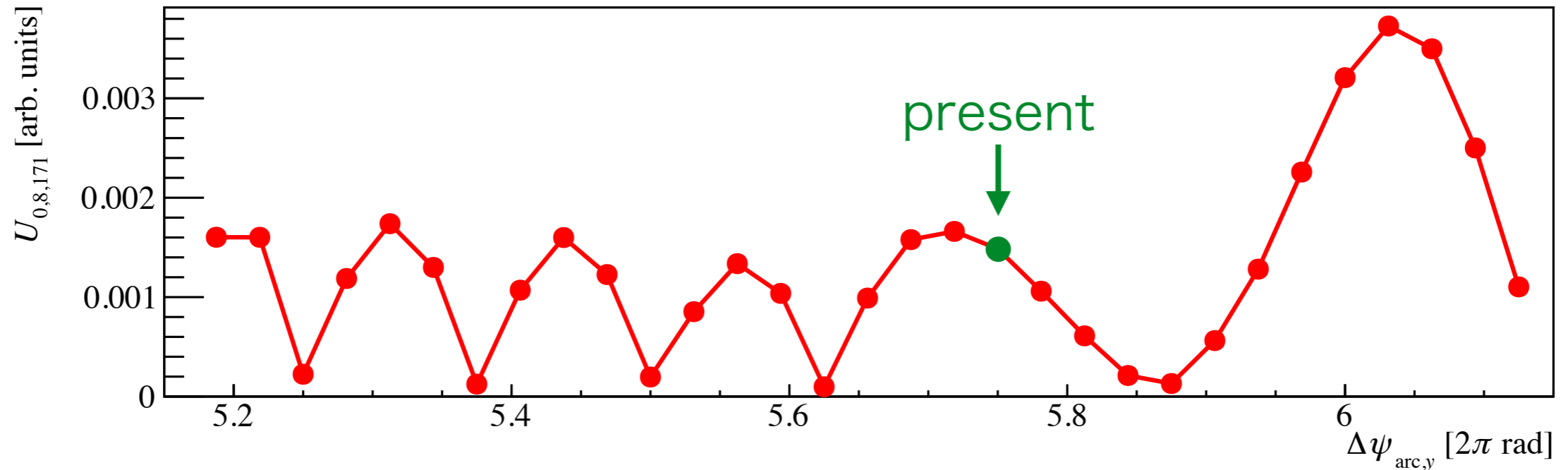
$\Delta\Psi_{\text{arc},y}$ scan

$\Delta\Psi_{\text{arc},y}$ vs $U_{0,8,171}$ ($\lambda=\lambda_{\text{max}}, J_x=0, J_y=66\pi$) (analytical)

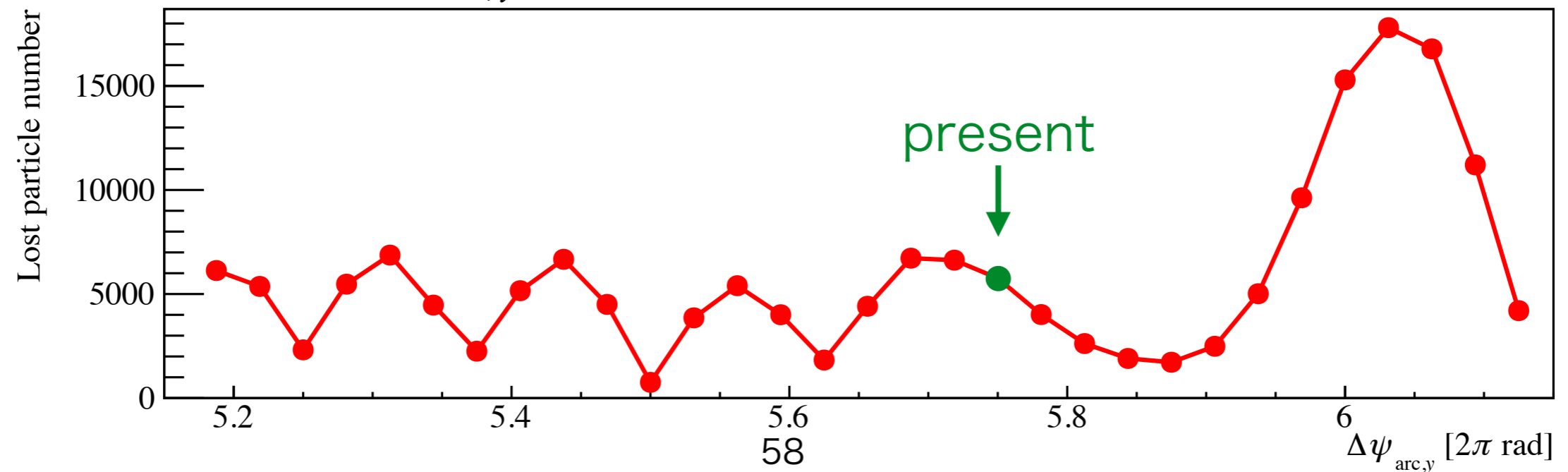


$\Delta\Psi_{\text{arc},y}$ scan

$\Delta\Psi_{\text{arc},y}$ VS $U_{0,8,171}$ ($\lambda=\lambda_{\text{max}}, J_x=0, J_y=66\pi$) (analytical)



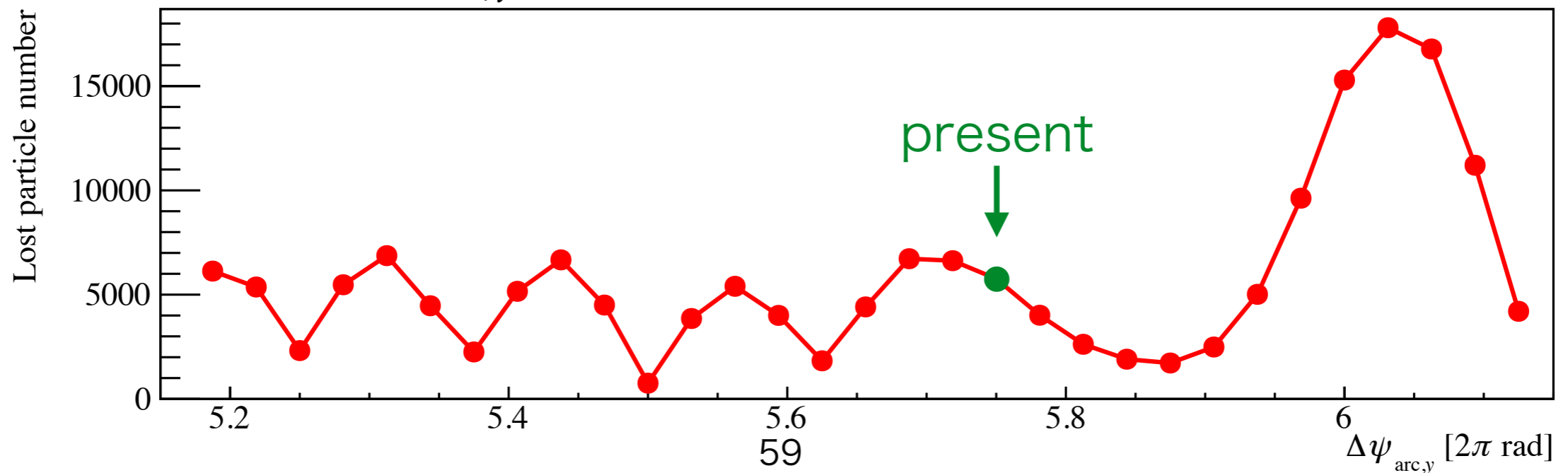
$\Delta\Psi_{\text{arc},y}$ VS **beam loss** (simulation)



$\Delta\Psi_{\text{arc},y}$ scan

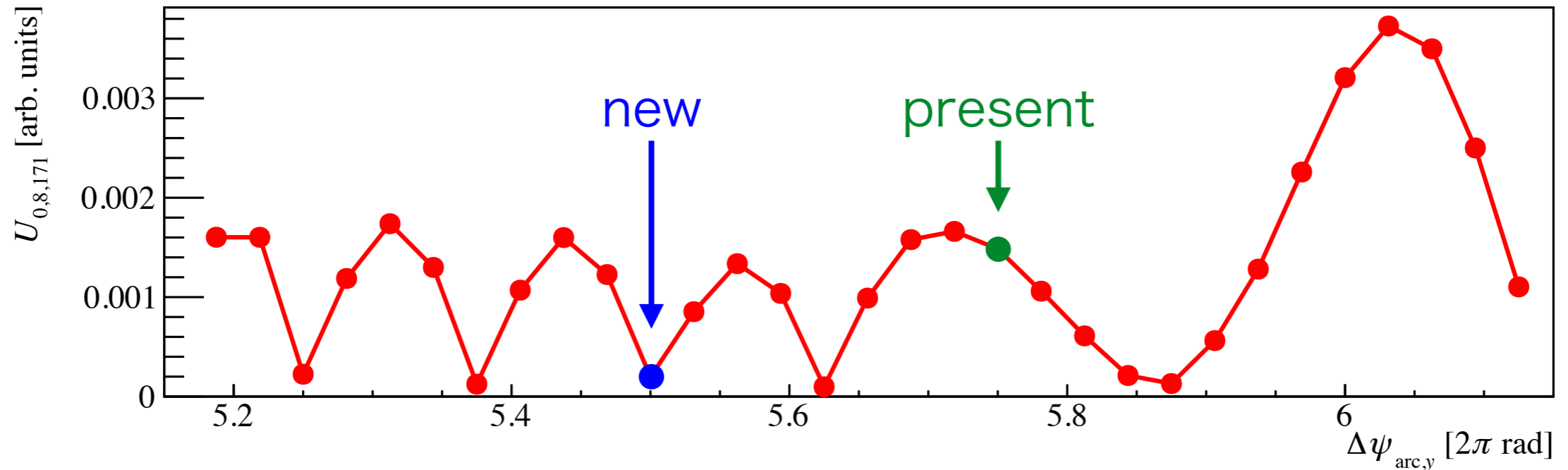


$\Delta\Psi_{\text{arc},y}$ VS **beam loss** (simulation)

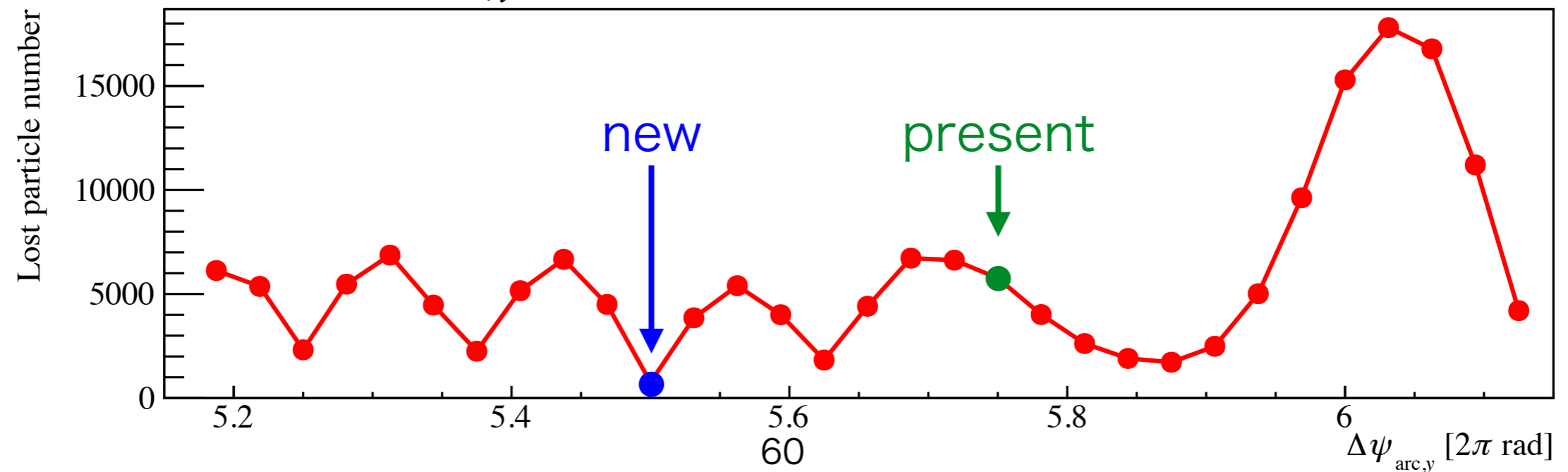


$\Delta\Psi_{\text{arc},y}$ scan

$\Delta\Psi_{\text{arc},y}$ VS $U_{0,8,171}$ ($\lambda=\lambda_{\text{max}}, J_x=0, J_y=66\pi$) (analytical)



$\Delta\Psi_{\text{arc},y}$ VS **beam loss** (simulation)



Resonance potential vs RDT

Resonance potential

- Fourier transform of a potential \rightarrow accurate
- depends on J_x, J_y

$$U_{\text{space charge}} = \sum_{m_x, m_y, n} U_{m_x, m_y, n} \cos(m_x \phi_x + m_y \phi_y - n\theta + \xi_{m_x, m_y, n})$$

$$U_{0,8,171} e^{i\xi_{0,8,171}} = 2 \frac{1}{(2\pi)^3} \oint d\theta \iint d\phi_x d\phi_y U_{\text{space charge}} e^{-i[8\phi_y - 171\theta]}$$

Resonance Driving Term

- Assume potential $x^{m_x} y^{m_y} \rightarrow$ One aspect of resonance potential
- independent of J_x, J_y

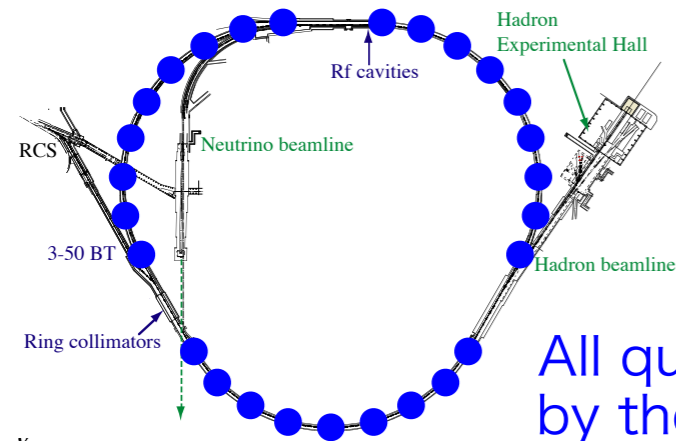
$$U_{0,8,171} = G_{0,8,171} J_y^4 + A_{0,5} J_y^5 + A_{0,6} J_y^6 + \dots + A_{1,4} J_x J_y^4 + \dots$$

$$G_{0,8,171} = \frac{1}{4!} \left. \frac{\partial^4 U_{0,8,171}(J_x, J_y)}{\partial J_y^4} \right|_{J_x=J_y=0}$$

Key for beam loss reduction

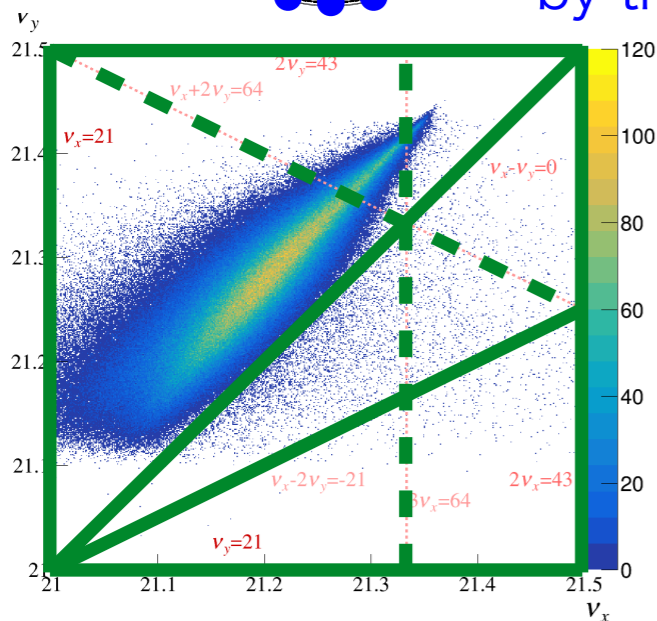
- adjustment of split families -

Before



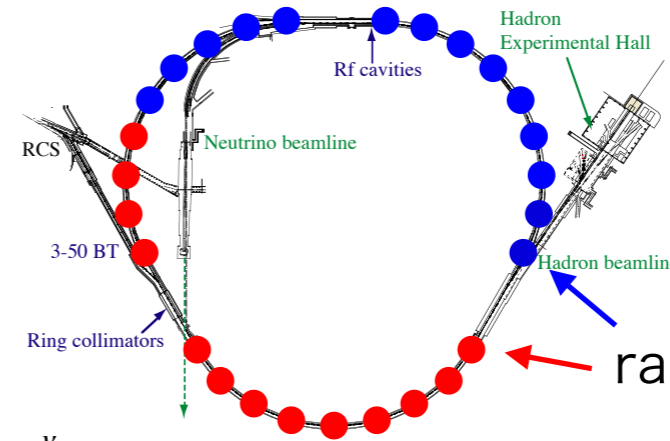
quad family QDX

All quads were ramped by the same PS.



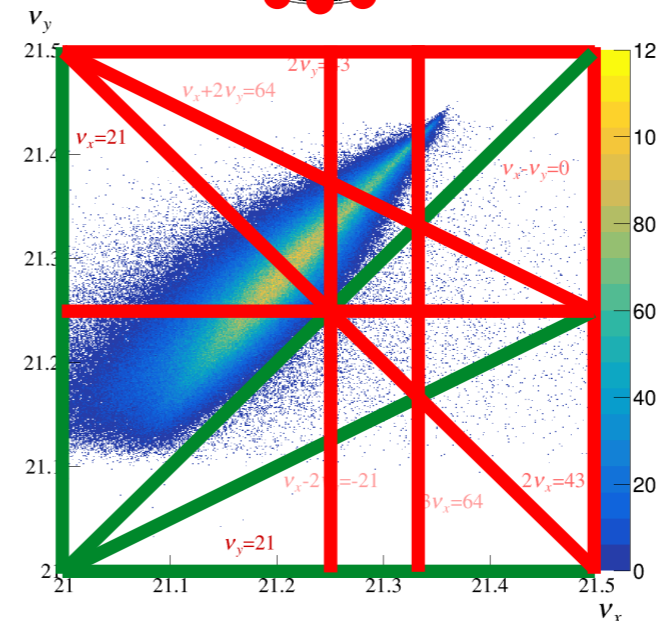
Green lines:
Strong resonances

After



Split!

ramped by different PSs



Red lines:
Reinforced or
newly appeared
resonances

Simulation suggested that the magnetic fields of the split families should be matched with an accuracy of about 0.1%.

T. Yasui, in Proc. IPAC'23, TUXG1

Precise adjustment of the split families was the key.

Bend field ripple reduction

Bend field ripples make quad field fluctuation in combination with sext fields, resulting in breaking three-fold symmetry.

$$\Delta x = \eta_x \frac{\Delta B}{B},$$

bend field error

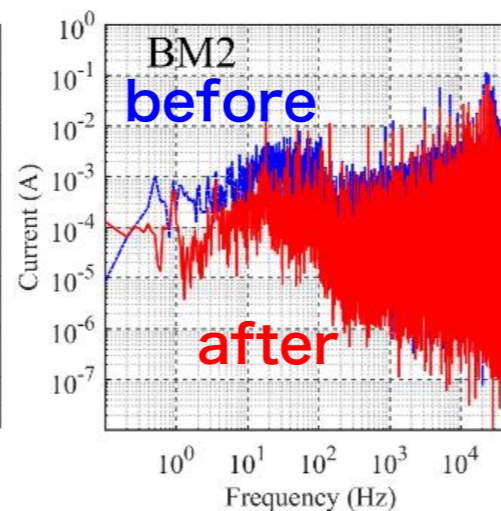
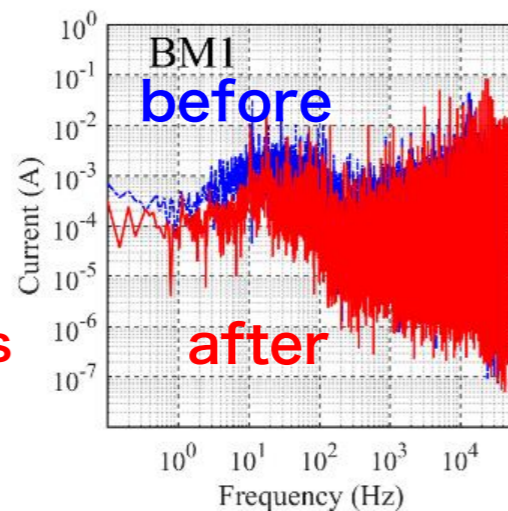
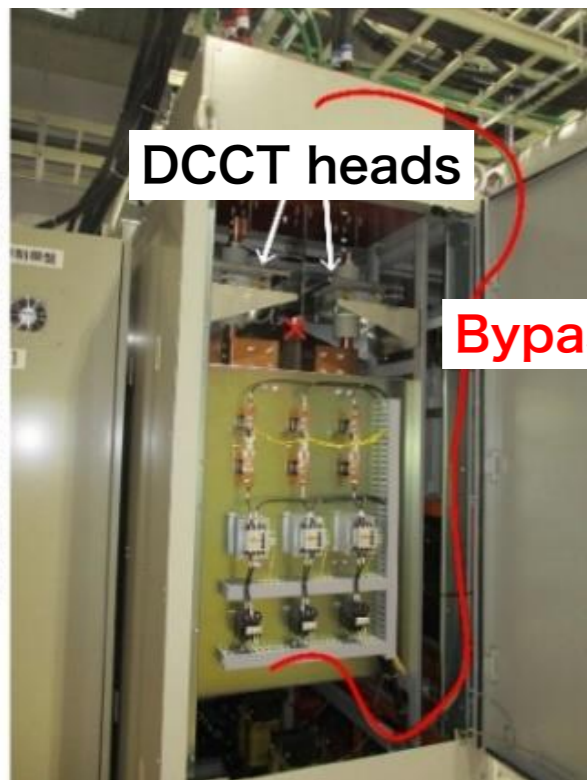
$$|\Delta K_1| = |K_2 \Delta x|$$

quad. field error

sext. field

**T. Yasui,
IPAC2023, TUXG1.**

The main source of ripple was identified as EM fields noise from the DCCT head, and the ground line was bypassed.



**Y. Morita *et al.*,
IPAC2024, TUAD2.**

**RMS of dB/B
(estimated by dl/l)**

	BM1	BM2
before	0.036%	0.035%
after	0.019%	0.013%